RANGE HOOD CAPTURE EFFICIENCY DESIGN MODELING

A Thesis

by

RYAN STEVEN COLLINS

Submitted to the Office of Graduate and Professional Studies of
Texas A&M University
in partial fulfillment of the requirements for the degree of

MASTER OF SCIENCE

Chair of Committee,	Michael Pate
Committee Members,	Jorge Alvarado
	Harry Hogan
Head of Department,	Andreas Polycarpou

December 2016

Major Subject: Mechanical Engineering

ABSTRACT

This study assessed and modeled the performance of a range-hood ventilation system and the important aspects such as major and minor pressure losses, volumetric airflow, and capture efficiency. Results can be classified into two parts: previous test data and the EES program model. Previous test data include fan performance curves produced by the Riverside Energy Efficiency Laboratory (REEL), vent cap performance data produced by a former student at the REEL facility (Escatel, 2011), and capture efficiency data published by Lawrence Berkeley National Laboratory (LBNL). An assortment of six (6) fans, twenty-two (22) vent caps, and the capture efficiency equations were used to complete a mathematical model in the EES program.

The vent cap performance data collected was for the two most common residential ventilation duct diameters, 4-inch and 6-inch in the variety of wall-mounted, roof-jack, and soffit. With most range-hoods using the larger duct size, all fan performance curves collected were 6-inch round. Trend lines using a spreadsheet calculator were constructed to fit the associated static pressure and flow rate data plots. It was shown that increasing the R^2 value to a maximum of one (1) did not necessarily produce trend lines similar to the experimental data. In fact, a third degree polynomial trend line in most cases fit the experimental data better than a larger degree polynomial. Graphing alongside the experimental data was determined to be the best way to quickly see how well the trend line fit the experimental data.

With the combination of fan and vent cap performance, associated ductwork, and the capture efficiency data from LBNL, a mathematical model was constructed and implemented in the Engineering Equation Solver (EES) software. Careful use of trend lines and initial variable guesses allowed the EES program to converge to a solution. Being dependent on airflow, capture efficiency range was from 49% - 94%.

ACKNOWLEDGEMENTS

First of all, I would like to thank Dr. Michael Pate for all the help during my tenure at Texas A&M University. To the members of my committee, Dr. Jorge Alvarado and Dr. Harry Hogan, thank you for support throughout my research.

I would also like to show appreciation for the team at the Riverside Energy Efficiency Laboratory, for their help and friendship. Jim, Kathy, and Wongyu, thank you so much for the answers to my many questions.

For my parents, Tom and Teresa, thank you for your support over the years. Last but not least, I would like to show my appreciation to my wife, Jaime, for her loyalty and encouragement.

NOMENCLATURE

α	Kinetic energy coefficient (dimensionless)
μ	Dynamic Viscosity ($\frac{lbf*s}{ft^2}$)
ASHRAE	American Society of Heating, Refrigeration and Air Conditioning Engineers
CE	Capture Efficiency
CFM	Volumetric flow rate ($\frac{ft^3}{min}$)
D	Diameter (ft) or (inches)
HVI	Home Ventilation Institute
K	Pressure loss coefficient
L	Length (ft) or (inches)
LBNL	Lawrence Berkeley National Laboratory
R_e	Reynold's Number (dimensionless)
P	Pressure (PSI) or (inches of water)
ΔP	Change in pressure or pressure loss (PSI) or (inches of water)
REEL	Riverside Energy Efficiency Laboratory
$\dot{V}$	Volumetric flow rate ($\frac{ft^3}{min}$)
ρ	Standard air density $0.075\frac{lbm}{ft^3}$

TABLE OF CONTENTS

Page

ABSTRACT ii

ACKNOWLEDGEMENTS iv

NOMENCLATURE v

TABLE OF CONTENTS vi

LIST OF FIGURES viii

LIST OF TABLES xii

1. INTRODUCTION 1

2. THEORY 3

- Major Losses 3
- Minor Losses 5
- System Curve 8
- First Iteration 11
- Second Iteration 12
- Third Through Sixth Iteration Table Data 13
- Entrance Length 16
- Capture Efficiency 19
- Capturing Gases 23
- Non Standard Air Density Correction 25

3. VENT CAP PERFORMANCE 28

- Vent Cap Performance Trend Lines 32

4. USE OF FLEXIBLE DUCTS 36

5. FAN TESTING OPERATION 39

- Range Hood Ratings 39

6. ANALYSIS OF REAL FANS 45

- Fan Laws 45
- Fan Performance Trend Lines 49

7. USE OF EES PROGRAM 54

Program Operation 54
Variable Description 55
Knowns 56
Activating Fan And Vent Cap Equations 56
Variable Information 58
Solving The EES Program 60

8. CORRECT SIZING DUCT LENGTHS AND DIAMETER 64

9. EES DATA 67

10. CONCLUSION 71

REFERENCES 73

APPENDIX A: FAN DATA 75

APPENDIX B: VENT CAP DATA (ESCATEL, 2011) 91

APPENDIX C: ELBOW DATA (ASHRAE, 2005) 131

APPENDIX D: PERSONAL AND PHONE INTERVIEWS 138

LIST OF FIGURES

Page

Figure 1: CD3-12 Elbow, 3 Gore, 90°, r/D = 0.75 – 2.06 (ASHRAE, 2005) 6

Figure 2: Loss Coefficient for Three Gore 90° Elbow 7

Figure 3: Adjustable Radius Elbow Duct (Oneida Air, 2016) 8

Figure 4: Typical Fan Curve 9

Figure 5: Total System Curve 15

Figure 6: Establishment of Uniform Velocity Profile (ASHRAE, 2013) 17

Figure 7: Entrance Length for Velocities Greater Than 2500 fpm 18

Figure 8: Entrance Length for Velocities Less Than 2500 fpm 19

Figure 9: Capture Efficiency Airflow Rates (Delp, 2012) 22

Figure 10: Range Hood Lacking Lip to Trap Gases 23

Figure 11: Fan With Increased Cavity Area 24

Figure 12: Holding Humidity Ratio Constant (ω = 0.009) 27

Figure 13: Vent Cap Orientation for Soffit, Wall-Mounted, and Roof (Truini, 2016) 28

Figure 14: Experimental and 6th Degree Trend Line Comparison 33

Figure 15: Experimental and 3rd Degree Trend Line Comparison 33

Figure 16: Reduced Performance of Compression (Abushakra, 2004) 37

Figure 17: Testing Setup Described As “Figure 12”(ANSI/AMCA 210-07, 2007) 41

Figure 18: Selection Guide (ANSI/AMCA 210-07,2007) 42

Figure 19: Green Chamber Constructed to “Figure 12” Specifications 43

Figure 20: RPM and Flow Rate Comparison 47

Figure 21: Excel Drawn 6th Degree Trend Line 51

Figure 22: Experimental and 6th Degree Trend Line Comparison 52

Figure 23: Experimental and 3rd Degree Trend Line Comparison 53
Figure 24: EES Operation Comments 54
Figure 25: EES Variables Sections 55
Figure 26: EES Knowns Section 56
Figure 27: Fan Static Pressure EES Trend Line Equations 57
Figure 28: Vent Cap Loss Coefficient EES Trend Line Equations 57
Figure 29: EES Variable Information Table 58
Figure 30: EES Variable Limit Defaults 59
Figure 31: EES Variable Limit Correction 60
Figure 32: EES Program Using Loss Coefficient Formula 61
Figure 33: EES Solution for Sample Problem in “System Curve” 62
Figure 34: Moody Diagram (Fox, 1985) 65
Figure 35: Fan A Performance 75
Figure 36: Fan B Performance 77
Figure 37: Fan C Performance 79
Figure 38: Fan D Performance 81
Figure 39: Fan E Performance 83
Figure 40: Fan F Performance 85
Figure 41: Fan A 88
Figure 42: Fan B 88
Figure 43: Fan C 89
Figure 44: Fan D 89
Figure 45: Fan E 90
Figure 46: Fan F 90

Figure 47: 4” Soffit Vent Cap Performance 91
Figure 48: 4” Wall-Mounted Vent Cap Performance 93
Figure 49: 4” Roof Jack Vent Cap Performance 97
Figure 50: 6” Soffit Vent Cap Performance 99
Figure 51: 6” Wall-Mounted Vent Cap Performance 101
Figure 52: 6” Roof Jack Vent Cap Performance 105
Figure 53: 4” Vent Cap Performance Average 107
Figure 54: 6” Vent Cap Performance Average 108
Figure 55: 4” Soffit Loss Coefficient Performance 109
Figure 56: 4” Wall-Mounted Loss Coefficient Performance 112
Figure 57: 4” Roof Jack Loss Coefficient Performance 115
Figure 58: 6” Soffit Loss Coefficient Performance 118
Figure 59: 6” Wall-Mounted Loss Coefficient Performance 119
Figure 60: 6” Roof Jack Loss Coefficient Performance 123
Figure 61: 4” Loss Coefficient Average 125
Figure 62: 6” Loss Coefficient Average 126
Figure 63: 4” Soffit Vent Caps 127
Figure 64: 4” Wall-Mounted Vent Caps 127
Figure 65: 4” Roof Jack Vent Caps 128
Figure 66: 6” Soffit Vent Cap 128
Figure 67: 6” Wall-Mounted Vent Caps 129
Figure 68: 6” Wall-Mounted Vent Caps 129
Figure 69: 6” Roof Jack Vent Caps 130
Figure 70: CD3-1 Elbow, Die Stamped, 90°, r/D=1.5 131

Figure 71: CD3-3 Elbow, Die Stamped, 45°, r/D = 1.5 131
Figure 72: CD3-5 Elbow, Pleated, 90°, r/D = 1.5 132
Figure 73: CD3-7 Elbow, Pleated, 45°, r/D = 1.5 133
Figure 74: CD3-9 Elbow, 5 Gore, 90°, r/D = 1.5 133
Figure 75: CD3-10 Elbow, 7 Gore, 90°, r/D = 2.5 134
Figure 76: CD3-12 Elbow, 3 Gore, 90°, r/D = 0.75 – 2.0 135
Figure 77: CD3-13 Elbow, 3 Gore, 60°, r/D = 1.5 135
Figure 78: CD3-14 Elbow, 3 Gore, 45°, r/D = 1.5 136
Figure 79: CD3-17 Elbow, Mitered, 45° 137

LIST OF TABLES

Page

Table 1: Solved Values For Iterative Solution 14

Table 2: Performance of U.S. Residential Range Hoods (Delp, 2012) 21

Table 3: Vent Cap Description (Escatel, 2011) 30

Table 4: Trend Line Equations 32

Table 5: Effects of Increasing Polynomial 35

Table 6: Pressure Drop Correction Factor of Common Duct Sizes (ASHRAE, 2005) 38

Table 7: Experimental Data and 1st Fan Law % Difference 46

Table 8: Experimental Data and 2nd Fan Law % Difference 48

Table 9: Effects of Increasing Trend Line Polynomial 50

Table 10: Trend Line Equations 51

Table 11: Table Data Using Loss Coefficient Trend Line 61

Table 12: Data Using Pressure Loss Trend Line 62

Table 13: Fan A and 6" Vent Cap Capture Efficiencies 67

Table 14: Fan B and 6" Vent Cap Capture Efficiencies 68

Table 15: Fan C and 6" Vent Cap Capture Efficiencies 68

Table 16: Fan D and 6" Vent Cap Capture Efficiencies 69

Table 17: Fan E and 6" Vent Cap Capture Efficiencies 69

Table 18: Fan F and 6" Vent Cap Capture Efficiencies 70

Table 19: Fan A Performance Trend Lines 75

Table 20: Fan A Experiment and Trend Line Comparison 76

Table 21: Fan B Performance Trend Lines 77

Table 22: Fan B Experiment and Trend Line Comparison 78

Table 23: Fan C Performance Trend Lines 79
Table 24: Fan C Experiment and Trend Line Comparison 80
Table 25: Fan D Performance Trend Lines 81
Table 26: Fan D Experiment and Trend Line Comparison 82
Table 27: Fan E Performance Trend Lines 83
Table 28: Fan E Experiment and Trend Line Comparison 84
Table 29: Fan F Performance Trend Lines 86
Table 30: Fan F Experiment and Trend Line Comparison 87
Table 31: 4” Soffit Vent Cap Performance Trend Lines 91
Table 32: 4" Soffit Experiment and Trend Line Comparison 92
Table 33: 4” Wall-Mounted Vent Cap Performance Trend Lines 94
Table 34: 4" Wall-Mounted Experiment and Trend Line Comparison 95
Table 35: 4” Roof Jack Vent Cap Performance Trend Lines 97
Table 36: 4" Roof Jack Experiment and Trend Line Comparison 98
Table 37: 6” Soffit Vent Cap Performance Trend Line 100
Table 38: 6" Soffit Experiment and Trend Line Comparison 100
Table 39: 6” Wall-Mounted Vent Cap Performance Trend Lines 102
Table 40: 6" Wall-Mount Experiment and Trend Line Comparison 103
Table 41: 6” Roof Jack Vent Cap Performance Trend Lines 105
Table 42: 6" Roof Jack Experiment and Trend Line Comparison 106
Table 43: 4” Average Vent Cap Performance Trend Line Data 108
Table 44: 6" Average Vent Cap Performance Trend Line Data 109
Table 45: 4” Soffit Loss Coefficient Performance Trend Lines 110
Table 46: 4" Soffit Data and Trend Line Comparison 111

Table 47: 4” Wall-Mounted Loss Coefficient Performance Trend Lines 113
Table 48: 4" Wall-Mounted Data and Trend Line Comparison.....114
Table 49: 4” Roof Jack Loss Coefficient Performance Trend Lines 116
Table 50: 4" Roof Jack Data and Trend Line Comparison 117
Table 51: 6” Soffit Loss Coefficient Performance Trend Line.....118
Table 52: 6" Soffit Data and Trend Line Comparison 119
Table 53: 6” Wall-Mounted Loss Coefficient Performance Trend Line.....120
Table 54: 6" Wall-Mounted Data and Trend Line Comparison.....121
Table 55: 6” Roof Jack Loss Coefficient Performance Trend Lines 123
Table 56: 6" Roof Jack Data and Trend Line Comparison 124
Table 57: 4” Average Loss Coefficient Trend Lines 125
Table 58: 6” Average Loss Coefficient Trend Lines 126
Table 59: CD3-1 Elbow, Die Stamped, 90°, r/D = 1.5 131
Table 60: CD3-3 Elbow, Die Stamped, 45°, r/D = 1.5 132
Table 61: CD3-5 Elbow, Pleated, 90°, r/D = 1.5 132
Table 62: CD3-7 Elbow, Pleated, 45°, r/D = 1.5 133
Table 63: CD3-9 Elbow, 5 Gore, 90°, r/D = 1.5 134
Table 64: CD3-10 Elbow, 7 Gore, 90°, r/D = 2.5 134
Table 65: CD3-12 Elbow, 3 Gore, 90°, r/D = 0.75 – 2.0 135
Table 66: CD3-13 Elbow, 3 Gore, 60°, r/D = 1.5 136
Table 67: CD3-14 Elbow, 3 Gore, 45°, r/D = 1.5 136
Table 68: CD3-17 Elbow, Mitered, 45° 137

1. INTRODUCTION

The most expensive operating cost of a household is the heating, ventilation, and air conditioning system. An air conditioning unit not only cools the air within the residence, but it also condenses water vapor out of the air and dehumidifies the indoor air. Depending on the climate, your air conditioning unit may be more useful dehumidifying air than cooling it. However, an air conditioning unit is not the only system in a residence that removes unwanted moisture or airborne particles. In fact, bathroom fans, range hoods, and even fenestrations help assist with ventilation of the residence.

Ventilation, being one of the most fundamental studies of Heating, Ventilation, and Air Conditioning (HVAC), is often overlooked. Fresh air to replace musty smells, reduction of humidity, and removal of airborne contaminants, specifically in and around the area of the stove can be obtained with the use of a kitchen range hood. One may use the range hood to ventilate hot air emanating from the heat source, but another important function of the range hood is the removal of the aforementioned airborne contaminants.

There are two main types of range hoods, recirculating range hoods and the ducted range hoods. A recirculating range hood draws air through a mechanical filter and exhausts the air back into the kitchen at eye level. Due to the physical impedance of the metal filter and grease being less nimble than air, the grease comes into contact with the filter and becomes trapped. Due to the lack of any ductwork, the airborne contaminants can only be reduced by adhering to the filter and not exiting the residence. Due to buildup of grease, bacteria, mold, and other airborne contaminants, it is much

more desirable to use a ducted range hood to not just trap airborne contaminants, but to exhaust them out of the residence. Therefore, a ducted range hood will be the focus of this study.

The ductwork must be constructed to direct the gases outside the house, and therefore creates a restriction on the air exhausted by the fan. Adequate duct sizing, necessary elbows to make 90° turns, and vent caps to reduce infiltration all create restrictions to airflow. It will be shown that there exists a direct correlation to airflow and the removal of these contaminants, known as capture efficiency.

Capture efficiency can also be explained by the capability of the range hood to capture the contaminants and direct them out of the kitchen. If we can mathematical analyze how well a fan and the associated duct system performs, with the use of Engineering Equation Solver (EES) we can produce a program that determines the associated capture efficiency. The computer program will be written to allow for fans, vent caps, and elbows for current Riverside Energy Efficiency Laboratory data and allow for future data as well.

2. THEORY

Many aspects go into the design of a fan-duct system. The duct system, which includes the major and minor losses (total head loss), diameter, vent caps, and even the duct material will affect what fan will be necessary to overcome the associated pressure loss. The following equations were taken from a common fluid mechanics textbook (Fox, 1985).

Major Losses

A major loss is the resulting pressure drop due to friction along a straight length of pipe. Three assumptions that must be made are: the straight pipe is in fact straight, flow is fully developed, and the area of the pipe is constant.

$$\left(\frac{p_1}{\rho} + \alpha_1 \frac{V_1^2}{2} + gz_1\right) - \left(\frac{p_2}{\rho} + \alpha_2 \frac{V_2^2}{2} + gz_2\right) = h_{l_T} \qquad \text{(Eqn. 1)}$$

p = pressure

ρ = fluid density

α = kinetic energy coefficient

V = fluid velocity

g = gravitational constant

z = relative height

h_{l_T} = total head loss per unit mass

To calculate major head losses, we use Eqn. 1 and make the following assumptions:

1. No minor losses exist, therefore total head loss (h_{l_T}) will become major head loss (h_l)

2. $\alpha_1 \frac{V_1^2}{2} = \alpha_2 \frac{V_2^2}{2}$ and the terms cancel out

3. The change in potential energy (Δz) can be considered negligible

The resulting major head loss formula is:

$$h_l = \frac{\Delta p}{\rho} \quad \text{(Eqn. 2)}$$

Given the flow rate as a function of pressure drop:

$$\dot{V} = \frac{\Pi \Delta p D^4}{128 \mu L} \quad \text{(Eqn.3)}$$

$\dot{V}$ = volumetric flow rate

Δp = pressure drop

D = diameter of pipe

μ = absolute viscosity

L = length of pipe

We can combine Eqn.2 and Eqn.3 and the result is the major head loss for laminar flow.

$$\Delta P_{major} = \left(\frac{64}{Re}\right)\left(\frac{L}{D}\right)\left(\rho \frac{V^2}{2}\right) \quad \text{(Eqn. 4)}$$

ΔP= major pressure loss

Re = Reynolds number

ρ = density of fluid ($\frac{lbm}{ft^3}$)

By substituting Eqn.5 below we arrive at the most commonly used form for major head loss in Eqn.6 known as the Darcy-Weisbach equation. Basic assumptions made when using this equation are fully developed flow and Newtonian fluids.

$$f_{laminar} = \frac{64}{Re} \quad \text{(Eqn.5)}$$

$$\Delta P_{major} = f(\frac{L}{D})(\rho\frac{V^2}{2}) \quad \text{(Eqn.6)}$$

The most commonly used formula for turbulent flow is the equation given below:

$$\frac{1}{\sqrt{f_{turbulent}}} = -2.0\log(\frac{\frac{e}{D}}{3.7} + \frac{2.51}{Re\sqrt{f_{turbulent}}}) \quad \text{(Eqn.7)}$$

Where Re: $4000<Re<3*10^6$

Minor Losses

Minor loss is the pressure reduction due to the necessary turns, changes in duct area, valves, fittings and applicable vent caps built into the system. The name given to the losses, "minor", is in fact, not minor at all. Depending on how sharp the turns are, typically 45°, 60°, or 90°, and how abrupt the interior panels are, you can lose as much pressure as due to the length of pipe itself. The equations for the minor losses are as follows:

$$\Delta P_{minor} = K * \rho * \frac{V^2}{2} \quad \text{(Eqn.8)}$$

h_{l_m} = minor head loss due to fitting and pipe bends

K = loss coefficient

V = velocity of fluid

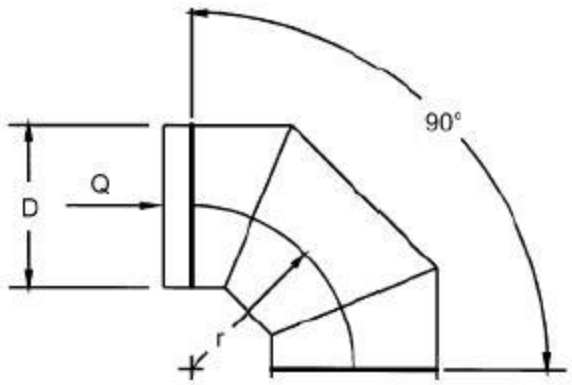

r/D	0.75	1.00	1.50	2.00
Loss Coefficient	0.54	0.42	0.34	0.33

Figure 1: CD3-12 Elbow, 3 Gore, 90°, r/D = 0.75 – 2.06 (ASHRAE, 2005)

Figure 1 above is a common elbow used to redirect the flow of air (Chen, 2015). The gores are rigid segments of straight pipe that are able to rotate and form the necessary 90° turn. These types of fittings are much more desirable due to the reduce pressure loss. With flexible duct, the internal ribs magnify the pressure loss of the moving fluid, and therefore reduce the efficiency of the system. Even though this is a more efficient way to construct the duct system, it is not without pressure loss. Below in Figure shows the Loss Coefficient for the above 90° Elbow given the radius of the bend, R, and the diameter of the duct D.

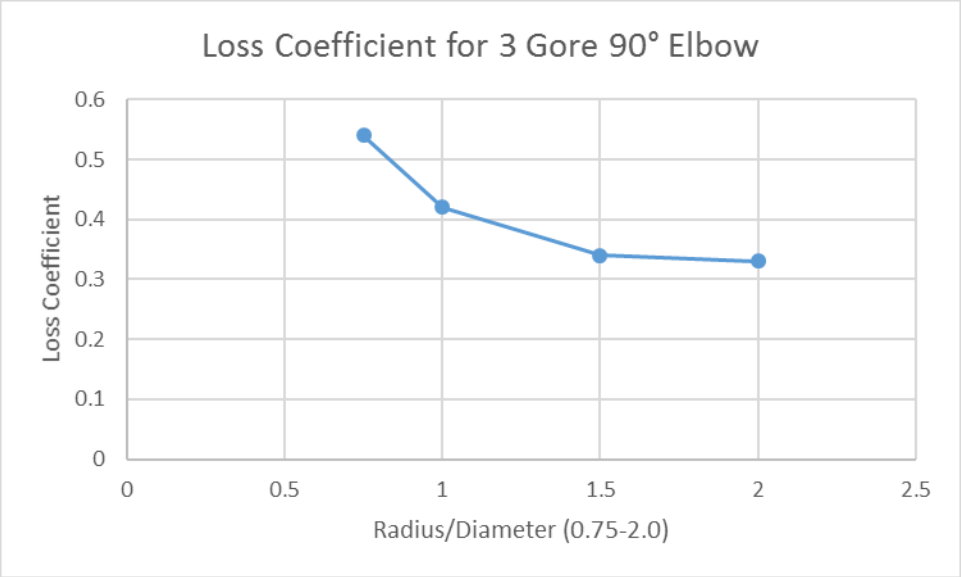

Figure 2: Loss Coefficient for Three Gore 90° Elbow

First we will calculate a trend line for the above Figure 2:

$$Y = -0.2293*x^3 + 1.172*x^2 - 2.000*x + 1.478 \qquad \text{(Eqn. 9)}$$

Next, we must determine the radius, R. In Figure 3 we can see the radius, R, is a function of the diameter, D.

Figure 3: Adjustable Radius Elbow Duct (Oneida Air, 2016)

Given a duct diameter of 6” we can determine what the radius and respective loss coefficient.

Radius = 1.75 * Diameter = 1.75 * 6 Inches = 10.5 Inches

With the radius, diameter, and the trend line for the 3 Gore, 90° Elbow, we can now calculate the loss coefficient.

Loss Coefficient = $-0.2293*(1.75)^3+1.172*(1.75)^2-2.000*(1.75)+1.478 = 1.849$ (Eqn.10)

With the above loss coefficient, we can determine what the associated minor pressure losses would be for each elbow in our system.

System Curve

Typically, fan curves are produced with the increase in pressure on the vertical axis, and the associated volumetric flow rate on the horizontal axis. Figure 4 shows a typical fan curve that loses pressure as we increase the volumetric flow rate.

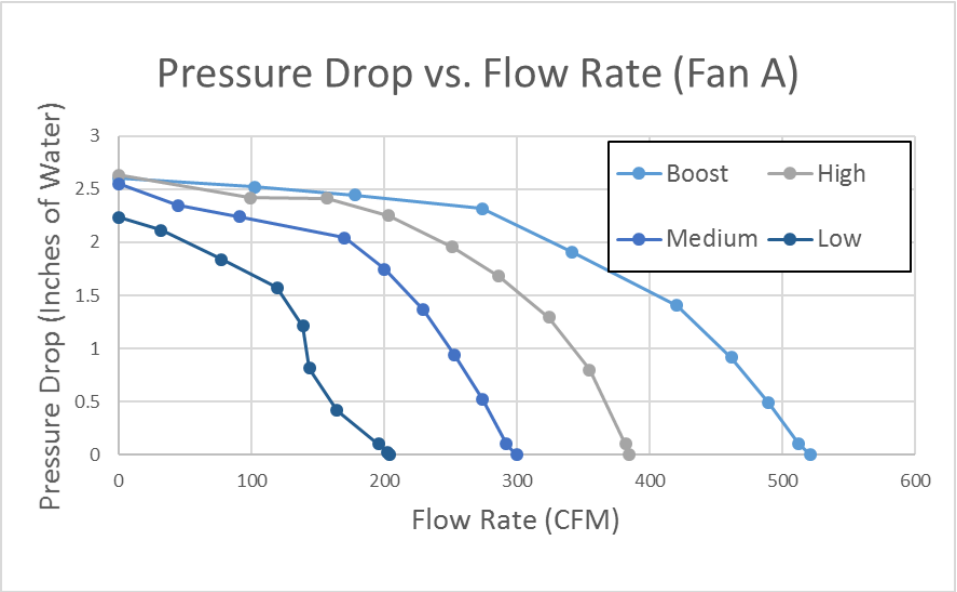

Figure 4: Typical Fan Curve

To better understand the loss in pressure due to increased flow rate, note Eqn. 11 below. Similar to Eqn.1, if we add in a fan, and neglect changes in height, we get the following equation:

$$\text{Fan} = h_{l_T} + \frac{\Delta P}{\rho} + \frac{V_2^2 - V_1^2}{2} \qquad \text{(Eqn. 11)}$$

With the mechanical energy of the fan added to the fluid being constant, we have one equation with three unknowns. Therefore we can deduce that P_2 = f(h_{l_T}, V_1, V_2, P_1) and V_2 = f(h_{l_T}, P_2, P_1, V_1) and see that the fan curve actually consists of many system curves.

A single speed on the fan performance curve represents an unlimited range of system constructions. With the addition of a ductwork and vent caps, the resistance created must intersect with the fan curve at one specific point. Since the fan performance curve

is a one to one function, the total pressure loss is associated with a single CFM value along the fan performance curve. To show this, major and minor pressure losses will be calculated and solved with the appropriate trend line.

- D (Diameter) = ½ foot
- L (Length of Straight Pipe) = 15 feet
- E (Roughness factor) = 0.0005
- ρ (Density of Air) = 0.075 $\frac{lbm}{ft^3}$
- m (Kinematic Viscosity) = 1.68E-04 $\frac{ft^2}{s}$

$$\Delta P_{major} = f(\frac{L}{D})(\rho\frac{V^2}{2}) \quad \text{(Eqn. 12)}$$

$$\Delta P_{minor} = K * \rho * \frac{V^2}{2} \quad \text{(Eqn. 13)}$$

$$\frac{1}{\sqrt{f_{turbulent}}} = -2.0\log(\frac{\frac{e}{D}}{3.7} + \frac{2.51}{Re\sqrt{f_{turbulent}}}) \quad \text{(Eqn. 14)}$$

$$R_e = \frac{V*D}{\mu} \quad \text{(Eqn. 15)}$$

First Iteration

If we want to manually solve this problem, we must initially guess a velocity and solve our equations from there. With the initial velocity guess of 32.85 $\frac{ft}{s}$ we find the following data:

$$R_e = \frac{32.85\ ft}{s} * 0.5\ ft * \frac{s}{1.68E{-}04\ ft^2} = 97{,}767 \quad \text{(Eqn. 16)}$$

$$\frac{1}{\sqrt{f_{turbulent}}} = -2.0\log\left(\frac{\frac{0.0005}{0.5}}{3.7} + \frac{2.51}{97{,}767\sqrt{f_{turbulent}}}\right) \quad \text{(Eqn. 7)}$$

$$f = 0.02222$$

$$\Delta P_{major} = 0.02222 * \left(\frac{15\ ft}{0.5\ ft}\right) * \left(0.075\ \frac{lbm}{ft^3}\right) * \left(\frac{(32.85\ \frac{ft}{s})^2}{2}\right) * \left(\frac{lbf*s^2}{32.2*lbm*ft}\right) * \left(\frac{1\ ft}{12\ inch}\right)^2 * \left(\frac{27.68\ "\ of\ Water}{PSI}\right) \quad \text{(Eqn.17)}$$

$$\Delta P_{major} = 0.16103\ Inches\ of\ Water$$

Taking our initial guess for our velocity of 32.85$\frac{ft}{s}$ and determining the resulting X (CFM) to be 387 $\frac{ft^3}{min}$ we can determine the associated pressure loss for the 6" Soffit vent cap, given the equation for "Product P" below.

ΔP_{Vent}= -1.000825E-09*x^3 + 2.492640125E-06*x^2 + 2.7180890E-04*x + 0.030254214 (Eqn. 18)

After solving we find the pressure drop for the vent cap to be ΔP_{Vent} = 0.4508. Assuming two 90° elbows (K=1.849) Eqn. 8 will determine the minor pressure loss for the elbows.

$$\Delta P_{Elbows} = (2 * 1.849) * \left(0.075\ \frac{lbm}{ft^3}\right) * \left(\frac{\left(32.85\frac{ft}{s}\right)^2}{2}\right) * \left(\frac{lbf*s^2}{32.2*lbm*ft}\right) * \left(\frac{1\ ft}{12\ inch}\right)^2 *$$

$$\left(\frac{27.68\ "\ of\ Water}{PSI}\right) = 0.8933 \quad \text{(Eqn. 19)}$$

$$\Delta P_{minor} = \Delta P_{Vent} + \Delta P_{Elbows} = 1.344 \text{ Inches of Water} \quad \text{(Eqn. 20)}$$

If we add the major pressure loss to the minor pressure loss, we arrive at the following total pressure loss:

$$\Delta P_{major} + \Delta P_{minor} = \Delta P_{Total} \quad \text{(Eqn. 20)}$$

$$0.16103 + 1.344 = 1.505 \text{ inches of Water}$$

Now that we have the total pressure loss we can refer to the "Fan A – High Speed" trend line and discover the resulting CFM.

$$1.505 \text{ inches of water} = -1.058E\text{-}07*x^3 + 3.535E\text{-}05*x^2 - 0.004645*x + 2.635 \quad \text{(Eqn. 21)}$$

After solving the trend line equation, we find the resulting X (CFM) is 305 $\frac{ft^3}{min}$ and a velocity of 25.94 $\frac{ft}{s}$.

Second Iteration

To get a more accurate volumetric flow rate, we would then complete the solving process again using the new velocity of 25.94$\frac{ft}{s}$.

$$R_e = \frac{25.94\ ft}{s} * 0.5\ ft * \frac{s}{1.68E{-}04\ ft^2} = 77{,}202 \quad \text{(Eqn. 22)}$$

Using the Reynold's Number, the relative roughness, and the Colebrook Equation, we again solve for the friction factor and get the following value:

$$f = 0.02107$$

$$\Delta P_{major} = 0.02107 * \left(\frac{15\ ft}{0.5\ ft}\right) * \left(0.075\ \frac{lbm}{ft^3}\right) * \left(\frac{(25.94\ \frac{ft}{s})^2}{2}\right) * \left(\frac{lbf*s^2}{32.2*lbm*ft}\right) * \left(\frac{1\ ft}{12\ inch}\right)^2 * \left(\frac{27.68\ "\ of\ Water}{PSI}\right) \quad \text{(Eqn. 23)}$$

$$\Delta P_{major} = 0.09521\ Inches\ of\ Water$$

Once again, taking our new velocity of 25.94 $\frac{ft}{s}$, we can determine the new volumetric flow rate to be 305 $\frac{ft^3}{min}$ and in turn, the ΔP_{Vent} = 0.3166

$$\Delta P_{Elbows} = (2 * 1.849) * \left(0.075\ \frac{lbm}{ft^3}\right) * \left(\frac{\left(25.94\ \frac{ft}{s}\right)^2}{2}\right) * \left(\frac{lbf*s^2}{32.2*lbm*ft}\right) * \left(\frac{1\ ft}{12\ inch}\right)^2 * \left(\frac{27.68\ "\ of\ Water}{PSI}\right) = 0.5570 \text{ inches of water}$$

$$\Delta P_{minor} = \Delta P_{Vent} + \Delta P_{Elbows} = 0.8736 \text{ inches of Water} \quad \text{(Eqn. 24)}$$

If we add the major pressure loss to the minor pressure loss, we arrive at the following total pressure loss:

$$\Delta P_{major} + \Delta P_{minor} = \Delta P_{Total} \quad \text{(Eqn.25)}$$

$$0.09521 + 0.8736 = 0.9688 \text{ Inches of Water}$$

After solving the trend line equation, we find the result of the second iteration to be 340.9 CFM and a velocity of 30.49 $\frac{ft}{s}$.

Third Through Sixth Iteration Table Data

To abbreviate the process, the 3rd, 4th, 5th, and 6th iterations take place and the information is given in Table 1.

Table 1: Solved Values For Iterative Solution

	Guess V $[\frac{ft}{s}]$	R_e	f	ΔP_{major} [inches of water]	ΔP_{Vent}	ΔP_{Elbow} [inches of water]	ΔP_{System} [inches of water]	CFM $[\frac{ft^3}{min}]$	Solved V $[\frac{ft}{s}]$
1st Iteration	32.85	97,767	0.02222	0.16103	0.4508	0.8933	1.505	305	25.94
2nd Iteration	25.94	77,202	0.02107	0.09521	0.3166	0.5570	0.9688	340.9	28.99
3rd Iteration	28.99	86,279	0.02074	0.1170	0.3729	0.6957	1.1856	327.7	27.87
4th Iteration	27.87	82,946	0.02085	0.1087	0.3518	0.6430	1.1035	332.9	28.31
5th Iteration	28.31	84,255	0.02081	0.1120	0.3601	0.6634	1.1355	330.9	28.14
6th Iteration	28.14	83,750	0.02082	0.1107	0.3569	0.6555	1.1231	331.7	28.21

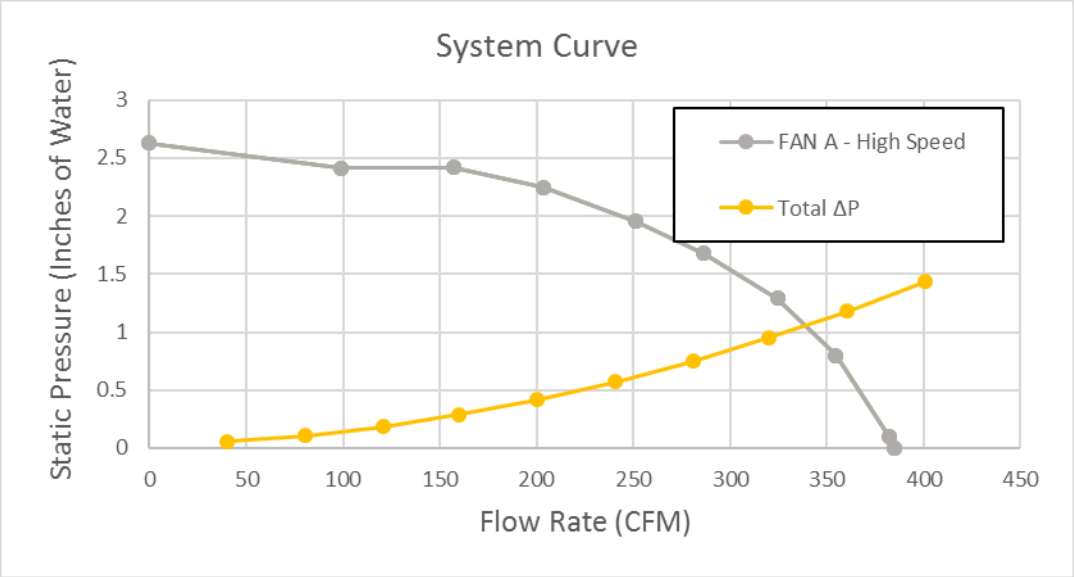

Figure 5: Total System Curve

Above in Figure 5, the "Fan A – High Speed" curve shown in gray represents the performance over the range of maximum resistance (CFM=0) to minimum resistance (CFM=358). Using the data solved in the previous iterative solution, a total system pressure drop curve was created and graphed in yellow. Therefore, for one given total pressure drop, there is only one possible flow rate for the system.

Entrance Length

Just as the Reynolds number is a way to gauge the turbulence for internal flow, calculating the entrance length allows us to determine how well the duct system is designed for ventilation. The entrance length is the distance from the entrance to the point within the duct where you have a fully developed velocity profile. When the airflow enters an elbow, if the flow is laminar the loss in performance will be greatly reduced. However, if the flow entering the elbow is turbulent, performance is greatly reduced because the airflow does not adhere to the duct walls very well. Therefore, unless it is absolutely necessary, installing any elbows or bends within the entrance length is not recommended (Bergstrom, 2016).

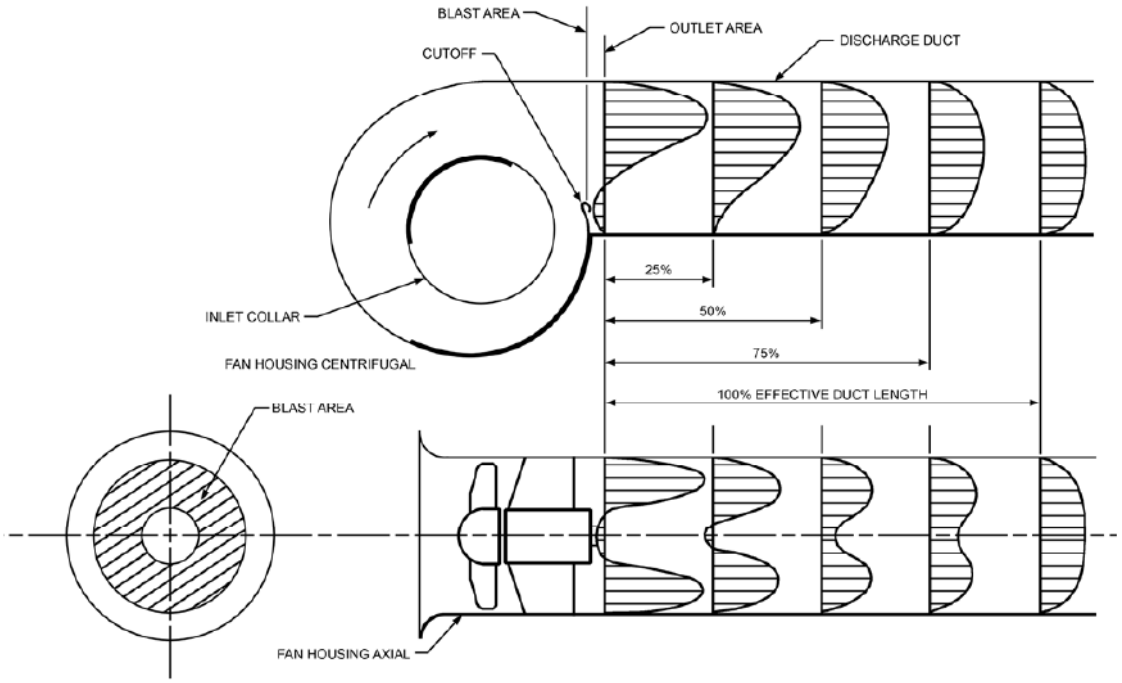

Figure 6: Establishment of Uniform Velocity Profile (ASHRAE, 2013)

In Figure 6 above, the velocity profile shows there is a transition length for different fans, specifically centrifugal and vane axial. In either case, the equations used to determine the fully developed flow length, L_e, is given by the following equations 26 and 27. The effects of entrance length due to airflow are shown in Figures 7 and 8.

Fluid velocities greater than 2500 $\frac{ft}{min}$:

$$L_e = \frac{V_0\sqrt{A_0}}{10600} \quad \text{(Eqn. 26)}$$

L_e = Effective duct length (ft)

A_0 = Duct Area (in^2)

V_0 = Duct Velocity ($\frac{ft}{min}$)

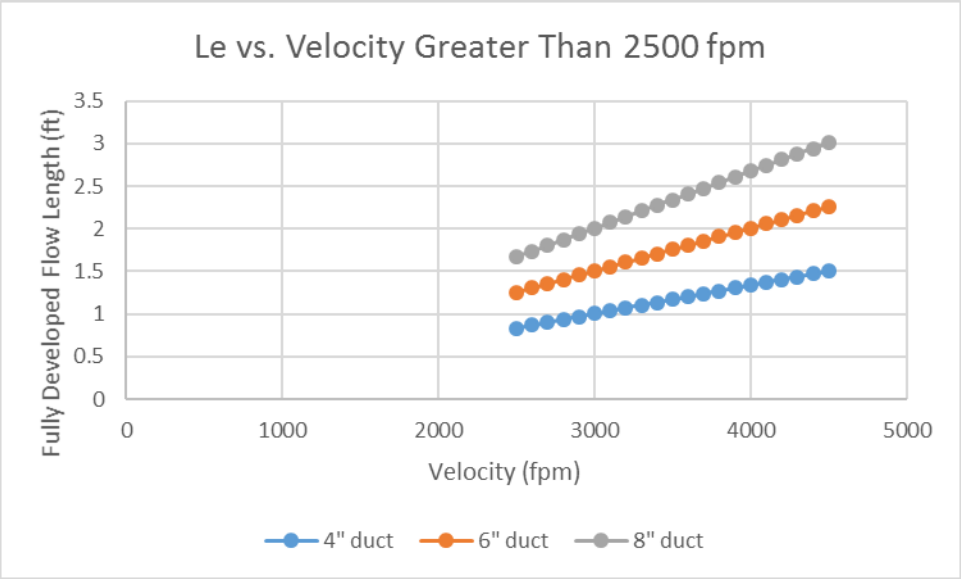

Figure 7: Entrance Length for Velocities Greater Than 2500 fpm

Fluid velocities less than 2500 $\frac{ft}{min}$:

$$L_e = \frac{\sqrt{A_0}}{4.3} \quad \text{(Eqn. 27)}$$

L_e = Effective Duct Length (ft)

A_0 = Duct Area (in^2)

V_0 = Duct Velocity ($\frac{ft}{min}$)

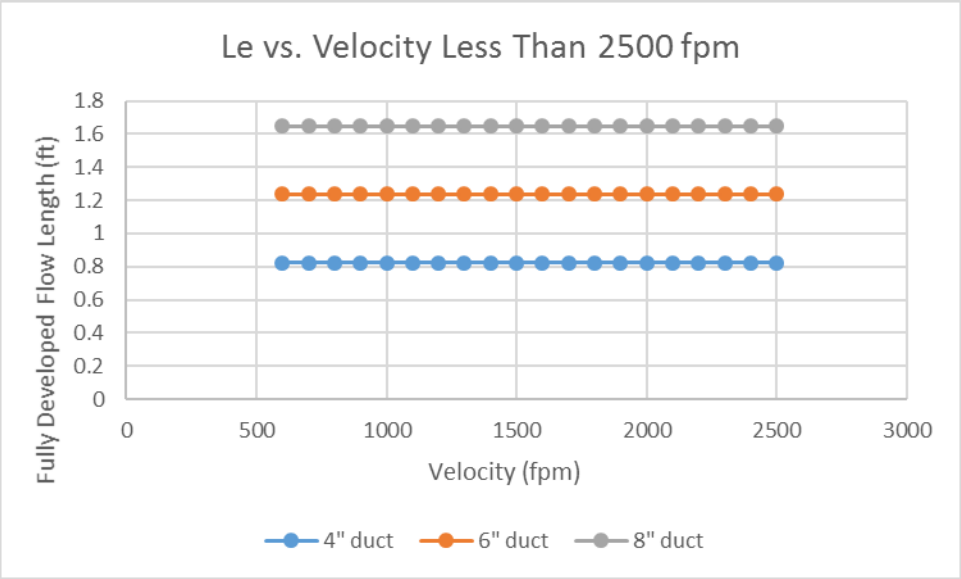

Figure 8: Entrance Length for Velocities Less Than 2500 fpm

Capture Efficiency

Anyone who has burned something on the stove can agree that a range hood removes unwanted air from the kitchen. In fact, if they are not exhausted from the

building, those airborne particles can deteriorate the structure, cause health problems to the occupants, or even force costly repairs to AC units due to formicary corrosion (Schofield, 2016). Therefore, it is important to discuss a range hood's ability to remove contaminants, capture efficiency. The equation given below is capture efficiency, ε_c (Li, 1996)

$$\varepsilon_c = \frac{q_f * C^C}{S_p^0 + c^T * (q_f + q_e)} \quad \text{(Eqn.28)}$$

ε_c = Capture efficiency of kitchen range hoods

q_f = Airflow rate through exhaust duct ($\frac{ft^3}{s}$)

c^C = Concentration of contaminant in the exhaust ($\frac{lbm}{ft^3}$)

S_p^0 = Release rate of contaminant source generated during cooking ($\frac{lbm}{ft^3}$)

c^T = Concentration of contaminant in the rest of the room ($\frac{lbm}{ft^3}$)

q_f = Airflow rate through the exhaust duct ($\frac{ft^3}{s}$)

q_e = Escaped flow rate at front canopy level ($\frac{ft^3}{s}$)

As Li and Delsante discussed, it is oversimplifying when capture efficiency is defined as the difference between produced and escaped contaminants over the produced contaminants. It is correct to consider the escaped contaminants may return to the

cooking area and exhaust at a later time. Therefore, Eqn. 28 is a better suited model for the capture efficiency of kitchen range hoods.

Table 2: Performance of U.S. Residential Range Hoods (Delp, 2012)

Hood Type	Hood Code	Capture Efficiency (CE)						
Single Grease Screen	L1	CFM	97	148	200			
		CE	66	81	87			
	B1	CFM	86	119	148	179	210	
		CE	52	65	77	86	96	
Microwave	M1	CFM	147	173	280	348		
		CE	77	79	99	90		
Flat Profile	A1	CFM	86	141	198	254	309	
		CE	51	61	68	81	95	
	E1	CFM	68	120	138	176	190	222
		CE	49	68	74	78	79	81
	E2	CFM	54	80	115	178	202	229
		CE	37	50	64	77	79	85
Open Capture	P1	CFM	183	210	232	252	262	
		CE	83	88	92	96	97	

The data provided in Table 2 by the Lawrence Berkeley National Laboratory used a carbon dioxide tracking system (Delp 2012). Three configurations were tested: back burners, front burners, and oven use. The above data is for back burner configuration because front burner and oven use showed no capture efficiency correlation to increase in volumetric flow rate (CFM). Therefore, for the purposes of this thesis, all capture efficiency values will assume the particle source is being placed on the back burner. Figure 9 shows a data plot with the associated averaged trend line to be used in the EES program.

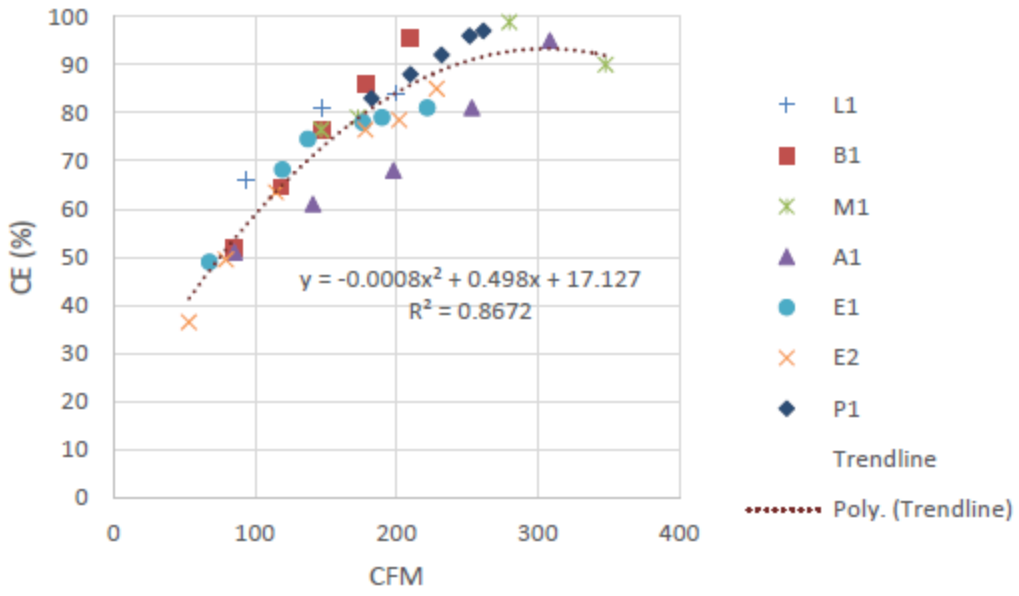

Figure 9: Capture Efficiency Airflow Rates (Delp, 2012)

The trend line to be used in the EES program is shown below:

$$CE = -0.0008X^2 + 0.498X + 17.127 \quad \text{(Eqn.29)}$$

CE = Capture Efficiency

X = Volumetric Flow Rate (CFM)

Once again, for the purpose of modeling capture efficiency as a function of CFM for cabinet range hoods with only back burner configurations, the above equation will be used. It is important to note that the Lawrence Berkeley National Laboratory did not conduct the capture efficiency experiments with ductwork attached to the fan exit. However, since the various theory has been covered to determine system performance due to vent cap, ductwork, and other associated restrictions, we can now determine the actual volumetric flow rate and in turn the expected capture efficiency.

Capturing Gases

Equation 12 describes the mathematical idea of capture efficiency, but the applicable design factors are as follows. First, the range hood is shaped to catch rising gases so the fan may move the gases through the ducting. The shape and cross sectional area directly affects the hoods ability to catch rising gases. Note the range hood in Figure 10, due to a smaller cavity, the range hood's ability to catch the rising gases is reduced. To visualize the capturing process, we can imagine an inverted cone of gases rising from the stove. Once again, the capture of these gases is directly related to the shape of the cavity, and its cross-sectional area.

Figure 10: Range Hood Lacking Lip to Trap Gases

Figure 11: Fan With Increased Cavity Area

With a different fan, as shown in Figure 11, the larger cavity traps the gases in the immediate area of the fan. Reducing the release rate of the airborne contaminants will help increase the capture efficiency. To describe the increased trapping of the gases, this reduces the escaped flow rate Q_e as seen in Equation 12. Other factors effecting capture efficiency not applied in the equation is the burner placement and contaminant types.

Non Standard Air Density Correction

Due to non-standard atmospheric conditions, the density of air may be different from experiment to experiment. Therefore, the AMCA210 Standard has distributed equations to help determine nonstandard pressures (ANSI/AMCA 210-07, 2007). The following equations are built in to the Figure 12 testing program at the Riverside Energy Efficiency Laboratory. Beginning with Eqn.13 defines atmospheric density in terms of ambient barometric pressure, dry bulb temperature, and the specific gas constant.

$$P = \frac{70.73*(P_b - 0.378*P_p)}{R*(t_d + 459.67)} \quad \text{(Eqn. 30)}$$

P = Atmospheric Air Density $[\frac{lbm}{ft^3}]$

P_b = Ambient Barometric Pressure [in. Hg]

P_p = Partial Vapor Pressure [in. Hg]

T_d = Dry Bulb Temperature [°F]

R = Gas Constant $[\frac{ft*lbf}{lbm*°R}]$

Eqn.14 calculates the partial vapor pressure in inches of mercury (in. Hg), in the terms of saturated vapor pressure, ambient barometric pressure, and the dry bulb temperature.

$$P_p = P_e - P_b*(\frac{T_d - T_w}{2700}) \quad \text{(Eqn.31)}$$

P_e = Saturated Vapor Pressure at T_w [in. Hg]

P_b = Ambient Barometric Pressure [in. Hg]

T_d = Dry Bulb Temperature [°F]

T_w = Wet Bulb Temperature [°F]

Eqn.15 determines the saturated vapor pressure in inches of mercury (in. Hg).

$$P_e = (2.96E\text{-}04) * T_w^2 - (1.59E\text{-}05) * T_w + 0.41 \qquad \text{(Eqn.32)}$$

T_w = Wet Bulb Temperature [°F]

To show the above calculations using Fan A – High Speed data, the following measurements are given:

P_b = 29.82 [in. Hg]

T_d = 73.3 [°F]

T_w = 63.7 [°F]

R = 53.35 $[\frac{ft*lbf}{lbm*°R}]$

We can now use the given information from the lab test data (Fan A – High Speed) to determine the corrected atmospheric density.

$$P_e = (2.96E\text{-}04) * 63.7^2 - (1.59E\text{-}05) * 63.7 + 0.41 = 1.6100 \text{ [in. Hg]} \qquad \text{(Eqn. 33)}$$

$$P_p = 1.6100 - 29.82*(\frac{73.3-63.7}{2700}) = 1.0549 \text{ [in. Hg]} \qquad \text{(Eqn. 34)}$$

$$P = \frac{70.73*(29.82-0.378*1.0549)}{53.35*(73.3+459.67)} = 0.073 \frac{lbm}{ft^3} \qquad \text{(Eqn. 35)}$$

The nonstandard temperatures and pressures yielded a value different of 0.075 $\frac{lbm}{ft^3}$. The air density value recorded by the experimental data was 0.073 $\frac{lbm}{ft^3}$ as well, which confirms the validity of the manually completed calculations.

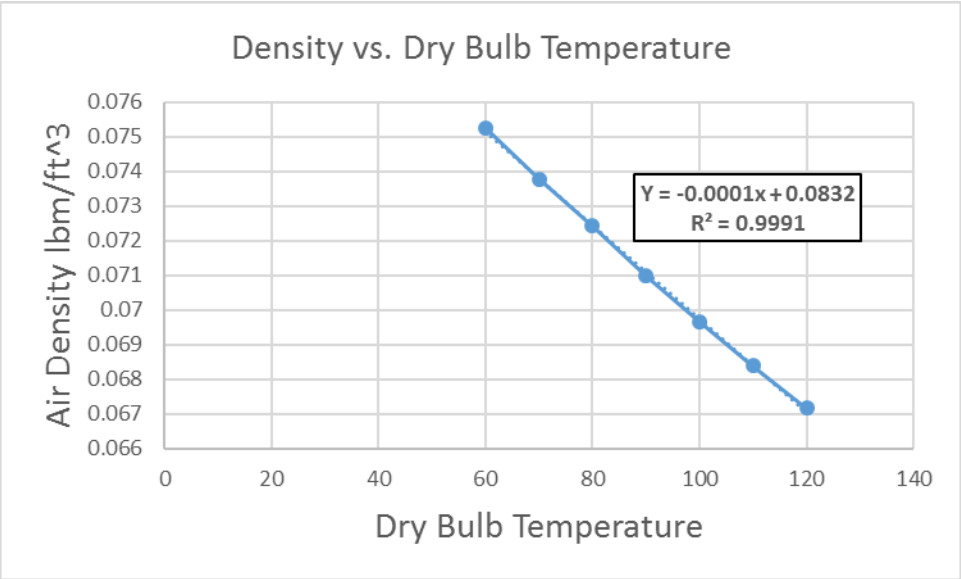

Figure 12: Holding Humidity Ratio Constant (ω = 0.009)

Using the above trend line estimation in Figure 12, an air density of 0.075 $\frac{lbm}{ft^3}$ is calculated instead of 0.073 $\frac{lbm}{ft^3}$ when using each individual equation. As suspected, using the equations would create a higher degree of accuracy.

3. VENT CAP PERFORMANCE

To reiterate the purpose of a kitchen range hood, we are tasked with capturing the unwanted gases, producing a pressure gradient with the fan, and ducting those gases out of the building. The duct system not only includes pipe to direct the exhaust gases, but a vent cap to limit outside air entering the duct system as well. These necessary fixtures are in most cases, the largest factor of system pressure drop (Chen, 2015). Figure 13 depicts the three main types of vent caps are wall mounted, roof jack, and soffit.

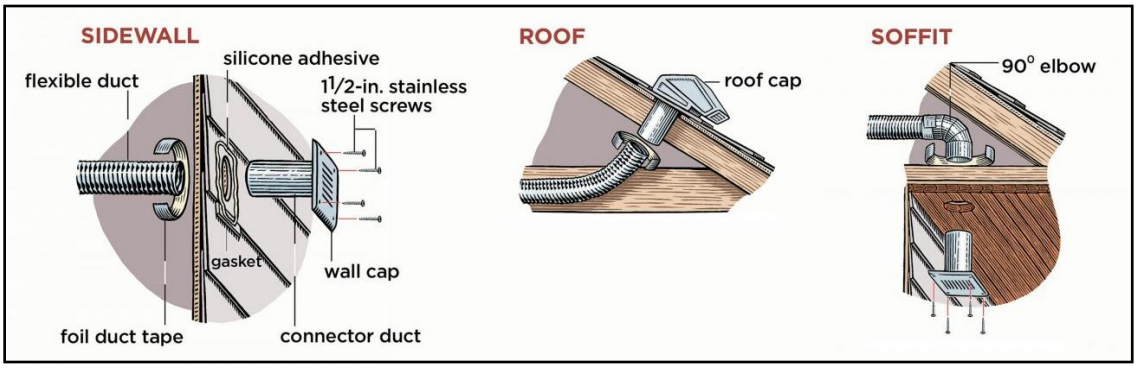

Figure 13: Vent Cap Orientation for Soffit, Wall-Mounted, and Roof (Truini, 2016)

Although the various types of vent caps all reduce the infiltration of outside air, all three vary in pressure loss performance. With the increase in pressure loss, you encounter the following adverse effects: the need for a larger fan, noisier operation, higher purchase price, and higher operating price. Therefore, given all available construction options, the smallest pressure loss will be the most beneficial.

A previous student at the Riverside Energy Efficiency Laboratory, Daniel Escatel, performed the vent cap performance experiments using the Figure 15 chamber (Escatel 2011). It is important to note that for bathroom fans 4" duct is a common diameter, and for range hoods 6" is a common diameter. The flow rate data for the vent caps stop at 200 CFM and 400 CFM respectively. For the majority of bathroom fans and range hoods, this is adequate data to model the system. However, there are times when a fan will exceed these limitations, and the trend line beyond the experimental data is considered unreliable. Therefore, in the EES program there will be a notation of "TRENDLINE IS UNRELIABLE AFTER 200 OR 400 CFM".

Other problems encountered while creating the trend lines were the lack of significant digits. The program used, Microsoft Excel, rounded the trend lines to two significant digits per each term in the trend line equation. The appropriate solution was to manually increase the significant digits (15) and in turn increase accuracy of the trend line.

The data collected by Daniel Escatel is located in Appendix B, however the vent cap description can be seen below in Table 3:

Table 3: Vent Cap Description (Escatel, 2011)

Product	Size	Type	Material	Damper	Spring-Loaded Damper	Grill
A	4”	Soffit	Plastic	Y		
B	4”	Soffit	Plastic	Y		
C	4”	Soffit	Plastic	Y		
E	4”	Wall-Mount	Steel			Y
F	4”	Wall-Mount	Aluminum			Y
G	4”	Wall-Mount	Galvanized	Y		
H	4”	Wall-Mount	Plastic			
I	4”	Wall-Mount	Plastic	Y		Y
J	4”	Wall-Mount	Plastic			Y
K	4”	Wall-Mount	Aluminum			Y
L	4”	Roof Jack	Plastic	Y		Y
M	4”	Roof Jack	Aluminum	Y		Y
N	4”	Roof Jack	Aluminum	Y		
O	4”	Roof Jack	Aluminum	Y		Y
P	6”	Soffit	Plastic	Y		Y
Q	6”	Wall-Mount	Copper	Y	Y	
R	6”	Wall-Mount	Plastic			
S	6”	Wall-Mount	Aluminum	Y	Y	

Table 3 Continued

Product	Size	Type	Material	Damper	Spring-Loaded Damper	Grill
T	6”	Wall-Mount	Aluminum	Y	Y	Y
U	6”	Wall-Mount	Plastic	Y	Y	Y
V	6”	Wall-Mount	Aluminum	Y		
W	6”	Roof Jack	Plastic	Y		Y
X	6”	Roof Jack	Plastic	Y		Y

Vent Cap Performance Trend Lines

When creating trend lines that best fit experimental data, a larger R^2 value would be assumed to give a better fit value. However, with the trend lines below in Table 4, graphs were produced to show how different degrees of polynomials perform in Figures 14 and 15.

Table 4: Trend Line Equations

3rd Degree Polynomial	Y =-0.000000001000825x^3+ 0.000002492640125x^2 + 0.000271808902902x + 0.030254214829606	R^2 = 0.999386622094397
6th Degree Polynomial	Y = 0.000000000000002x^6 - 0.000000000002979x^5 + 0.000000001397074x^4 - 0.000000316936144x^3 + 0.000038109450114x^2 - 0.001586938396715x + 0.064645582575619	R^2 = 0.999832063495252

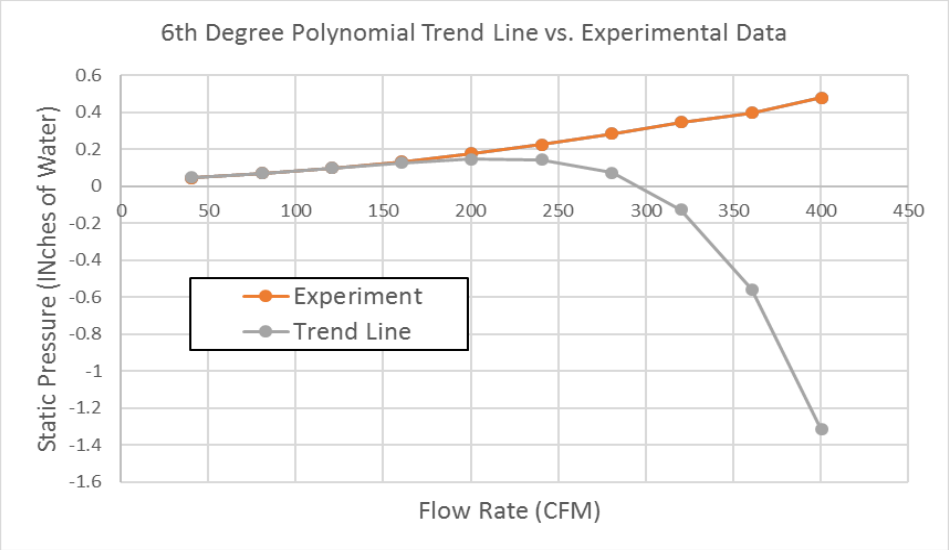

Figure 14: Experimental and 6th Degree Trend Line Comparison

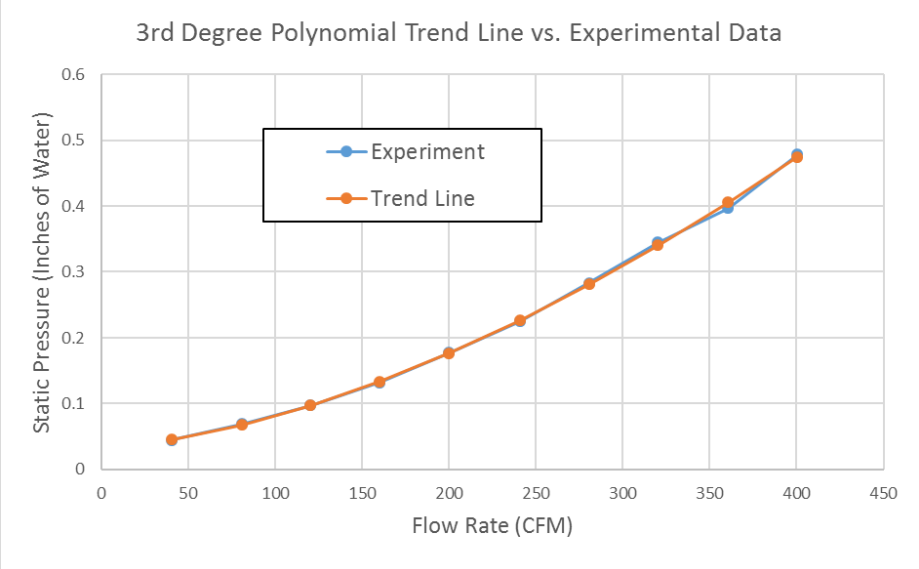

Figure 15: Experimental and 3rd Degree Trend Line Comparison

By visually inspecting Figures 14 and 15 we can see that a higher degree polynomial may not produce the best results. The numerical data shown in Table 5 describes the pressure loss observed in the experiment, the pressure loss using the trend line, and the percent difference between the two.

Table 5: Effects of Increasing Polynomial

Product P - 3rd Degree Polynomial			
CFM	dP(Exp) [inWC]	dP(Eqn) [inWC]	%Diff
400.5	0.478	0.474	0.702828
360.7	0.397	0.405	2.174295
320.3	0.345	0.340	1.405098
280.7	0.283	0.280	0.771379
240.7	0.225	0.226	0.505164
200.1	0.177	0.176	0.322093
160.2	0.132	0.133	1.253368
120.5	0.097	0.097	0.463723
80.7	0.069	0.067	1.599282
40.3	0.045	0.045	0.424179

Product P - 6th Degree Polynomial			
CFM	dP(Exp) [inWC]	dP(Eqn) [inWC]	%Diff
400.5	0.478	-1.31	375.4051
360.7	0.397	-0.558	240.6819
320.3	0.345	-0.127	136.9115
280.7	0.283	0.072	74.35265
240.7	0.225	0.142	36.72158
200.1	0.177	0.146	17.39041
160.2	0.132	0.125	5.251778
120.5	0.097	0.097	0.239755
80.7	0.069	0.067	1.726924
40.3	0.045	0.045	0.424179

4. USE OF FLEXIBLE DUCTS

The Lawrence Berkeley National Laboratory has conducted a study on the use of pressure loss using flexible ductwork (Abushakra, 2004). If the flexible duct is stretched fully, the interior walls are relatively smooth. However, to stretch the duct and remain connected to the various ventilation fittings remains a problem. Therefore, the use of flexible duct without some compression is not feasible. To discuss compression, first we must define it as the change in length divided by the fully stretched length. See Eqn. 36 below:

$$r_c = \frac{\Delta X}{L} \qquad \text{(Eqn.36)}$$

r_c = Compression Ratio

ΔX = Change in Length

L = Fully Stretched Length

The Lawrence Berkeley National Laboratory results show compression ratio ranges from fully stretched to fully compressed, with compression ratios of 0 and 0.3 respectively. Due to the buckling of the flexible duct, compression was not tested beyond 0.3. The effects of compression are prevalent in two forms, increased friction factor, and reduced cross sectional area. As shown in Figure 16, a less than fully stretched duct will increase interior roughness and reduce performance.

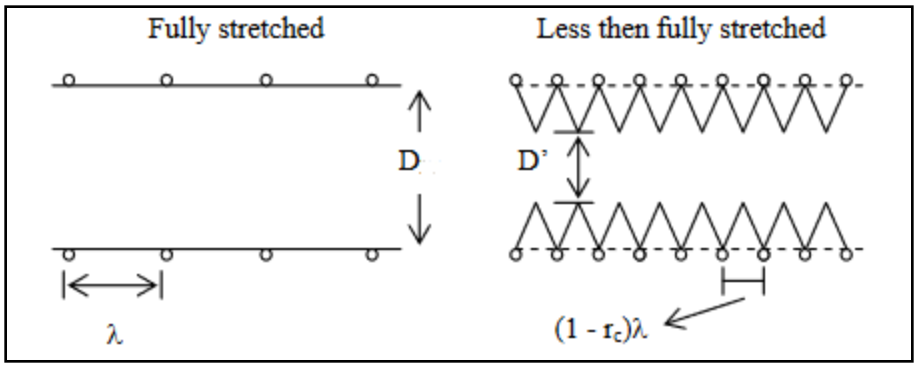

Figure 16: Reduced Performance of Compression (Abushakra, 2004)

To better describe the effects of compressed flexible duct, the following equation is used to determine expected pressure loss using the pressure drop correction factor (PDCF), which is a function of the compression ratio, and the pressure drop when the duct is fully stretched (ΔP_{FS}).

$$\text{PDCF} = \frac{\Delta P}{\Delta P_{FS}} \qquad \text{(Eqn.37)}$$

PDCF = Pressure Drop Correction Factor

ΔP = Pressure Drop with Compression

ΔP_{FS} = Pressure Drop When Fully Stretched

Table 6: Pressure Drop Correction Factor of Common Duct Sizes (ASHRAE, 2005)

Diameter in (mm)	**Pressure Drop Correction Factor PDCF**
6 (150)	$1 + 25.35\ r_c$
8 (200)	$1 + 21.61\ r_c$
10 (250)	$1 + 16.18\ r_c$
ASHRAE-all sizes	$\mathbf{1 + 9.86\ r_c}$

If we take the data from Table 6, we can determine that for a 6" duct with an average compression ratio of 0.15, the resulting pressure loss is almost four times that of the pressure loss when fully stretched. A large reduction in performance can be expected if you allow moderate compression of the flexible duct.

To reduce the material cost and reduce installation time, some construction companies may use flexible duct even with the reduction in performance. Acceptable for bathroom fan ducting, but for range hood duct system the reduced performance and exhaustion of grease may become a fire hazard. Therefore, most building codes restrict the use of flexible duct in range hoods for violation of building code.

5. FAN TESTING OPERATION

Several different means of fan performance evaluation are needed to issue a certification. Specifically, volumetric airflow, loudness, power consumption, and capture efficiency best describe the performance of a fan. The Home Ventilating Institute (HVI) has set a standard by which the Riverside Energy Efficiency Laboratory must evaluate the above criteria. Although these are all necessary for the fan certification, only airflow is directly related to the main purpose of this thesis, capture efficiency.

Range Hood Ratings

Riverside Energy Efficiency Laboratory (REEL) conducts various types of tests for the Home Ventilation Institute (HVI). Specifically, HVI contracts the lab to conduct airflow tests on inline fans, bathroom fans, and range hoods. Many different testing chambers can be used to create fan performance curves for the aforementioned fans, but for the purposes of this thesis, we will strictly deal with the testing chamber known as "Figure 12." "Figure 12" references strict construction standards set forth by the Air Movement and Control Association International (AMCA) and the American Society of Heating, Refrigeration and Air Conditioning Engineers (ASHRAE).

By varying the assist blower on the testing chamber (will be discussed later), the system curve changes and produces a different operating point. The pump curve is a trend line that closely matches the various operating points produced by the airflow testing chamber. So, in effect, one pump curve allows us to estimate the volumetric flow rate for any ductwork system.

Airflow rating points are usually 0.1” of water column (WC) for range hoods. It is important to note that the rating point is a general area of where the manufacturer expects the system to be operating at. A system analysis, like the one this thesis is based on, will show the actual pressure loss operating point.

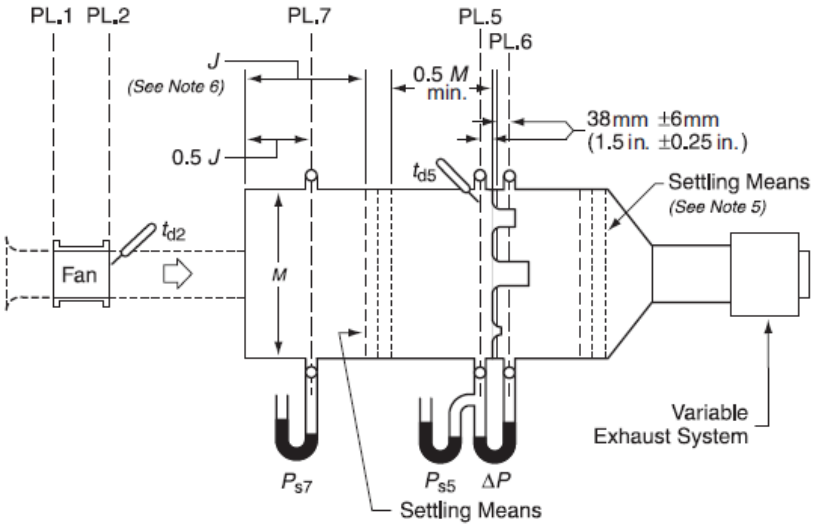

Notes:

1. Dotted lines on fan inlet indicate an inlet bell and one equivalent duct diameter which may be used for inlet duct simulation. The duct friction shall not be considered.

2. Dotted lines on fan outlet indicate a uniform duct 2 to 3 equivalent diameters long and of an area within ±1% of the fan outlet area and a shape to fit the fan outlet. This may be used to simulate an outlet duct. The outlet duct friction shall not be considered.

3. The fan may be tested without outlet duct in which case it shall be mounted on the end of the chamber.

4. Variable exhaust system may be an auxiliary fan or a throttling device.

5. The distance from the exit face of the largest nozzle to the downstream settling means shall be a minimum of 2.5 throat diameters of the largest nozzle.

6. Dimension *J* shall be at least 1.0 times the fan equivalent discharge diameter for fans with axis of rotation perpendicular to the discharge flow and at least 2.0 tmes the fan equivalent discharge diameter for fans with axis of rotation parallel to the discharge flow. **Warning!** A small dimension *J* may make it difficult to meet the criteria given in Annex A. By making dimension *J* at least 0.35*M* this condition is improved, as well as meeting the criteria given in section 5.3.1 for any fan.

7. Temperature t_{d2} may be considered equal to t_{d5}.

8. For the purpose of calculating the density at Plane 5 only, P_{s5} may be considered equal to P_{s7}.

Figure 17: Testing Setup Described As "Figure 12"(ANSI/AMCA 210-07, 2007)

	Installation Type			
Setup Figure	**A**	**B**	**C**	**D**
7A, 7B, 8A, 8B, 9A, 9B, 9C, 10A, 10B, 10C		NS		NS (a)
11,12,13,14, or 15	Y (b)	Y (c)	Y (a,d)	Y (a,c)
16			Y	Y (c)

NS = Not suitable for fans with significant swirl
Y = Suitable for all fan types

Notes:

(a) A simulated inlet duct may be used
(b) An auxiliary inlet bell or outlet duct may not be used
(c) An outlet duct or a short outlet duct, per Section 5.2.3, may be used
(d) No outlet duct may be used

Figure 18: Selection Guide (ANSI/AMCA 210-07,2007)

The "Setup Figure 12" at the Riverside Laboratory is a ducted inlet and free outlet (Type C) and can be shown in Figure 18 to be suitable for all fan types. Note that a simulated inlet duct, also called a venturi inlet, may be used to reduce the effects of a vena contracta. A vena contracta, also known as a contracted vein, is the entering airstream is contracts due to an orfice. This contraction reduces the airflow significantly, and with the addition of a venture inlet, the setup can return 15% airflow for vane axial fans and 12% for propeller fans (Bleier, 1998). Obviously, a venturi inlet will not be present for actual residential or commercial installation, but for the sake of fan performance curve consistency, a standard must be set.

The standard adhered to at the Riverside Laboratory is the HVI standard 916 which complies with the ANSI/AMCA 210 standard mentioned previously. The "Green Chamber" shown in Figure 19 below is constructed to the standards shown previously in Figure 17.

Figure 19: Green Chamber Constructed to "Figure 12" Specifications

Referring to Figure 17, you can see the interior of the Green Chamber consists of multiple nozzles that are used in combination to produce different airflow and pressure drop specifications. The nozzle arrangement is used to produce variances in pressure from maximum airflow to shutoff, which is zero pressure and maximum pressure respectively.

6. ANALYSIS OF REAL FANS

Like the vent cap performance data, the fan performance curves in Appendix A were produced by Figure 12 testing chamber in the Riverside Energy Efficiency Laboratory. The fan curves are made of 10 points and show the progression through different system curves. Fan Laws are used to estimate the values you may expect during the progression of these fan performance curves and are used for a reference.

Similar to the vent cap performance, the trend lines were constructed by using a spreadsheet calculator. As stated before, the spreadsheet calculator defaults the trend line with two significant digits per term. Increasing the significant digits to 15 then increased the accuracy of the EES program. Increasing the R^2 value may on average and produce a trend line closer to the experimental data.

Fan Laws

To understand how a fan performs, first we must discuss fundamentals of fan construction and the the fan laws. The 1st Fan Law is given below:

$$CFM_{new} = \frac{RPM_{new}}{RPM_{old}} * CFM_{old} \quad \text{(Eqn.38)}$$

In ventilation systems, the fan performs the work and with each revolution it discharges the same amount of air (New York Blower Company, 2016). If the fan increases RPM, then the air discharged will increase proportional to that RPM. To confirm the 1st fundamental fan law, we will see if the values match with the experimental data given the data collected for the Fan A – High Speed:

Point 2:

CFM_{old} = 382

RPM_{old} = 1659

Point 1:

RPM_{new} = 1589

Using the 1st Fan Law, we arrive at an expected volumetric flow rate below:

$$CFM_{new} = \frac{1589\ RPM}{1659\ RPM} * 382\text{CFM} = 366\text{CFM}$$

Table 7: Experimental Data and 1st Fan Law % Difference

	Experimental Values	Fan Law Calculation
CFM_{old}	382 CFM	382 CFM
CFM_{new}	384.8 CFM	366 CFM
% Difference from Exp.	N/A	4.88 %

From Table 7, you can see the difference between the experimental data and the fan law calculation is within 5 %. While this may not get a precise value for volumetric flow rate estimation, it will give a rough estimate for the fan. Figure 20 shows the effects of Flow rate and RPM.

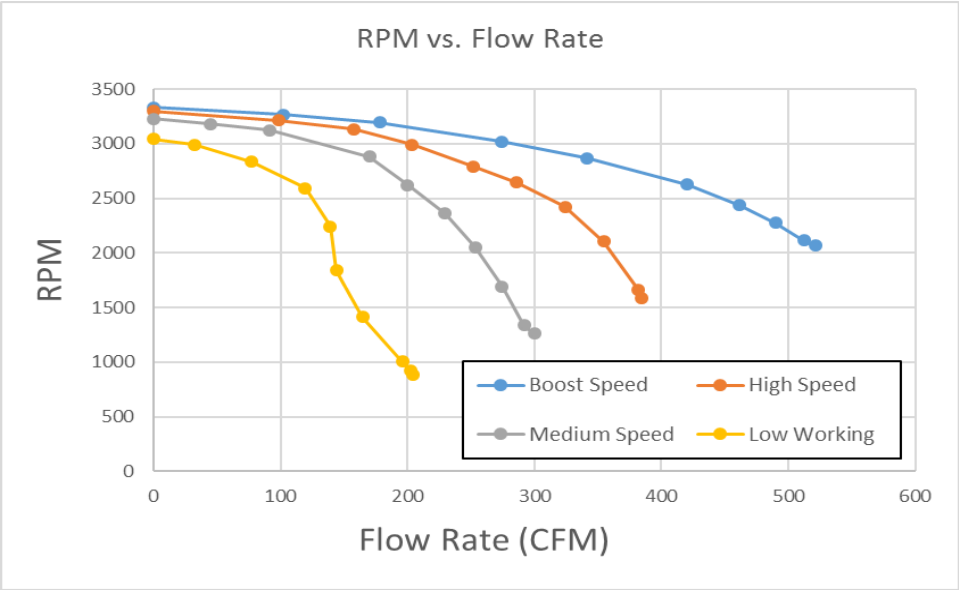

Figure 20: RPM and Flow Rate Comparison

Next, the 2nd Fan Law given below:

$$SP_{new} = (\frac{RPM_{new}}{RPM_{old}})^2 * SP_{old} \quad \text{(Eqn.39)}$$

The static pressure (SP) varies as the square of the change in CFM (New York Blower Company, 2016). To confirm the 2nd fundamental fan law, we will see if the values match the experimental data collected for Fan A – High Speed:

Point 4:

SP_{old} = 1.293

RPM_{old} = 2421

Point 5:

RPM_{new} = 2646

Using the 2nd Fan Law, we arrive at an expected static pressure drop below:

$$SP_{new} = (\frac{2646\ RPM}{2421\ RPM})^2 * 1.293\ SP = 1.54\ SP$$

Table 8: Experimental Data and 2nd Fan Law % Difference

	Experimental Values	Fan Law Calculation
SP_{old}	1.293	1.293
SP_{new}	1.680	1.54
% Difference from Exp.	N/A	8.33%

This time, Table 8 shows the data with slightly larger errors from the actual experimental data. Again, the 2nd Fan Law may provide an estimate for the expected static pressure, therefore using actual experimental data is recommended.

The 3rd and final Fan Law shows as the fan speed changes, the brake horsepower (BHP) will vary proportionally as the cube of the change in RPM (New York Blower Company, 2016). The 3rd Fan Law is given below:

$$BHP_{new} = (\frac{RPM_{new}}{RPM_{old}})^3 * BHP_{old} \quad \text{(Eqn.40)}$$

Due to the reports produced by the Riverside Energy Efficiency Laboratory, results of the 3rd Fan Law are unable to be verified. However, it has been shown that the Fan Laws can have significant differences from than actual experimental test data and should be used only for general reference.

Fan Performance Trend Lines

Table 9 shows the comparison between a 3rd degree and 6th degree polynomial trend line. Note, the calculation was manually solved and the volumetric flow rate resides in the larger CFM range where the trend line has a larger error difference. Much like increasing the terms in a Taylor series expansion, it was proposed that an increase in R^2 value by raising the degree of the trend line polynomial would yield results closer to that of the experimental data. However, there seems to be an inherent error within the spreadsheet calculator and graphing the trend line equation next to the experimental data will provide a better indication of trend line accuracy. To reiterate the problem and the solution, the spreadsheet calculator produced incorrect R^2 values and the best way to determine trend line accuracy was to graph the trend line and the experimental data together.

Table 9: Effects of Increasing Trend Line Polynomial

Fan A - High Speed 3rd Degree Polynomial			
CFM	dP(Exp) [inWC]	dP(Eqn) [inWC]	%Diff
384.8	0.002	0.052	2513.767
382	0.101	0.120	18.93836
354.7	0.8	0.713	10.86598
324.4	1.293	1.23	4.360073
286.3	1.68	1.72	2.41082
251.5	1.957	2.02	3.240798
203.5	2.249	2.26	0.602623
157.3	2.42	2.36	2.177106
98.9	2.414	2.41	0.189294
0	2.63	2.63	0.172614

Fan A - High Speed 6th Degree Polynomial			
CFM	dP(Exp) [inWC]	dP(Eqn) [inWC]	%Diff
384.8	0.002	-0.857	42996.33
382	0.101	-0.727	820.6449
354.7	0.8	0.273	65.82835
324.4	1.293	0.980	24.20412
286.3	1.68	1.53	8.472134
251.5	1.957	1.88	3.581935
203.5	2.249	2.23	0.78366
157.3	2.42	2.41	0.181723
98.9	2.414	2.41	0.008254
0	2.63	2.62	4.68E-05

To visually explain the difference, in Figure 21 below, the spreadsheet calculator shows the trend line following the experimental data closely. The 3rd and 6th degree trend line polynomials are given below in Table 10.

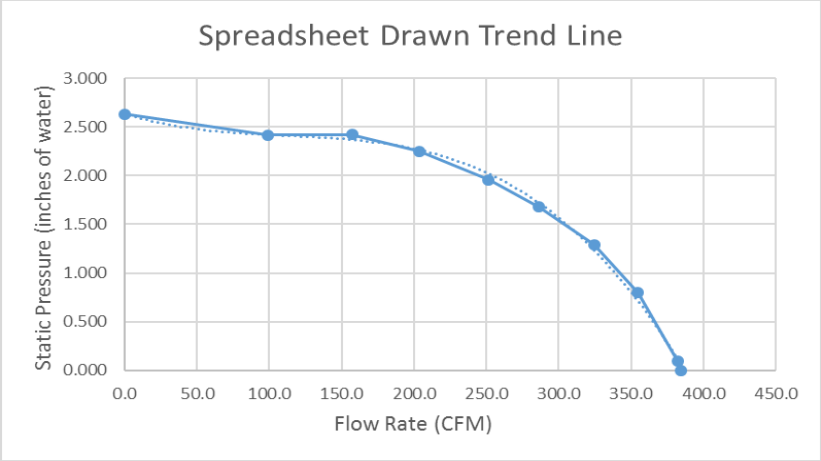

Figure 21: Excel Drawn 6th Degree Trend Line

Table 10: Trend Line Equations

6th Degree Polynomial	$Y = -0.000000000000002x^6 - 0.000000000002659x^5 + 0.000000003680994x^4 - 0.000001492128672x^3 + 0.000238520430376x^2 - 0.014468409721303x + 2.629998767980970$	0.999992880996089
3rd Degree Polynomial	$Y = -0.000000106096694x^3 + 0.00003548496125x^2 - 0.004655431621344x + 2.63453975814541$	0.997366634402583

However, after encountering problems with the EES program, it was prudent to graph the trend line using different equations. Again, the equations in Table 10 are formatted by the same spreadsheet calculator. Below in Figures 22 and 23, shows the difference in experimental values and the trend line values.

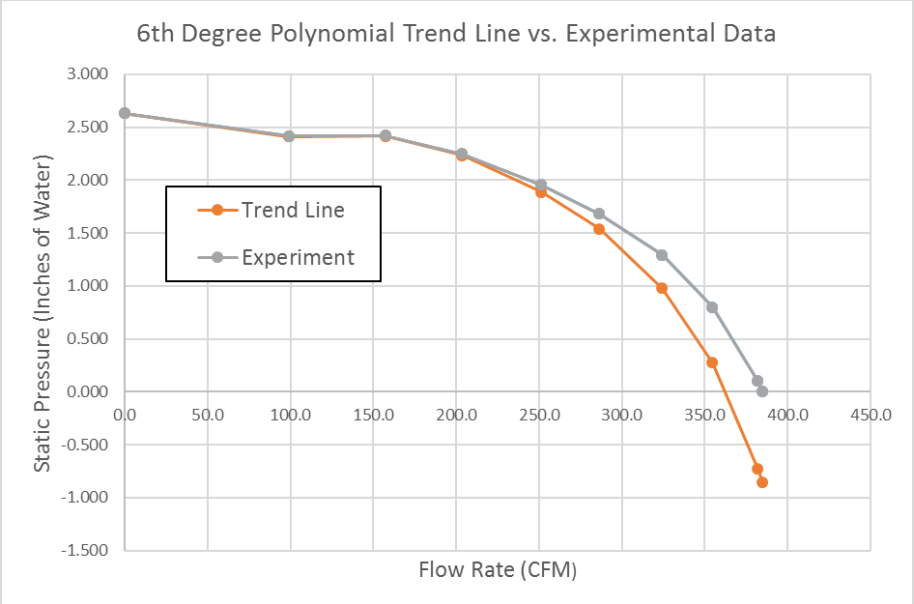

Figure 22: Experimental and 6th Degree Trend Line Comparison

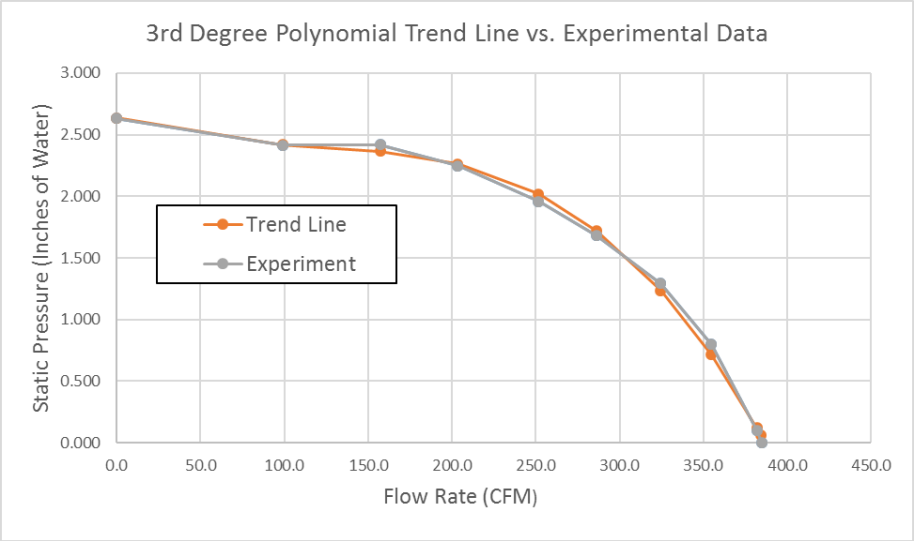

Figure 23: Experimental and 3rd Degree Trend Line Comparison

Thus, for each individual trend line, each trend line must be tested to see how closely it performs to the actual experimental test data.

7. USE OF EES PROGRAM

It is very important to adequately design the range hood, ductwork, vent caps, and the resulting system. Failure to do so will produce an unwanted drop in performance that may severely reduce the effects of air ventilation within the kitchen area. Exhaustion of heat and airborne particles being the main reasons for installing a kitchen range hood, it is therefore appropriate to use the EES design program to determine the expected performance.

Program Operation

An important practice in EES programs is the use of detailed comments, which are highlighted with quotation marks and are displayed with blue text. These comments describe the mathematical equations that are used in the EES program. It is important to note, that comments are not recognized by the EES program and will not participate in the operation of the program. This is helpful because information can be given within the program that helps the user with the operation. For example, below in Figure 24 are the instructions given within the EES program.

```
"Program Operation:
1. Choose a fan and speed by highlighting and uncommenting that mathematical equation.
2. Choose the appropriate 4 or 6 Inch vent cap by highlighting and uncommenting that mathematical equation.
3. Change knowns as necessary for duct diameter, roughness factor, air density etc.
4. Variables section serves no program function and is there for reference only.
5. Press F2 to solve"
```

Figure 24: EES Operation Comments

Variable Description

To define the information contained within the EES program, it was necessary to use a variables description section that contained the appropriate units as shown in Figure 25. The standard English unit for pressure is pounds per square inch (PSI), but the industry standard for pressure is inches of water. Since the major and minor loss formulas are in PSI, a conversion factor from PSI to inches of water was needed for correct program operation. Without a variables section, the user may overlook this small detail during addition of other fan or vent cap performance curves. Needless to say, this section is helpful for understanding the EES program code.

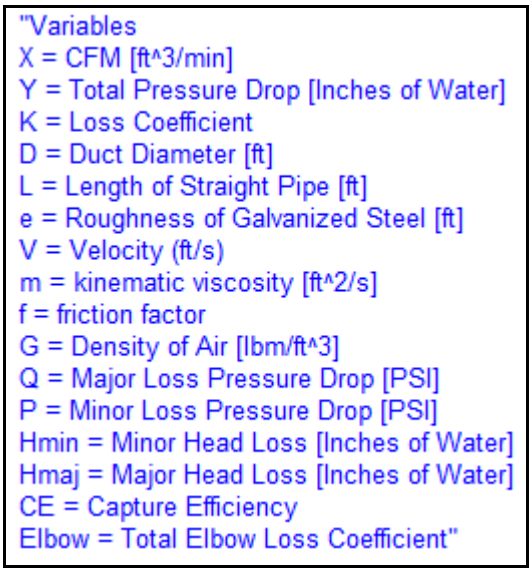

Figure 25: EES Variables Sections

Knowns

For ease of use, a knowns section was created where the user could quickly change information within the program as shown in Figure 26. While these variables don't change values during the completion of the EES program, they may change from system to system. Therefore, it was prudent to group the knowns section with the variable description section so the user could save time changing the values throughout the program.

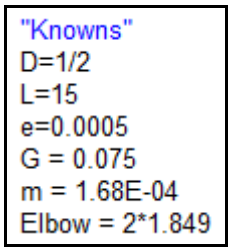

Figure 26: EES Knowns Section

Activating Fan And Vent Cap Equations

The Fan Static Pressure vs. Flow Rate curve describes how the volumetric flow rate behaves from minimum to maximum resistances. To activate a fan equation, select a fan speed equation as seen in Figure 27, highlight the appropriate equation, and select "undo comment." Note, you must select the mathematical equation only, because activating "Fan A High Speed" will create errors in the EES program. Figure 28 shows the relation between the loss coefficient and flow rate and must be selected in the same

way to activate the equation. In the Figures below, Fan A – High Speed and Product P equations have been activated successfully.

Below in Figure 28 it states “TRENDLINE IS UNRELIABLE AFTER 400 CFM” this is due to the limitations of the Vent Cap Performance data discussed previously. The spreadsheet calculator produced a trend line to a high R^2 value, but once again the data past 400 CFM is considered unreliable.

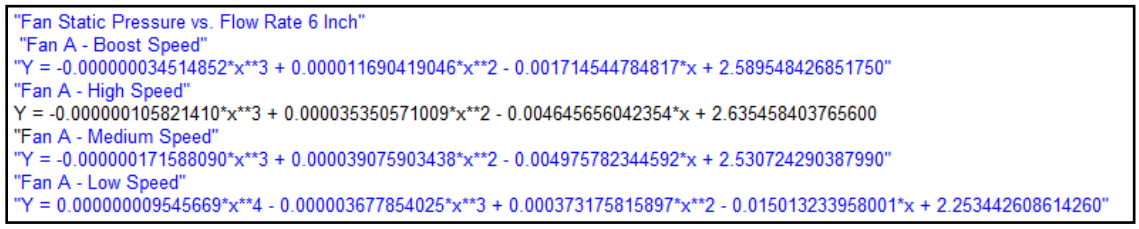

Figure 27: Fan Static Pressure EES Trend Line Equations

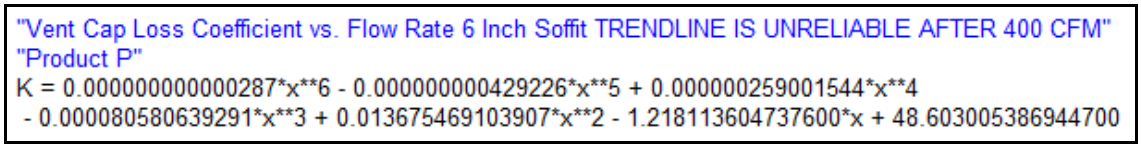

Figure 28: Vent Cap Loss Coefficient EES Trend Line Equations

Variable Information

Given the fact that the program must initially guess a velocity, like we did in a previous section, it will solve iteratively. Setting up the initial guesses and proper limits will help the EES program converge to an accurate solution. To do this we must select "Options" then "Variable Information." A table will appear like Figure 29 below:

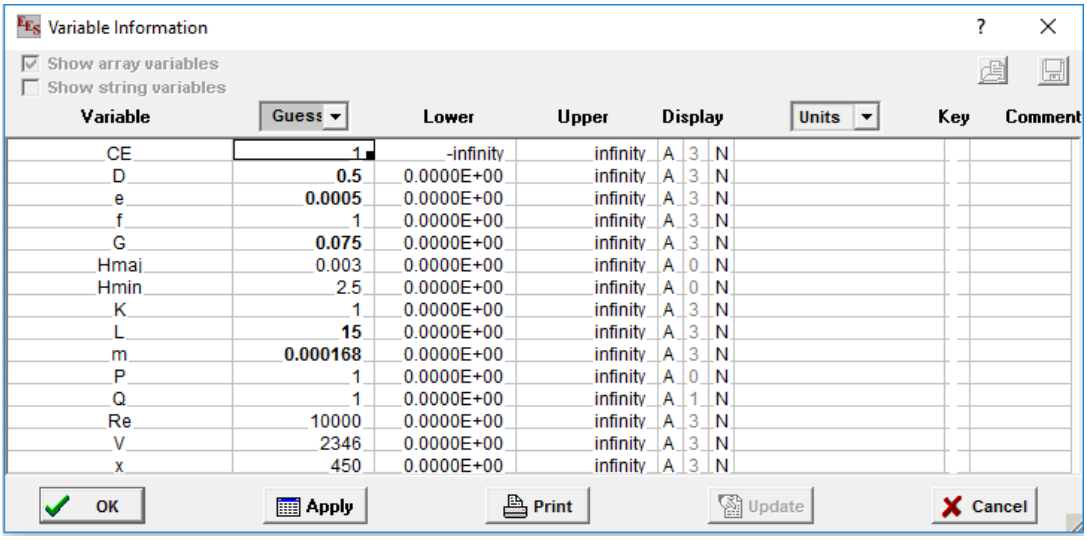

Figure 29: EES Variable Information Table

Notice every variable you have written into the program is displayed in the first column. While the initial guess for those variables are in the second column, the numbers in black are actually defined as constants within the program by the various equations you have written. It is important to note, if you change the guess for a constant in this window, it does not change the value of the constant you have written

into your program. These initial guesses are in fact guesses, and not defining the variable.

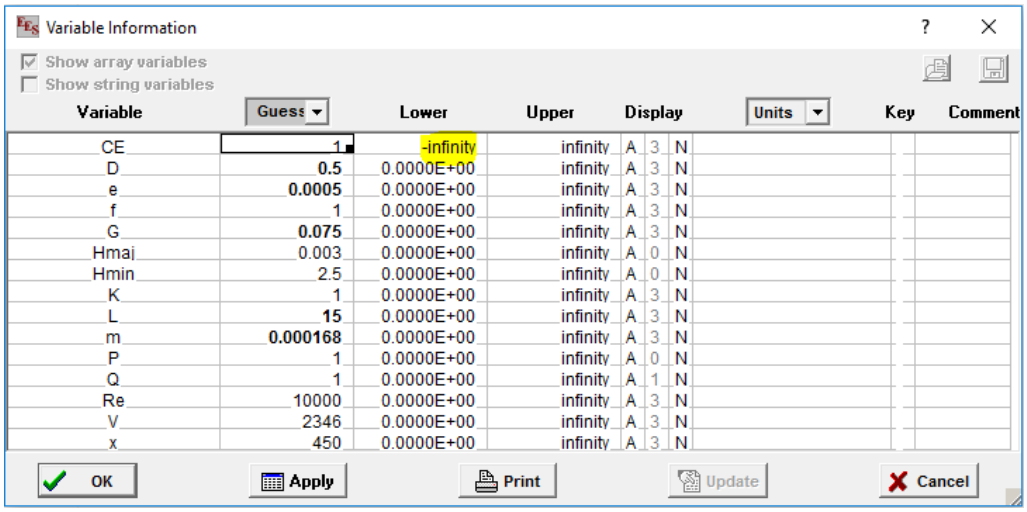

Figure 30: EES Variable Limit Defaults

In Figure 30 above, EES may manually default the variable limit to negative infinity. This creates problems for the EES program, and may inhibit convergence of a solution. To remedy this problem, realistic values should replace the default ones. Therefore, in Figure 31 a lower limit of negative infinity was replaced with a realistic value of zero.

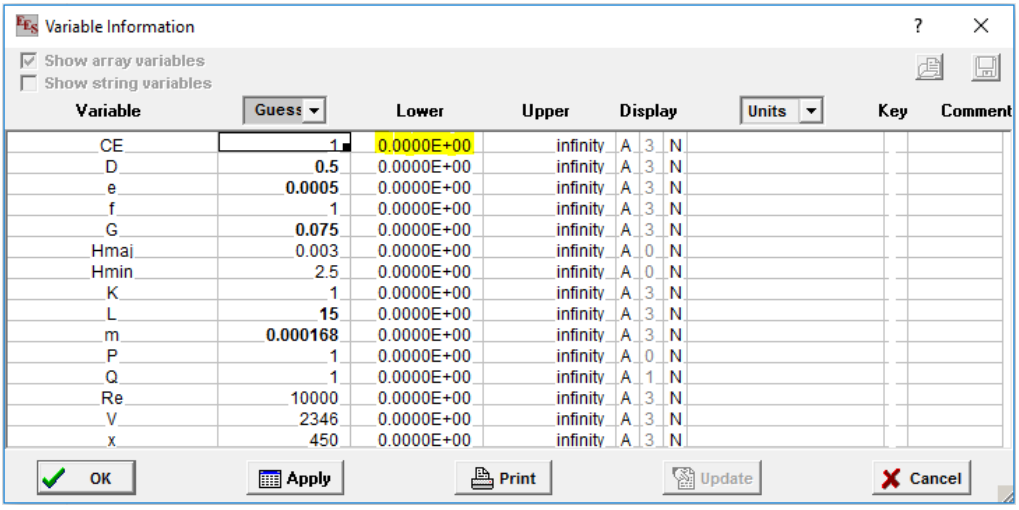

Figure 31: EES Variable Limit Correction

Solving The EES Program

In a previous section titled "System Curve" we manually solved for the volumetric flow rate using the Fan A – High Speed, Vent Cap P, and "knowns". The volumetric flow rate calculated was 331.7 CFM with a velocity of 28.21 $\frac{ft}{s}$, and showed the general process of analyzing the fan performance and system curve with multiple iterations. In Figure 32, we used the EES program to solve not only for the volumetric flow rate, but the subsequent capture efficiency as well.

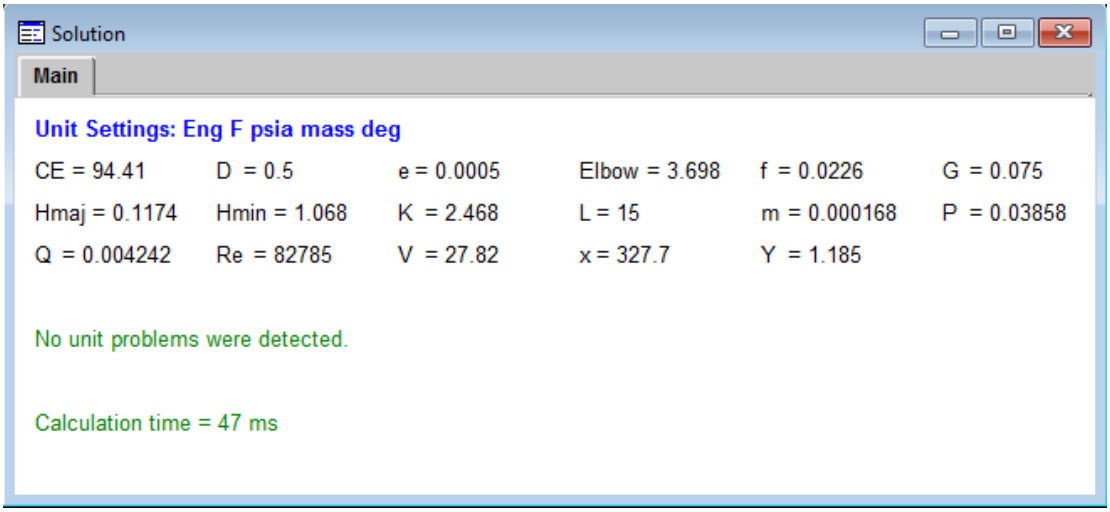

Figure 32: EES Program Using Loss Coefficient Formula

The data in Table 11 below shows a discrepancy in the data due to some sort of unexpected error. It is possible that rounding error or truncating digits may have produced this result, but further investigation has shown something else may be the problem.

Table 11: Table Data Using Loss Coefficient Trend Line

	R_e	f	ΔP_{major}	ΔP_{minor}	CFM	V $[\frac{ft}{s}]$
Manual	83,750	0.02082	0.1107	1.0124	331.7	28.21
EES (K)	82,785	0.0226	0.1174	1.068	327.7	27.82
% Difference	1.15%	8.54%	5.7%	5.49%	1.20%	1.38%

Trying to work out the data discrepancy in the EES program, it was decided to try a different idea. Daniel Escatel provided not only loss coefficient data, but Pressure Drop vs. Flow Rate data as well. To create a simpler program and reduce the solving issues for EES, we can use the Pressure Drop vs. Flow Rate curves to determine the resulting solution as shown in Figure 33.

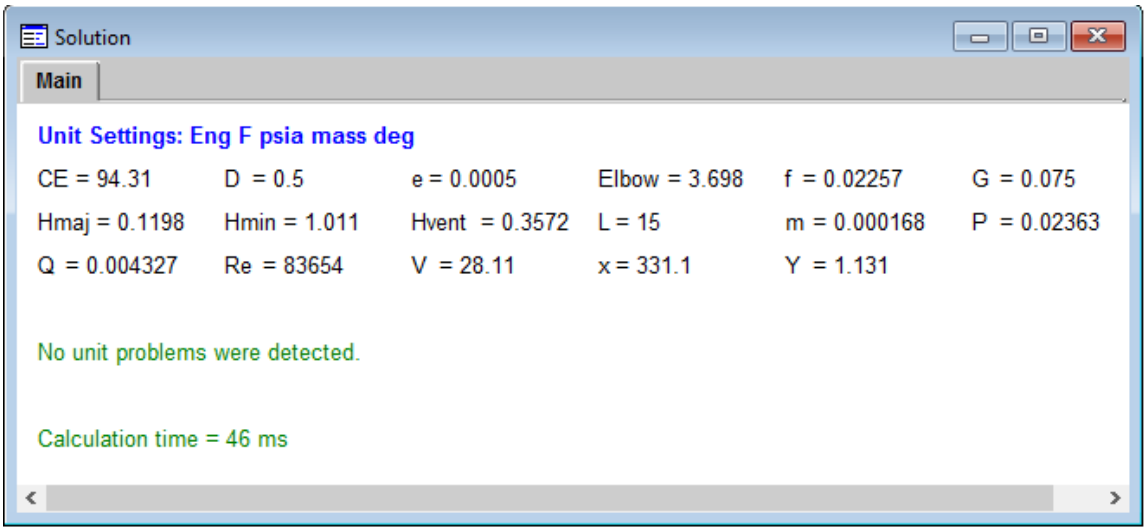

Figure 33: EES Solution for Sample Problem in "System Curve"

Table 12: Data Using Pressure Loss Trend Line

	R_e	f	ΔP_{major}	ΔP_{minor}	CFM	V $[\frac{ft}{s}]$
Manual	83,750	0.02082	0.1107	1.0124	331.7	28.21
EES (ΔP)	83,654	0.02257	0.1198	1.011	331.1	28.11
% difference	0.11%	8.40%	8.22%	0.138%	0.180%	0.354%

Table 12 shows the change in the EES programming produced an increase in CFM accuracy by about 1%. Therefore, it can be shown that using the static pressure method instead of the loss coefficient method will produce results closer to the manually solved values. As explained before in a previous section, the fan and vent cap trend lines do not match the experimental data perfectly, and careful selection of trend lines will produce more accurate results

As determined before, increasing the R^2 value may not produce results closer to the manually calculated value. It is proposed that a trend lines with smoother shape will better suit the use of the program. A six degree polynomial may give a better R^2 value, but the turns due to the trend line may be the cause for the difference in solved values.

8. CORRECT SIZING DUCT LENGTHS AND DIAMETER

One of the most overlooked part of installing a range hood and the appropriate ductwork is the size of the duct transporting the gases. As we have discussed before, the pressure loss is a function of the velocity squared. For example, given a roughness (e) of 0.0005 feet for galvanized steel, we find the following relative roughness for 6" galvanized pipe:

$$\text{Relative roughness} = \frac{0.0005\ feet}{0.5\ feet} = 0.001\ \frac{ft}{ft} \qquad \text{(Eqn.41)}$$

If we assume a volumetric flow rate of 600CFM, given a 6" circular pipe, the velocity of the fluid is 12.73 $\frac{ft}{s}$, we can then find the Reynolds number using Eqn. below

$$Re = \frac{\rho V D}{\mu} \qquad \text{(Eqn.42)}$$

Re = Reynold's number (Dimensionless)

ρ = Fluid density ($\frac{lbm}{ft^3}$)

V = Velocity of fluid ($\frac{ft}{s}$)

D = Hydraulic diameter of pipe (ft)

μ = absolute viscosity ($\frac{ft^2}{lbf*s}$)

$$Re_{6"} = (0.075\ \frac{lbm}{ft^3})*(50.929\ \frac{ft}{s})*(0.5\ \text{ft})*(\frac{ft^2}{3.85*10^{-7}\ lbf*s})*(\frac{lbf*s^2}{32.2*ft*lbm}) = 154{,}056 \qquad \text{(Eqn.43)}$$

We find the Reynolds number is 38,507 and given the relative roughness for galvanized steel found previously, we can reference the moody diagram in Figure 34 and determine friction factor to be 0.022.

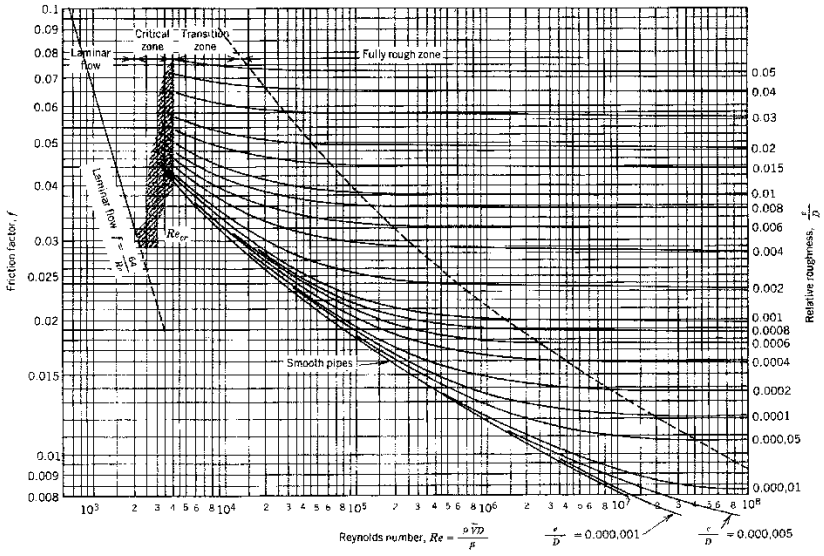

Figure 34: Moody Diagram (Fox, 1985)

Using Eqn.6 discussed previously, we find the pressure drop for 6" circular pipe and 600cfm below:

$$\Delta P = f\rho(\frac{L}{D})(\frac{V^2}{2}) \quad \text{(Eqn.44)}$$

ΔP = 0.022*(0.075$\frac{lbm}{ft^3}$)*($\frac{100ft}{0.5ft}$)*$\frac{(50.92\,\frac{ft}{s})^2}{2}$*$\frac{lbf*s^2}{32.2*lbm*ft}$*($\frac{1\,ft}{12\,in}$)^2 = 0.0922 PSI per 100 ft pipe

If we decide to reduce the cost of supplies and use a 4" circular pipe instead of the 6" circular pipe used previously, we must calculate a new velocity for the smaller pipe. Once again, assuming a 600cfm flow rate, a 4" circular pipe, we get a fluid velocity of 28.64 $\frac{ft}{s}$. Calculating our new Reynolds number below:

$Re_{4"}$ = (0.075 $\frac{lbm}{ft^3}$)*(114.591 $\frac{ft}{s}$)*($\frac{1}{3}$ ft)*($\frac{ft^2}{3.85*10^{-7}lbf*s}$)*($\frac{lbf*s^2}{32.2*ft*lbm}$) = 231,087 (Eqn.45)

This time, referencing the Moody Diagram in Figure 34, we find our friction factor to be 0.0235. Once again, using Eqn.6 we determine the pressure loss to be the following:

$$\Delta P = 0.022*(0.075\frac{lbm}{ft^3})*(\frac{100ft}{0.3ft})*\frac{(114.591\frac{ft}{s})^2}{2}*\frac{lbf*s^2}{32.2*lbm*ft}*(\frac{1\ ft}{12\ in})^2$$

$$= 0.7787 \text{ PSI per 100 ft pipe} \qquad \text{(Eqn.46)}$$

It is important to note that due to the reduction in pipe diameter, there was an increase of nearly 744% in pressure loss.

9. EES DATA

Using the fluid mechanics theory, the main performance reduction is due to the minor losses. Therefore, the EES data will show the capture efficiency differences due to the various vent caps. Using the EES program, the following Tables 13 through 18 show capture efficiency data that was compiled using the following system:

- Duct Diameter = 6 inches
- Length of Straight Pipe = 15 feet
- Roughness = 0.0005
- Two 90°, 3 Gore Elbows (ASHRAE CD3-12)

Table 13: Fan A and 6" Vent Cap Capture Efficiencies

	Soffit	Wall-Mounted						Roof-Jack	
Fan Speed	Prod P	Prod Q	Prod R	Prod S	Prod T	Prod U	Prod V	Prod W	Prod X
High	94%	94%	94%	94%	94%	94%	94%	95%	95%
Medium	93%	93%	93%	93%	93%	93%	93%	92%	92%
Low	90%	79%	89%	89%	89%	90%	90%	90%	90%

Table 14: Fan B and 6" Vent Cap Capture Efficiencies

	Soffit	Wall-Mounted						Roof-Jack	
Fan Speed	Prod P	Prod Q	Prod R	Prod S	Prod T	Prod U	Prod V	Prod W	Prod X
High	86%	88%	88%	89%	87%	85%	87%	79%	81%
Low	78%	79%	79%	80%	79%	77%	79%	73%	75%

Table 15: Fan C and 6" Vent Cap Capture Efficiencies

	Soffit	Wall-Mounted						Roof-Jack	
Fan Speed	Prod P	Prod Q	Prod R	Prod S	Prod T	Prod U	Prod V	Prod W	Prod X
High	84%	86%	86%	87%	86%	83%	85%	77%	80%
Low	77%	78%	79%	80%	78%	76%	78%	72%	74%

Table 16: Fan D and 6" Vent Cap Capture Efficiencies

	Soffit	Wall-Mounted						Roof-Jack	
Fan Speed	Prod P	Prod Q	Prod R	Prod S	Prod T	Prod U	Prod V	Prod W	Prod X
High	94%	94%	94%	93%	94%	94%	94%	95%	95%
Low	90%	90%	90%	91%	90%	89%	90%	87%	88%

Table 17: Fan E and 6" Vent Cap Capture Efficiencies

	Soffit	Wall-Mounted						Roof-Jack	
Fan Speed	Prod P	Prod Q	Prod R	Prod S	Prod T	Prod U	Prod V	Prod W	Prod X
High	93%	94%	94%	94%	94%	93%	93%	92%	92%
Medium	70%	70%	72%	72%	71%	69%	71%	66%	68%
Working	51%	49%	53%	51%	51%	48%	54%	46%	50%

Table 18: Fan F and 6" Vent Cap Capture Efficiencies

	Soffit	Wall-Mounted						Roof-Jack	
Fan Speed	Prod P	Prod Q	Prod R	Prod S	Prod T	Prod U	Prod V	Prod W	Prod X
High	94%	94%	94%	94%	94%	94%	94%	92%	93%
Medium	87%	88%	88%	88%	88%	87%	87%	85%	85%
Low	71%	72%	72%	73%	72%	71%	72%	69%	70%

Once again, capture efficiency was not effected with the change of duct length, roughness, or air temperature. Only slight capture efficiency changes were noticed varying the diameter of the duct, and it is recommended that the adequate duct size is used. Generally, capture efficiency was only changed by the amount of elbows within the duct system, the vent cap used, and the speed setting on the fan itself.

10. CONCLUSION

Many homeowners worry about initial purchase and installation cost, noise levels, and the general aesthetic appearance of their kitchen range hood. However as stated before, the main purpose of the kitchen range hood is to remove the unhealthy particles in the immediate area of the source. Many household activities affect indoor air quality and installing a kitchen range hood could greatly increase that air quality. Before installation, or even purchasing the kitchen range hood itself, it would be prudent to have a design program to ascertain the performance of the various products. With the completion of a system model solved by an EES program, we could determine how well our kitchen range hood will perform at little to no cost.

With the use of Microsoft Excel, trend lines to estimate the experimental data produced by the Riverside Energy Efficiency Laboratory were created to input into the EES Program. Trial and error has shown that increasing the R^2 value does not necessarily make a trend line fit the experimental data any better. In fact, it has been shown that sometimes it makes the trend line veer away from the experimental data. Thus, the trend line graph produced by Microsoft Excel must not be used to verify the accuracy of the equation. To see how well the equation performs, it must be graphed side by side with the experimental data. Also, tables were created to show the percent difference between experimental data and the trend line equation. The tables along with visual verification will determine how well the equation suits the experimental data.

The program allows for comments to be highlighted in blue and anyone with basic programming skills could determine how well the fan and duct system would work. If

possible, it is recommended to use the “Static Pressure vs. Flow” instead of using the minor loss equation. Once again, this is due to smoother experimental curves produced of the “Static Pressure vs. Flow”. With these smoother curves, a successful and accurate trend line will be easier to achieve.

Another factor that affects capture efficiency is the well-designed duct system. We can reduce the turbulence by keeping the velocity at a maximum of 30 fps (Seloff, 2016). Less turbulence can be achieved by allowing adequate duct length between elbows due to entrance length, correctly sizing the duct diameter, and installing the range hood vertical round when possible. Reducing minor losses like elbows increase system performance as well. With these factors we can increase overall capture efficiency and alleviate poor indoor air quality within the residence.

When adequate design for ventilation applications are planned for, increased air quality, longer lifespan of air handling units, and general cleanliness in the kitchen stove area can be greatly increased. Modern technology allows for a computer program to be easily distributed and tailored to the various HVAC companies in the industry. Thanks to the work from the Energy Efficiency Laboratory, we can produce something that will have lasting effects for kitchen range hood analysis and design.

REFERENCES

Abushakra, Bass, Iain Walker, and Max Sherman. "Compression Effects on Pressure Loss in Flexible HVAC Ducts." HVAC&R Research 10.3 (2004): 275-89. IBS Advisors. July 2004. Web. 01 Oct 2016.

ANSI/AMCA 210-07: Laboratory Methods of Testing Fans for Aerodynamic Performance Rating. www.amca.org. ANSI/AMCA, 17 Aug. 2007. Web. 08 Aug 2016.

ASHRAE Handbook: Fundamentals. Atlanta, GA: ASHRAE, 2005. Print.

ASHRAE Handbook: Fundamentals. Atlanta, GA: ASHRAE, 2013. Print.

Bergstrom, Erik "Range Hood Basics." Telephone interview. 30 June 2016.

Bleier, Frank P. Fan Handbook: Selection, Application, and Design. 1st ed. New York: McGraw-Hill, 1998. Print.

Chen, Meinan, and Michael B. Pate. Performance Assessment of a Typical Range Hood Ventilation System. Thesis. Texas A&M University, 2015. Print.

Delp, William, and Brett Singer. "Performance Assessment of U.S. Residential Cooking Exhaust Hoods." Department of Energy. May 2012. Web. Oct. 2016.

Escatel, D. S. An Experimental Study and Analysis on Vent Cap Performance. Dissertation. Texas A&M University, 2011. Print.

Fox, Robert W., and Alan T. McDonald. Introduction to Fluid Mechanics. 9th ed. New York: Wiley, 1985. Print.

Li, Yuguo, and Angelo Delsante. "Derivation of Capture Efficiency of Kitchen Range Hoods in a Confined Space." Derivation of Capture Efficiency of Kitchen Range Hoods in a Confined Space. Elsevier Science Ltd., 1996. Web. 19 July 2016.

New York Blower Company, “Fan Laws and System Curves.pdf.” Scribd., Web. 04 Mar 2016.

Oneida Air. "Adjustable Large Radius Elbow Duct." Web. 21 Sept. 2016. <http%3A%2F%2Fwww.oneida-air.com%2FinventoryD.asp%3Fitem_no%3DSCOLLECT4>.

Schofield, Roquey. "Range Hood Installation." Personal interview. 14 July 2016. Construction Specialist at Integrity Comfort Solutions – Conroe, TX.

Seloff, Bob. "Kitchen Range Hoods." Telephone interview. 30 June 2016.

Truini, Joseph. "Installing a Bathroom Vent Fan." This Old House. 23 July 2016. Web. 18 Nov. 2016.

APPENDIX A: FAN DATA

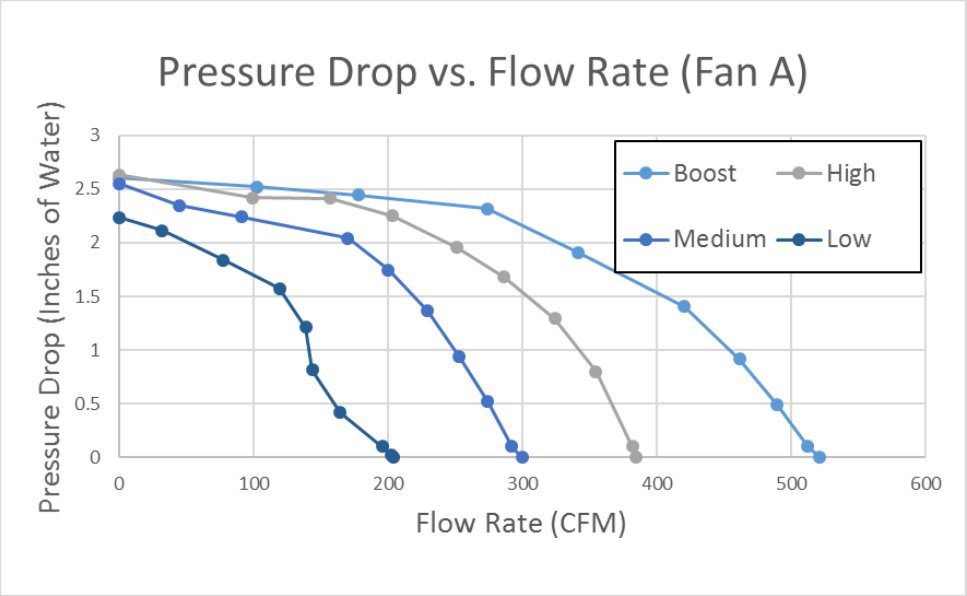

Figure 35: Fan A Performance

Table 19: Fan A Performance Trend Lines

	Trend Line	R^2 Value
Boost Speed	$Y = -.000000034514852x^3 + 0.000011690419046x^2 - 0.001714544784817x + 2.589548426851750$	0.985
High Speed	$Y = -0.000000105821410x^3 + 0.000035350571009x^2 - 0.004645656042354x + 2.635458403765600$	0.997
Medium Speed	$Y = -0.000000171588090x^3 + 0.000039075903438x^2 - 0.004975782344592x + 2.530724290387990$	0.9997
Low Speed	$Y = 0.000000009545669x^4 - 0.000003677854025x^3 + 0.000373175815897x^2 - 0.015013233958001x + 2.253442608614260$	0.987

Table 20: Fan A Experiment and Trend Line Comparison

Fan A - Boost Speed			
CFM	**dP(Exp) inWC**	**dP(Eqn) inWC**	**%Diff**
521.3	0.003	0.108	3507.8
512.5	0.101	0.217	115.57
489.8	0.491	0.489	0.3867
461.6	0.919	0.804	12.510
420.6	1.406	1.21	13.369
341.2	1.909	1.87	1.9439
273.9	2.317	2.27	1.8809
178.2	2.519	2.60	3.3397
102.6	2.445	2.66	8.928
0	2.601	2.46	5.3379

Fan A - Medium Speed			
CFM	**dP(Exp) inWC**	**dP(Eqn) inWC**	**%Diff**
300	0	-0.078	7805.7
292.1	0.102	0.134	32.268
274.3	0.522	0.564	8.169
253.2	0.939	0.990	5.5039
229.7	1.366	1.369	0.2899
200.2	1.744	1.723	1.152
170.2	2.04	1.969	3.4408
91.4	2.238	2.271	1.4906
44.7	2.348	2.371	0.9821
0	2.55	2.530	0.7559

Fan A - High Speed			
CFM	**dP(Exp) inWC**	**dP(Eqn) inWC**	**%Diff**
384.8	0.002	0.0527	2537.07
382	0.101	0.120	19.3218
354.7	0.8	0.712	10.8956
324.4	1.293	1.235	4.4107
286.3	1.68	1.719	2.3609
251.5	1.957	2.019	3.2028
203.5	2.249	2.262	0.5876
157.3	2.42	2.367	2.1687
98.9	2.414	2.419	0.224
0	2.63	2.635	0.2075

Fan A - Low Speed			
CFM	**dP(Exp) inWC**	**dP(Eqn) inWC**	**%Diff**
204.2	0.002	0.0296	1380.5
202.6	0.029	0.027	6.8741
196	0.102	0.0416	59.185
164.5	0.418	0.500	19.674
144	0.817	0.952	16.543
139.1	1.21	1.060	12.344
119.4	1.571	1.460	7.0266
77.4	1.838	1.964	6.8687
32.2	2.113	2.044	3.246
0	2.234	2.253	0.870

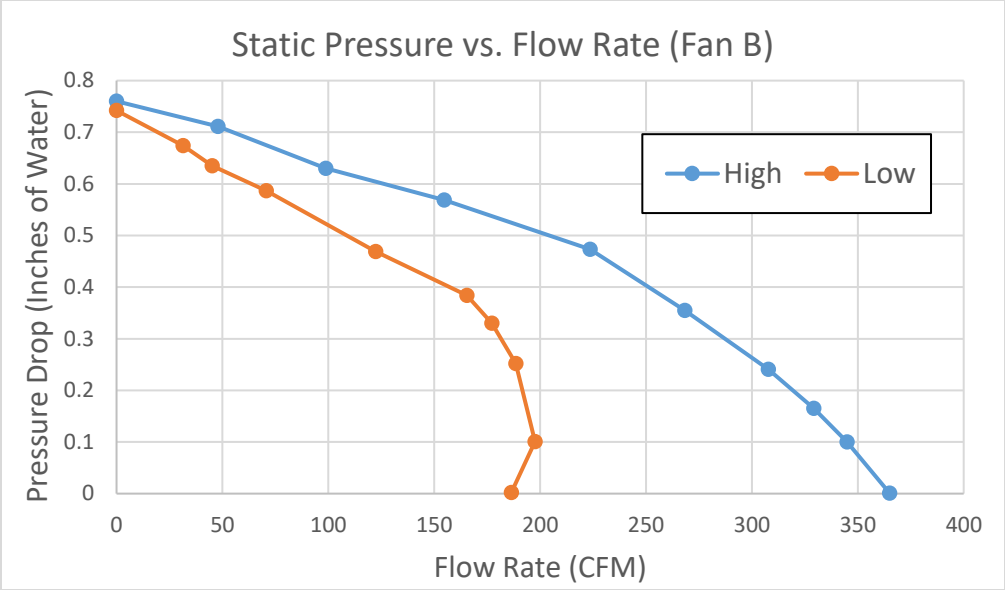

Figure 36: Fan B Performance

Table 21: Fan B Performance Trend Lines

	Trend Line	R^2 Value
High Speed	$Y = -0.000000017551567x^3 + 0.000005111201732x^2 - 0.001611466679855x + 0.764985332642593$	0.9999
Low Speed	$Y = 0.000000000010797x^5 - 0.000000007194695x^4 + 0.000001460995020x^3 - 0.000109845260672x^2 + 0.000323730442716x + 0.740186176303947$	0.912

Table 22: Fan B Experiment and Trend Line Comparison

Fan B - High Speed			
CFM	**dP(Exp) inWC**	**dP(Eqn) inWC**	**%Diff**
365	0.001	0.004258	325.7603
344.9	0.1	0.097094	2.9058
329.2	0.165	0.16223	1.6785
307.8	0.241	0.24139	0.1619
268.3	0.355	0.361575	1.8521
223.6	0.473	0.463991	1.9046
154.7	0.569	0.573032	0.7086
98.7	0.63	0.638849	1.4047
47.9	0.711	0.697594	1.8855
0	0.76	0.764985	0.656

Fan B - Low Speed			
CFM	**dP(Exp) inWC**	**dP(Eqn) inWC**	**%Diff**
186.4	0.002	0.190101	9405.054
197.6	0.101	0.071214	29.4914
188.5	0.252	0.169626	32.6882
177.2	0.33	0.270218	18.1159
165.4	0.384	0.35142	8.4845
122.3	0.469	0.495171	5.5802
70.7	0.587	0.569633	2.9587
45.1	0.635	0.637631	0.4144
31.4	0.674	0.680615	0.9814
0	0.742	0.740186	0.2445

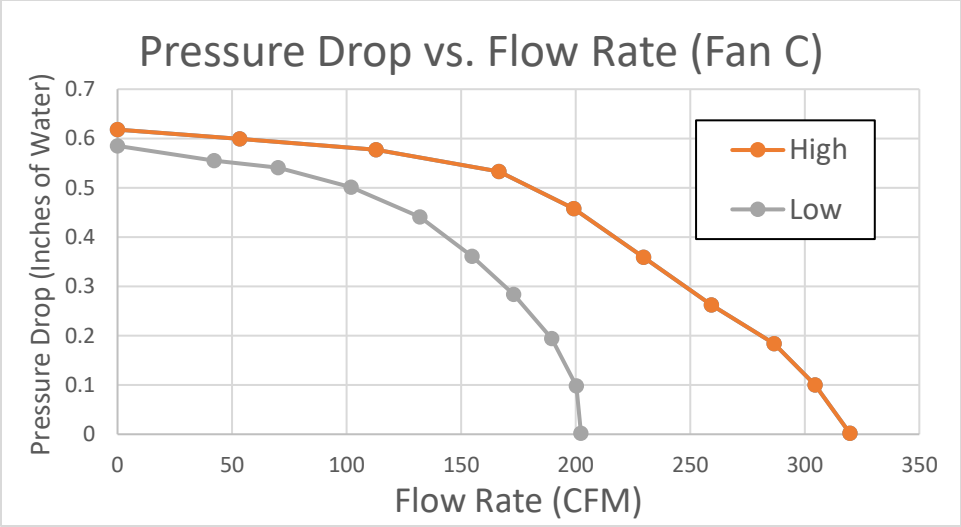

Figure 37: Fan C Performance

Table 23: Fan C Performance Trend Lines

	Trend Line	R^2 Value
High Speed	$Y = -0.000000015099144x^3 - 0.000001096886840x^2 + 0.000008191341421x + 0.613688211129658$	0.996
Low Speed	$Y = -0.000000001079263x^4 + 0.000000306593201x^3 - 0.000033491303174x^2 + 0.000500369539147x + 0.583131580093620$	0.989

Table 24: Fan C Experiment and Trend Line Comparison

Fan C - High Speed			
CFM	**dP(Exp) inWC**	**dP(Eqn) inWC**	**%Diff**
319.7	0.002	0.010818	440.8878
304.5	0.1	0.08818	11.8201
286.6	0.0184	0.170486	826.5549
259.3	0.262	0.278817	6.4185
229.6	0.359	0.374991	4.4543
199.2	0.458	0.452445	1.2128
166.5	0.533	0.51495	3.3865
112.9	0.577	0.578903	0.3298
53.3	0.599	0.608722	1.6231
0	0.618	0.613688	0.6977

Fan C - Low Speed			
CFM	**dP(Exp) inWC**	**dP(Eqn) inWC**	**%Diff**
202.3	0.002	0.044422	2121.095
200.3	0.098	0.066276	32.3715
189.6	0.194	0.169021	12.876
172.9	0.284	0.288633	1.6314
154.8	0.361	0.375594	4.0427
132	0.441	0.443123	0.4814
101.9	0.501	0.494396	1.3181
70.1	0.541	0.533182	1.4451
42.2	0.555	0.564223	1.6617
0	0.585	0.583132	0.3194

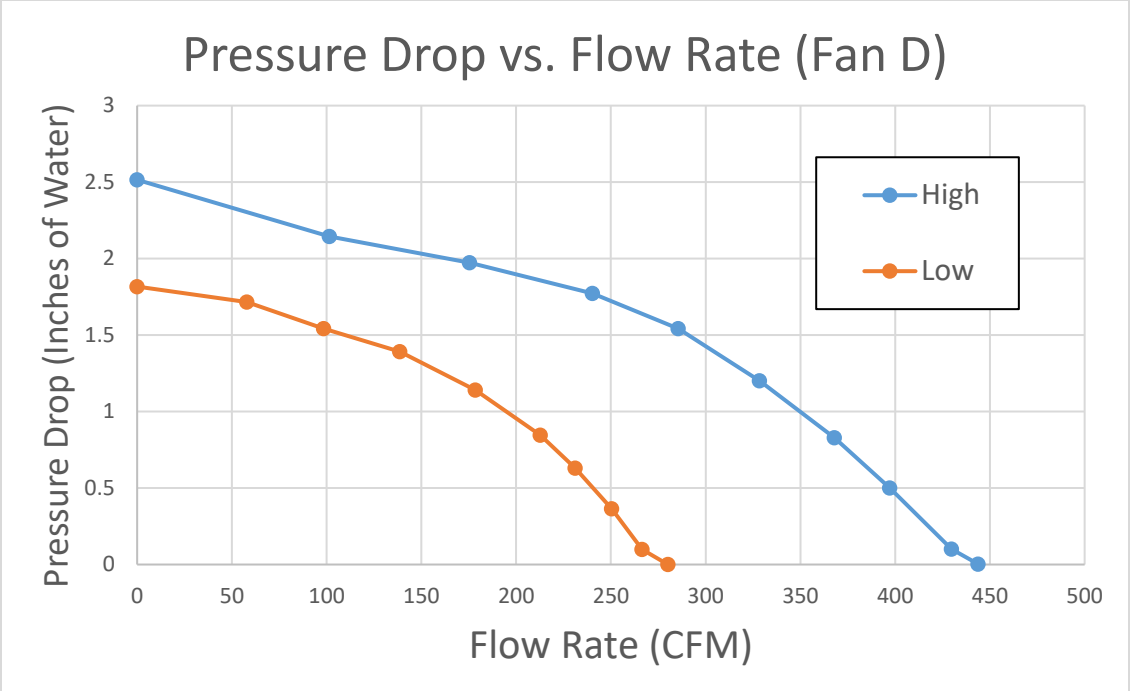

Figure 38: Fan D Performance

Table 25: Fan D Performance Trend Lines

	Trend Line	R^2 Value
High Speed	$Y = 0.000000000149575x^4 - 0.000000171656288x^3 + 0.000050305239458x^2 - 0.007328167919011x + 2.517610456235260$	0.999
Low Speed	$Y = 0.000000000161538x^4 - 0.000000149944793x^3 + 0.000015313208839x^2 - 0.002734402169520x + 1.822169329267510$	0.997

Table 26: Fan D Experiment and Trend Line Comparison

Fan D - High Speed			
CFM	**dP(Exp) inWC**	**dP(Eqn) inWC**	**%Diff**
443.8	0.003	-0.02868	1056.155
429.7	0.1	0.137246	37.246
397.2	0.501	0.509529	1.7023
367.9	0.829	0.82289	0.737
328.5	1.201	1.195594	0.4501
285.5	1.542	1.524932	1.1069
240.3	1.773	1.778336	0.3009
175.4	1.973	1.995177	1.124
101.5	2.144	2.128437	0.7259
0	2.515	2.51761	0.1038

Fan D - Low Speed			
CFM	**dP(Exp) inWC**	**dP(Eqn) inWC**	**%Diff**
280.1	0	-0.04312	4311.731
266.4	0.099	0.159212	60.8206
250.4	0.365	0.37852	3.7042
231.2	0.63	0.616994	2.0645
212.7	0.846	0.821091	2.9443
178.5	1.141	1.133188	0.6847
138.6	1.391	1.39773	0.4839
98.5	1.543	1.573311	1.9645
57.9	1.715	1.687894	1.5805
0	1.817	1.822169	0.2845

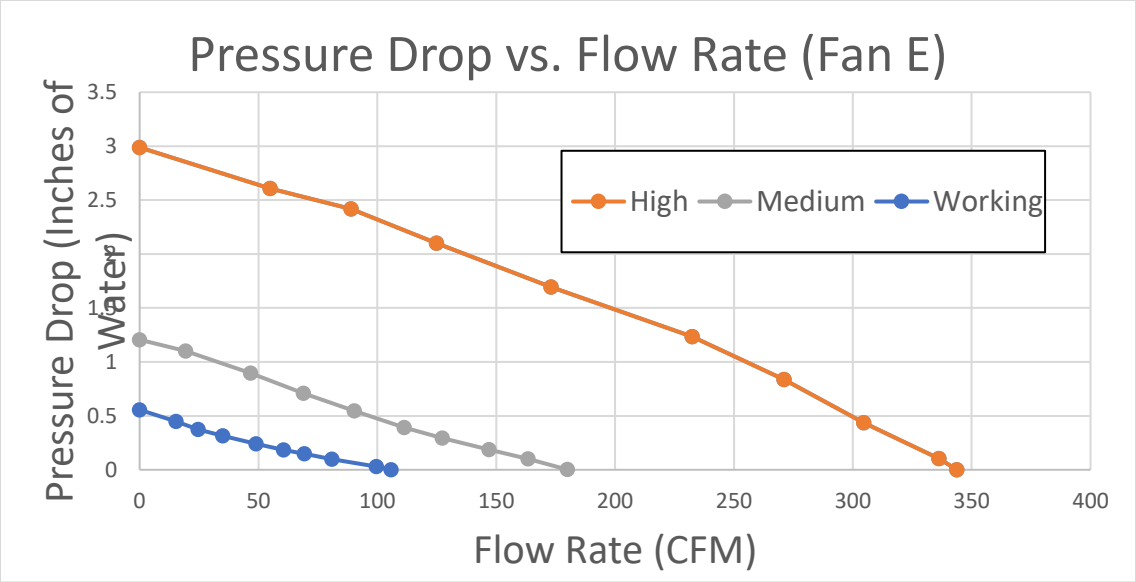

Figure 39: Fan E Performance

Table 27: Fan E Performance Trend Lines

	Trend Line	R^2 Value
High Speed	$Y = -0.000000013258575x^3 - 0.000001409414595x^2 - 0.006640520583425x + 2.990401925904360$	0.999
Medium Speed	$Y = -0.000000001756276x^4 + 0.000000733210223x^3 - 0.000090894347547x^2 - 0.003833596493678x + 1.205304509402200$	0.999
Working Speed	$Y = -0.000000002065441x^4 + 0.000000284672444x^3 + 0.000016647149423x^2 - 0.007753532812457x + 0.556935320619788$	0.999

Table 28: Fan E Experiment and Trend Line Comparison

Fan E - High Speed			
CFM	**dP(Exp) inWC**	**dP(Eqn) inWC**	**%Diff**
343.8	0.001	0.002017	1.01662
336.2	0.103	0.094715	0.080434
304.6	0.436	0.46223	0.06016
271.1	0.837	0.8224	0.017443
232.4	1.234	1.204603	0.023823
173	1.694	1.73076	0.0217
124.9	2.099	2.11318	0.006756
88.9	2.419	2.379605	0.016286
54.8	2.609	2.620087	0.00425
0	2.988	2.990402	0.000804

Fan E - Medium Speed			
CFM	**dP(Exp) inWC**	**dP(Eqn) inWC**	**%Diff**
179.9	0.002	0.003319	0.659718
163.3	0.102	0.099393	0.025557
147	0.187	0.186598	0.00215
127.3	0.294	0.295664	0.00566
111.3	0.391	0.394059	0.007823
90.3	0.545	0.54107	0.007211
68.8	0.71	0.710738	0.001039
46.7	0.895	0.894367	0.000707
19.3	1.101	1.102486	0.00135
0	1.206	1.205305	0.000577

Fan E - Working Speed			
CFM	**dP(Exp) inWC**	**dP(Eqn) inWC**	**%Diff**
105.7	0.001	0.001738	73.81585
99.5	0.03	0.028249	5.835591
80.8	0.098	0.101266	3.332924
69.3	0.149	0.146669	1.564642
60.5	0.184	0.184147	0.079912
48.9	0.241	0.239071	0.800316
35	0.314	0.31506	0.337678
24.6	0.375	0.379754	1.26776
15.3	0.448	0.44311	1.091609
0	0.556	0.556935	0.168223

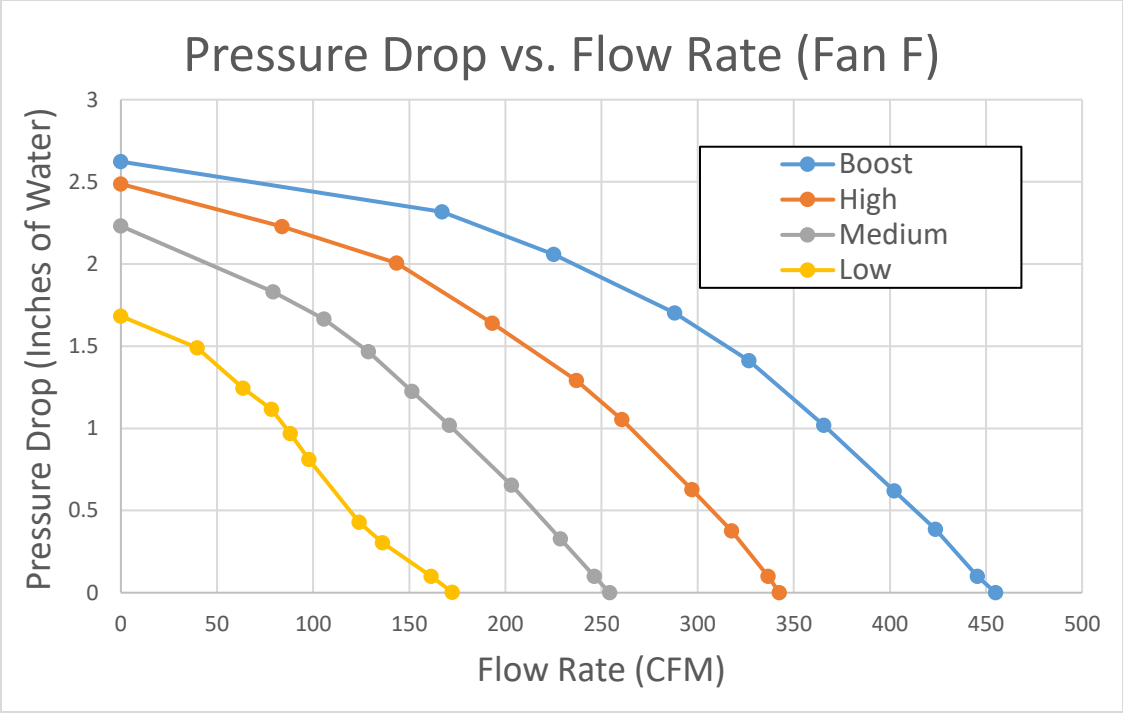

Figure 40: Fan F Performance

Table 29: Fan F Performance Trend Lines

	Trend Line	R^2 Value
Boost Speed	$Y = 0.000000000054331x^4 - 0.000000065299031x^3 + 0.000010196837853x^2 - 0.002026803700355x + 2.623441021375230$	0.999
High Speed	$Y = 0.000000000045992x^4 - 0.000000056913851x^3 + 0.000000572608497x^2 - 0.002591406550024x + 2.485337954121350$	0.999
Medium Speed	$Y = 0.000000000340180x^4 - 0.000000159173606x^3 + 0.000000140104265x^2 - 0.004109350683487x + 2.230395703591600$	0.999
Low Speed	$Y = 0.000000534628799x^3 - 0.000155490000962x^2 + 0.001258781511144x + 1.675767447281900$	0.999

Table 30: Fan F Experiment and Trend Line Comparison

Fan F - Boost Speed			
CFM	**dP(Exp) inWC**	**dP(Eqn) inWC**	**%Diff**
455	0	-0.01009	1009.494
445.5	0.1	0.110749	10.7488
423.7	0.386	0.379357	1.721
402.2	0.619	0.631003	1.9391
365.7	1.018	1.024054	0.5947
326.6	1.412	1.392472	1.383
288.1	1.702	1.698693	0.1943
225.2	2.058	2.078096	0.9765
167.1	2.317	2.307168	0.4244
0	2.623	2.623441	0.0168

Fan F - High Speed			
CFM	**dP(Exp) inWC**	**dP(Eqn) inWC**	**%Diff**
342.5	0.001	0.011186	1018.645
336.7	0.1	0.09638	3.6199
317.7	0.377	0.36336	3.6181
297.1	0.628	0.631773	0.6007
260.6	1.054	1.053765	0.0223
236.9	1.292	1.291746	0.0197
193.2	1.639	1.6597	1.2629
143.4	2.005	1.977125	1.3903
83.9	2.228	2.240616	0.5662
0	2.487	2.485338	0.0668

Fan F - Medium Speed			
CFM	**dP(Exp) inWC**	**dP(Eqn) inWC**	**%Diff**
254.2	0	0.000698	69.8473
246.2	0.1	0.101633	1.6332
228.6	0.327	0.3258	0.3668
203.2	0.655	0.645633	1.43
170.9	1.019	1.02788	0.8714
151.4	1.225	1.237794	1.0444
128.8	1.467	1.456947	0.6853
105.7	1.665	1.652092	0.7752
79.2	1.83	1.840122	0.5531
0	2.231	2.230396	0.0271

Fan F - Low Speed			
CFM	**dP(Exp) inWC**	**dP(Eqn) inWC**	**%Diff**
172.4	0.003	0.007991	166.3744
161.4	0.1	0.090824	9.1765
136.1	0.305	0.303304	0.556
123.9	0.428	0.442821	3.4628
97.8	0.811	0.811594	0.0733
88.2	0.968	0.955109	1.3317
78.4	1.117	1.095187	1.9528
63.6	1.244	1.279913	2.8869
39.8	1.49	1.478551	0.7684
0	1.683	1.683862	0.0512

Figure 41: Fan A

Figure 42: Fan B

Figure 43: Fan C

Figure 44: Fan D

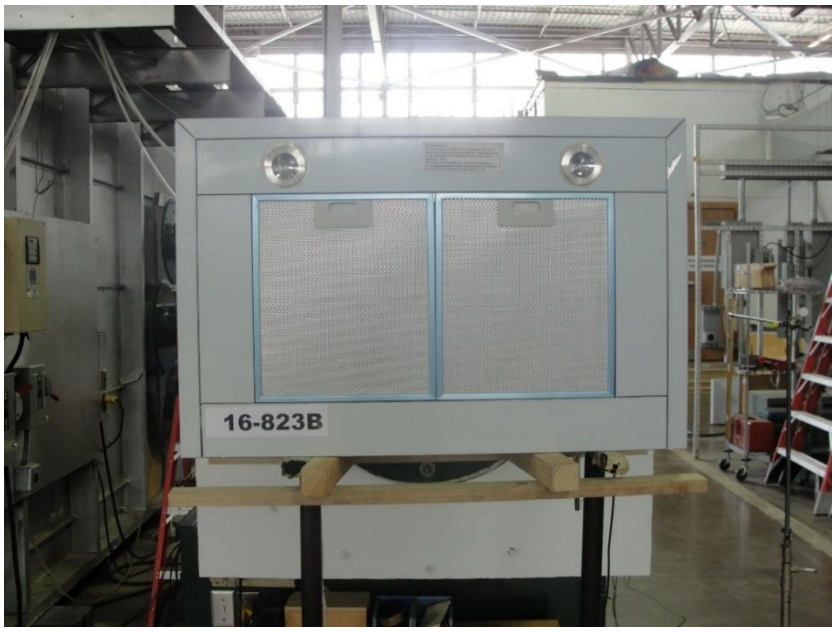

Figure 45: Fan E

Figure 46: Fan F

APPENDIX B: VENT CAP DATA (ESCATEL, 2011)

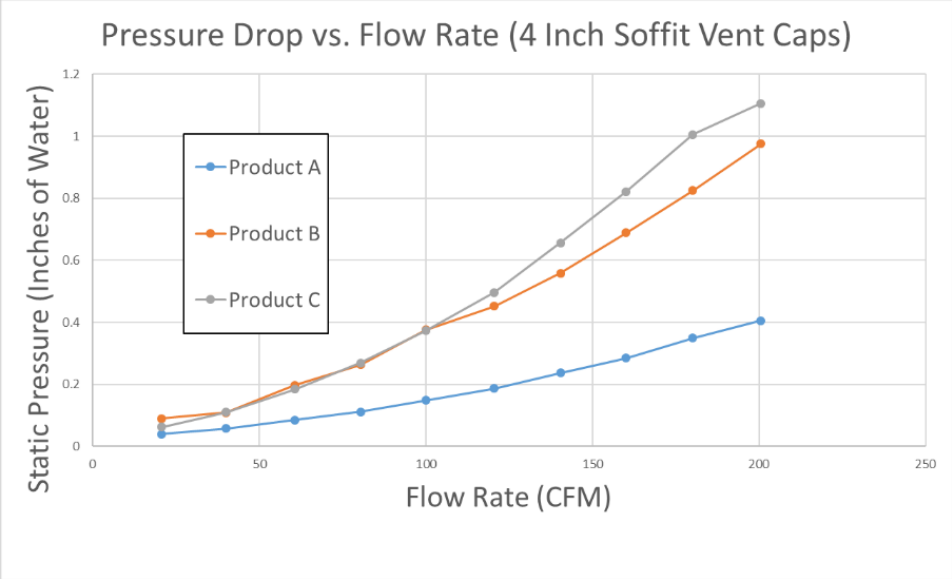

Figure 47: 4" Soffit Vent Cap Performance

Table 31: 4" Soffit Vent Cap Performance Trend Lines

	Trend Line	R^2 Value
Product A	$Y = -0.000000003273794x^3 + 0.000007876647506x^2 + 0.000442223157142x + 0.027996301679561$	0.9996
Product B	$Y = -0.000000002013453x^3 + 0.000015801757729x^2 + 0.001560369261724x + 0.040833910588412$	0.9987
Product C	$Y = -0.000000106681792x^3 + 0.000054052479134x^2 - 0.001308790685007x + 0.075925548633840$	0.996

Table 32: 4" Soffit Experiment and Trend Line Comparison

Product A			
CFM	**dP(Exp) inWC**	**dP(Eqn) inWC**	**%Diff**
200.6	0.405	0.407239	0.5527
180.1	0.349	0.344003	1.4318
160.1	0.285	0.287256	0.7916
140.4	0.237	0.23629	0.2997
120.5	0.187	0.189927	1.5652
100	0.149	0.147711	0.8649
80.4	0.112	0.112766	0.6835
60.7	0.085	0.083128	2.2018
40.1	0.058	0.058184	0.3174
20.7	0.04	0.040496	1.2409

Product B			
CFM	**dP(Exp) inWC**	**dP(Eqn) inWC**	**%Diff**
200.6	0.976	0.973459	0.2603
180.5	0.825	0.825465	0.0564
160.6	0.689	0.690654	0.24
140.9	0.559	0.568767	1.7472
120.1	0.452	0.452671	0.1485
100.6	0.375	0.355677	5.1529
80.1	0.263	0.266169	1.2049
60.8	0.197	0.193665	1.6928
40.3	0.109	0.129248	18.5766
20.4	0.09	0.079224	11.9729

Product C			
CFM	**dP(Exp) inWC**	**dP(Eqn) inWC**	**%Diff**
200.4	1.106	1.125815	1.7916
180.3	1.005	0.971809	3.3026
160.4	0.822	0.816412	0.6798
140.9	0.657	0.666194	1.3994
120	0.496	0.51288	3.4033
100.6	0.373	0.382678	2.5947
80	0.269	0.262537	2.4026
60.3	0.184	0.170155	7.5247
40.7	0.11	0.105003	4.5429
20	0.062	0.070517	13.7375

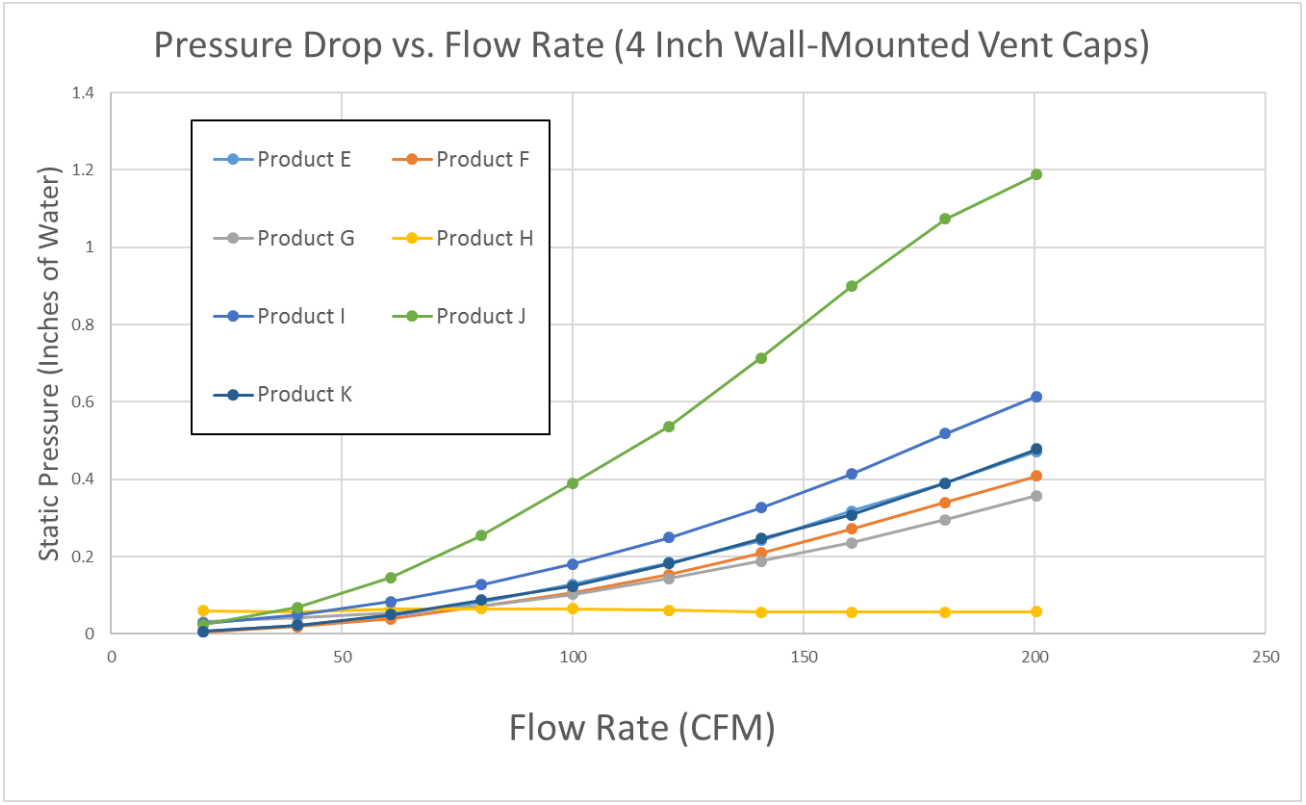

Figure 48: 4" Wall-Mounted Vent Cap Performance

Table 33: 4" Wall-Mounted Vent Cap Performance Trend Lines

	Trend Line	R^2 Value
Product E	$Y = -0.000000015851247x^3 + 0.000015711021952x^2 - 0.000177252455421x + 0.003795149639709$	0.9996
Product F	$Y = -0.000000012436489x^3 + 0.000013578269898x^2 - 0.000197219110252x + 0.004335314169471$	0.9997
Product G	$Y = -0.000000010579457x^3 + 0.000012408836457x^2 - 0.000470235429657x + 0.037545325862393$	0.9996
Product H	$Y = 0.000000000000040x^6 - 0.000000000032109x^5 + 0.000000010202020x^4 - 0.000001586763557x^3 + 0.000122313102810x^2 - 0.004159974933070x + 0.105602722780341$	0.968
Product I	$Y = -0.000000009317615x^3 + 0.000016428499644x^2 + 0.000058171480871x + 0.020933476140906$	0.9998
Product J	$Y = -0.000000181442886x^3 + 0.000078012406825x^2 - 0.002615673961524x + 0.053146052526256$	0.9993
Product K	$Y = -0.000000000972512x^3 + 0.000011310032727x^2 + 0.000170607703930x - 0.001683165033632$	0.9998

Table 34: 4" Wall-Mounted Experiment and Trend Line Comparison

Product E			
CFM	**dP(Exp)**	**dP(Eqn)**	**%Diff**
200.5	0.472	0.47208	0.016866963
180.7	0.39	0.391242	0.31857105
160.3	0.318	0.313801	1.320500169
140.7	0.242	0.245727	1.54020306
120.8	0.184	0.183706	0.159833561
100	0.128	0.127329	0.524315142
80.1	0.082	0.082253	0.308525607
60.6	0.047	0.047223	0.473539148
40.4	0.022	0.021232	3.491670594
20	0.006	0.006408	6.794988935

Product F			
CFM	**dP(Exp)**	**dP(Eqn)**	**%Diff**
200.2	0.408	0.409279	0.313471
180.6	0.34	0.338334	0.490011
160.4	0.272	0.270722	0.469704
140.3	0.209	0.209596	0.285064
120.1	0.153	0.154958	1.279985
100.1	0.108	0.108174	0.161339
80.8	0.071	0.070487	0.722222
60.1	0.039	0.038828	0.442162
40.3	0.019	0.017626	7.232958
20.8	0.005	0.005996	19.91489

Product G			
CFM	**dP(Exp)**	**dP(Eqn)**	**%Diff**
200.8	0.357	0.357799	0.223789185
180.2	0.295	0.293844	0.391915676
160.1	0.236	0.236909	0.385295269
140	0.188	0.185896	1.119398798
120.4	0.143	0.142345	0.45822793
100.3	0.102	0.10454	2.489966448
80.3	0.071	0.074321	4.677277004
60.5	0.055	0.052173	5.140442123
40.5	0.041	0.038152	6.94734071
20.2	0.031	0.033023	6.52474713

Product H			
CFM	**dP(Exp)**	**dP(Eqn)**	**%Diff**
200.5	0.058	0.080751	39.22595
180.5	0.057	0.06892	20.91187
160.5	0.056	0.062161	11.00128
140.9	0.057	0.059955	5.184004
120.6	0.061	0.06165	1.0658
100.3	0.065	0.06504	0.062241
80.6	0.065	0.066358	2.089411
60.2	0.064	0.062767	1.926626
40.9	0.056	0.056564	1.006887
20.3	0.06	0.05991	0.150198

Table 34 Continued

Product I			
CFM	**dP(Exp)**	**dP(Eqn)**	**%Diff**
200.2	0.614	0.61627	0.369635672
180.8	0.518	0.513408	0.886467737
160.3	0.413	0.414027	0.248556484
140.5	0.326	0.327567	0.480615443
120.1	0.249	0.248744	0.102975994
100.2	0.181	0.182331	0.735590892
80.2	0.127	0.126461	0.424324636
60.7	0.084	0.082911	1.296123019
40.5	0.05	0.049617	0.765405344
20.1	0.028	0.028664	2.37263005

Product J			
CFM	**dP(Exp)**	**dP(Eqn)**	**%Diff**
200.1	1.188	1.199646	0.980282
180.6	1.073	1.056444	1.542954
160.1	0.899	0.889407	1.067071
140.3	0.713	0.720683	1.077621
120.2	0.537	0.550765	2.563283
100	0.39	0.39026	0.066625
80.7	0.254	0.254757	0.298202
59.9	0.146	0.13738	5.903804
40.4	0.069	0.062837	8.931385
20.7	0.024	0.03082	28.41577

Product K			
CFM	**dP(Exp) inWC**	**dP(Eqn) inWC**	**%Diff**
200	0.478	0.47706	0.196738738
180.3	0.39	0.391045	0.267915398
159.9	0.308	0.310796	0.907822001
140.6	0.247	0.243182	1.545730246
120.3	0.182	0.180828	0.644166346
100	0.124	0.127505	2.82695212
80.7	0.087	0.08523	2.03420655
60.6	0.05	0.049974	0.052508177
40.6	0.023	0.023821	3.571432464
20.5	0.007	0.006559	6.300630886

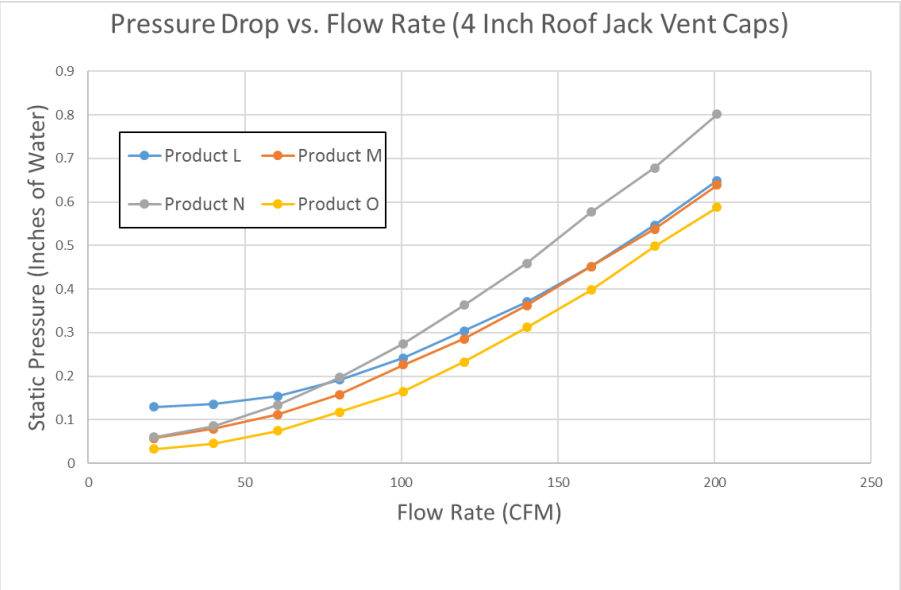

Figure 49: 4" Roof Jack Vent Cap Performance

Table 35: 4" Roof Jack Vent Cap Performance Trend Lines

	Trend Line	R^2 Value
Product L	$Y = -0.000000017512824x^3 + 0.000020308244772x^2 - 0.000831070581585x + 0.137042389951397$	0.9997
Product M	$Y = -0.000000023485359x^3 + 0.000019482866651x^2 - 0.000030755636013x + 0.049240319904090$	0.9995
Product N	$Y = -0.000000044061150x^3 + 0.000028369738475x^2 - 0.000178244272160x + 0.051144382378564$	0.9992
Product O	$Y = -0.000000030573321x^3 + 0.000023761735382x^2 - 0.000790556473361x + 0.040453518144967$	0.9992

Table 36: 4" Roof Jack Experiment and Trend Line Comparison

Product L			
CFM	**dP(Exp) inWC**	**dP(Eqn) inWC**	**%Diff**
200.9	0.649	0.677541	4.39766
180.9	0.547	0.560795	2.521952
160.7	0.452	0.451658	0.075657
140.1	0.371	0.350338	5.569191
120.1	0.304	0.262475	13.65969
100.7	0.242	0.187938	22.33947
80.3	0.192	0.121768	36.57933
60.6	0.154	0.070568	54.17669
40	0.136	0.031258	77.01582
20.9	0.129	0.008597	93.3356

Product M			
CFM	**dP(Exp) inWC**	**dP(Eqn) inWC**	**%Diff**
200.7	0.639	0.637985	0.158916
180.5	0.538	0.540334	0.433907
160.6	0.452	0.449528	0.546952
140.6	0.362	0.364784	0.769186
120.3	0.286	0.28661	0.213421
100.9	0.226	0.220363	2.494136
80.5	0.158	0.160767	1.751242
60.4	0.112	0.113284	1.146716
40.8	0.079	0.078822	0.224827
20.4	0.057	0.056522	0.839453

Product N			
CFM	**dP(Exp) inWC**	**dP(Eqn) inWC**	**%Diff**
200.4	0.802	0.800149	0.230786
180.4	0.678	0.683577	0.82255
160.4	0.577	0.570624	1.105068
140.3	0.459	0.462886	0.846731
120.1	0.363	0.362614	0.106208
100	0.275	0.272956	0.743204
80.5	0.197	0.197654	0.331864
60.4	0.134	0.134167	0.124589
40.3	0.086	0.087152	1.339893
20.7	0.06	0.05922	1.299893

Product O			
CFM	**dP(Exp) inWC**	**dP(Eqn) inWC**	**%Diff**
200.7	0.588	0.591759	0.639363
180.3	0.498	0.491168	1.371846
160.3	0.398	0.398377	0.094712
140.1	0.312	0.312019	0.006104
120.6	0.233	0.237085	1.75301
100	0.165	0.168442	2.086002
80.1	0.118	0.113873	3.49732
60.5	0.075	0.072828	2.895426
40.6	0.045	0.045479	1.063885
20.5	0.033	0.03397	2.938142

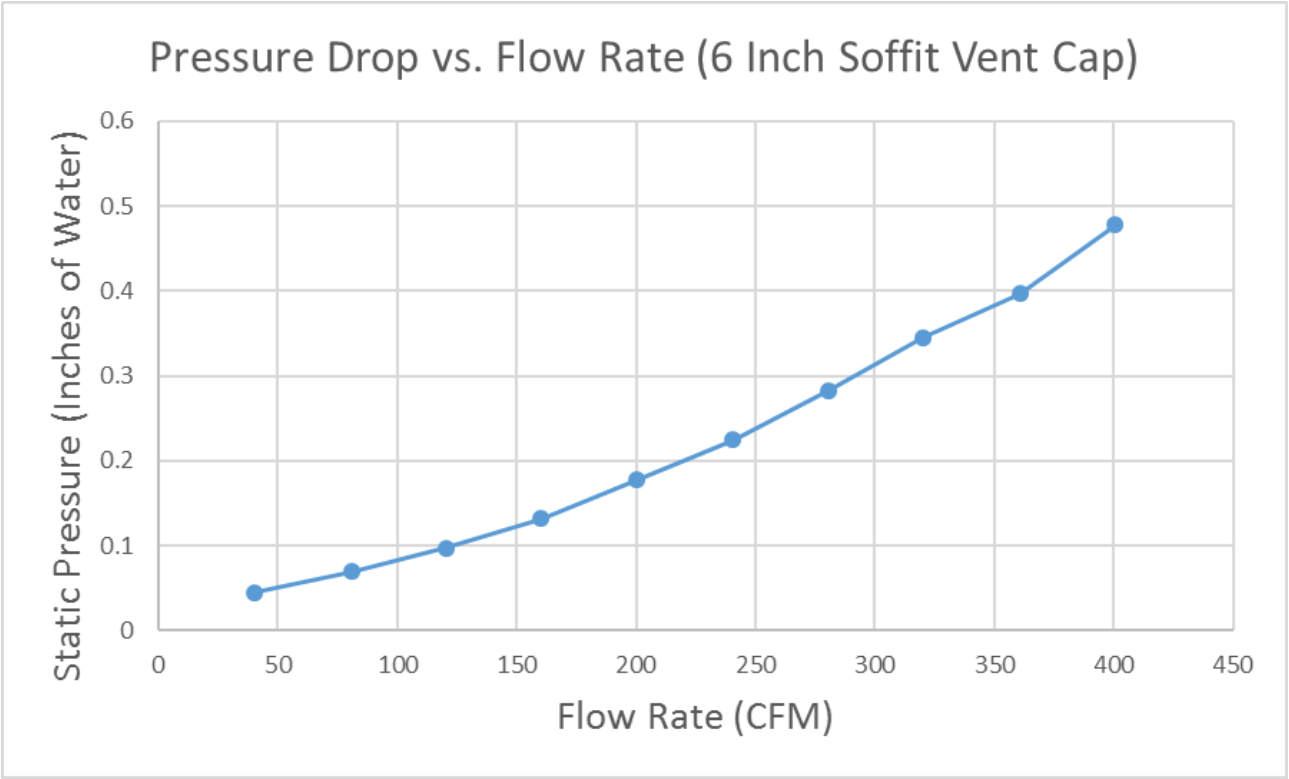

Figure 50: 6" Soffit Vent Cap Performance

Table 37: 6" Soffit Vent Cap Performance Trend Line

	Trend Line	R^2 Value
Product P	$Y = -0.000000001000825x^3 + 0.000002492640125x^2 + 0.000271808902902x + 0.030254214829606$	0.9993

Table 38: 6" Soffit Experiment and Trend Line Comparison

Product P			
CFM	**dP(Exp) inWC**	**dP(Eqn) inWC**	**%Diff**
400.5	0.478	0.47464	0.702828
360.7	0.397	0.405632	2.174295
320.3	0.345	0.340152	1.405098
280.7	0.283	0.280817	0.771379
240.7	0.225	0.226137	0.505164
200.1	0.177	0.17643	0.322093
160.2	0.132	0.133654	1.253368
120.5	0.097	0.09745	0.463723
80.7	0.069	0.067896	1.599282
40.3	0.045	0.045191	0.424179

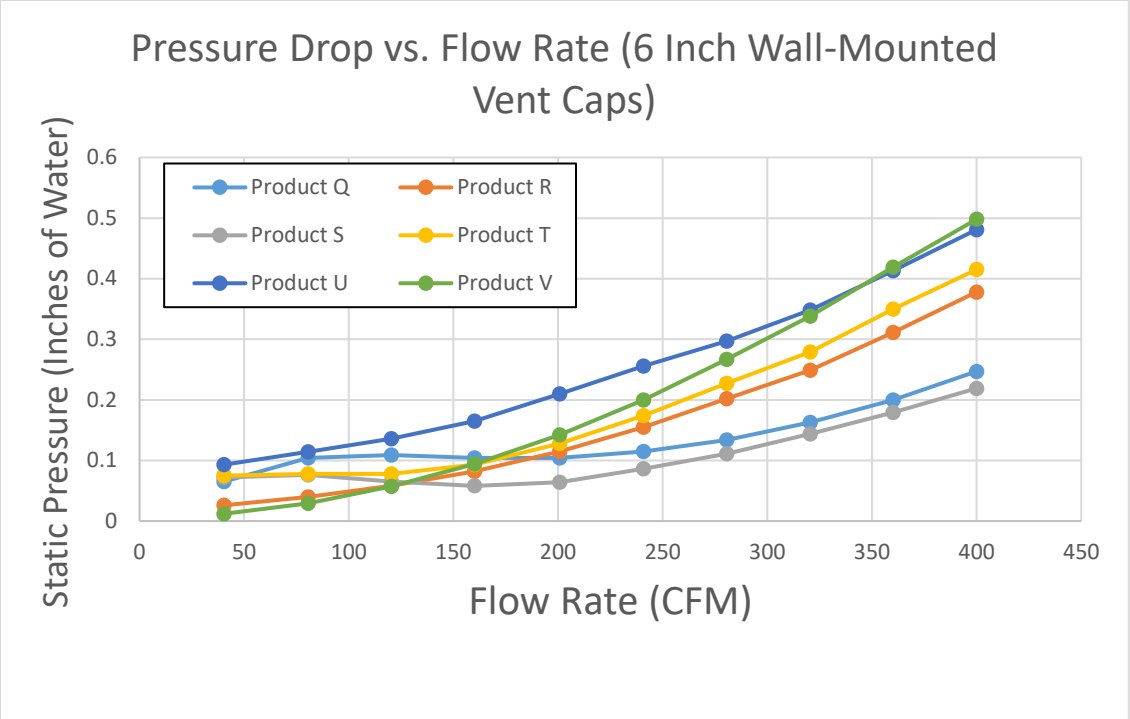

Figure 51: 6" Wall-Mounted Vent Cap Performance

Table 39: 6" Wall-Mounted Vent Cap Performance Trend Lines

	Trend Line	R^2 Value
Product Q	$Y = 0.000000010260360x^3 - 0.000005307710937x^2 + 0.001011421457558x + 0.040167171783979$	0.9839
Product R	$Y = 0.000000000524253x^3 + 0.000001760914471x^2 + 0.000107540064417x + 0.018894033063307$	0.9998
Product S	$Y = 0.000000000148095x^3 + 0.000002119225373x^2 - 0.000563115877042x + 0.097626093743791$	0.990
Product T	$Y = -0.000000003872553x^3 + 0.000005565087303x^2 - 0.000823489351220x + 0.102952842365828$	0.999
Product U	$Y = 0.000000000229541x^3 + 0.000001652865453x^2 + 0.000307423408572x + 0.077054981924263$	0.999
Product V	$Y = -0.000000002835456x^3 + 0.000004508723897x^2 - 0.000131573652305x + 0.010979354967451$	0.999

Table 40: 6" Wall-Mount Experiment and Trend Line Comparison

Product Q			
CFM	**dP(Exp) inWC**	**dP(Eqn) inWC**	**%Diff**
400	0.247	0.252165	2.091111
360	0.2	0.195107	2.446542
320.5	0.163	0.156908	3.737248
280.5	0.134	0.132703	0.967863
240.8	0.115	0.119214	3.664429
200.7	0.104	0.11231	7.990415
160	0.104	0.108144	3.984269
120.3	0.109	0.102891	5.604852
80.6	0.104	0.092579	10.98141
40.3	0.065	0.072979	12.27509

Product R			
CFM	**dP(Exp) inWC**	**dP(Eqn) inWC**	**%Diff**
400.1	0.378	0.377385	0.162598
360.6	0.311	0.311231	0.074243
320.7	0.249	0.251781	1.11696
280.8	0.202	0.199544	1.215682
240.4	0.155	0.153797	0.775945
200.1	0.115	0.11512	0.104479
160.6	0.082	0.083755	2.139873
120	0.058	0.058062	0.106756
80.1	0.04	0.039075	2.311344
40.8	0.026	0.026249	0.956009

Product S			
CFM	**dP(Exp) inWC**	**dP(Eqn) inWC**	**%Diff**
400.7	0.219	0.221777	1.268198
360.9	0.179	0.177386	0.901884
320.3	0.144	0.139542	3.095641
280.3	0.111	0.10955	1.306626
240.7	0.086	0.08693	1.081178
200.2	0.064	0.071017	10.96445
160.5	0.058	0.06245	7.672539
120.7	0.065	0.060792	6.473333
80.2	0.076	0.066172	12.93219
40.3	0.072	0.078384	8.866708

Product T			
CFM	**dP(Exp) inWC**	**dP(Eqn) inWC**	**%Diff**
400.1	0.415	0.416305	0.314377
360	0.35	0.347054	0.841669
320.1	0.279	0.28256	1.276073
280	0.227	0.223668	1.467672
240.1	0.174	0.172448	0.891874
200	0.128	0.129878	1.467219
160.4	0.093	0.098063	5.444481
120.2	0.078	0.077649	0.450333
80.6	0.078	0.070705	9.352927
40	0.075	0.07867	4.892753

Table 40 Continued

Product U			
CFM	**dP(Exp) inWC**	**dP(Eqn) inWC**	**%diff**
400	0.481	0.479173	0.379742
360.7	0.413	0.41376	0.18399
320.4	0.348	0.35278	1.373593
280.1	0.297	0.297886	0.298246
240	0.256	0.249215	2.650459
200.5	0.21	0.206989	1.433755
160.2	0.165	0.169667	2.828574
120.3	0.136	0.138358	1.733871
80.8	0.114	0.112807	1.046629
40.8	0.093	0.092365	0.682933

Product V			
CFM	**dP(Exp) inWC**	**dP(Eqn) inWC**	**%Diff**
400.6	0.498	0.499546	0.310354
360.1	0.419	0.415854	0.750915
320.8	0.338	0.339164	0.344497
280.7	0.267	0.266588	0.1542
240.6	0.2	0.200833	0.416653
200.6	0.142	0.14313	0.795732
160.2	0.094	0.093956	0.047137
120.8	0.057	0.055881	1.962936
80.7	0.029	0.028234	2.640744
40.3	0.012	0.012814	6.782727

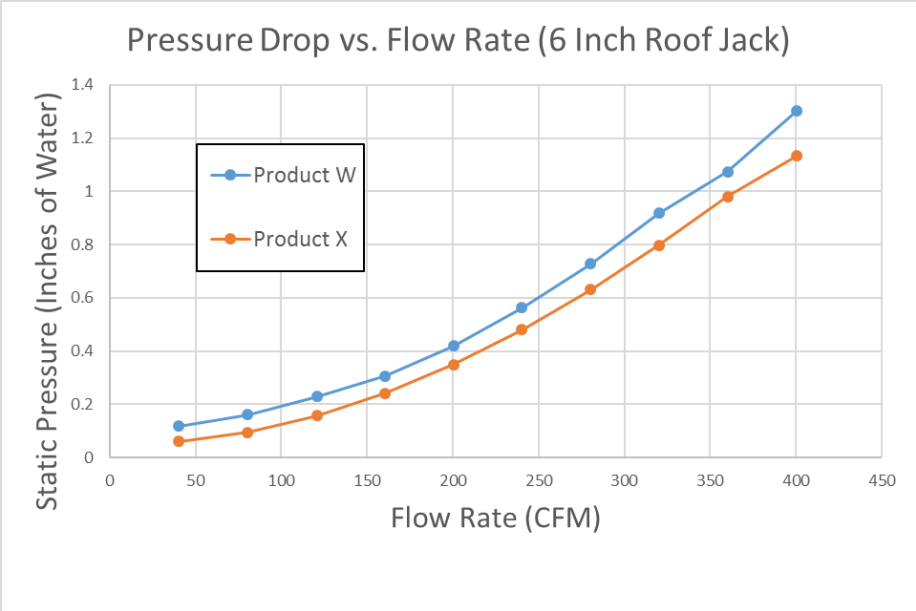

Figure 52: 6" Roof Jack Vent Cap Performance

Table 41: 6" Roof Jack Vent Cap Performance Trend Lines

	Trend Line	R^2 Value
Product W	$Y = -0.000000005823482x^3 + 0.000010498984870x^2 - 0.000319776247073x + 0.117303607622539$	0.999
Product X	$Y = -0.000000010183990x^3 + 0.000012443316285x^2 - 0.000680576345367x + 0.071903380425450$	0.999

Table 42: 6" Roof Jack Experiment and Trend Line Comparison

Product W			
CFM	**dP(Exp) inWC**	**dP(Eqn) inWC**	**%Diff**
400.2	1.302	1.297585	0.339108
360.1	1.074	1.09165	1.64337
320.2	0.918	0.90017	1.942297
280.3	0.727	0.724307	0.370414
240.2	0.563	0.565538	0.450792
200.3	0.42	0.427675	1.82734
160.5	0.307	0.312359	1.745502
120.7	0.229	0.221421	3.309667
80.3	0.161	0.156309	2.913862
40.1	0.117	0.120988	3.40816

Product X			
CFM	**dP(Exp) inWC**	**dP(Eqn) inWC**	**%Diff**
400.6	1.134	1.14146	0.657815
360.7	0.98	0.96743	1.282703
320	0.797	0.794606	0.300432
280.7	0.631	0.636066	0.802795
240.4	0.481	0.48593	1.025028
200.3	0.35	0.352972	0.84909
160	0.241	0.239846	0.478656
120.1	0.158	0.152007	3.793219
80.7	0.094	0.092666	1.419611
40.3	0.061	0.064019	4.948637

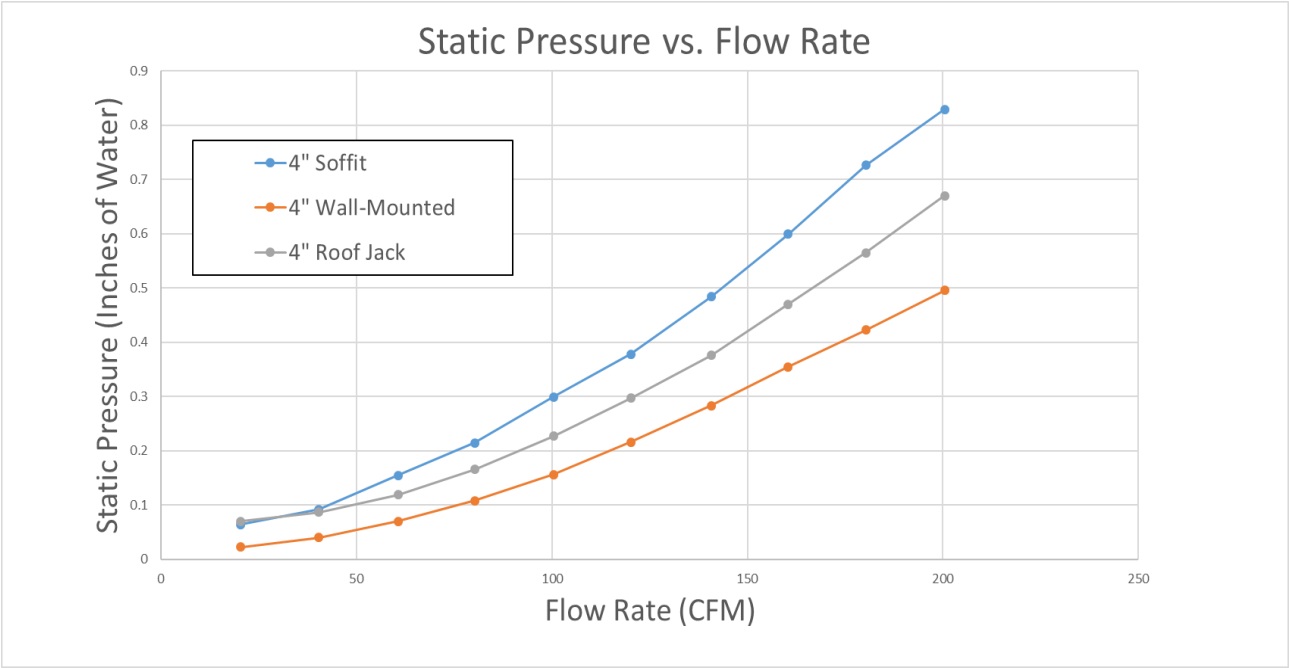

Figure 53: 4" Vent Cap Performance Average

Table 43: 4" Average Vent Cap Performance Trend Line Data

	Trend Line	R^2 Value
4" Soffit Average	$Y = -0.000000038168659x^3 + 0.000026194577085x^2 + 0.000206580531660x + 0.048613632727994$	0.999
4" Roof Jack Average	$Y = -0.000000028922608x^3 + 0.000023024810719x^2 - 0.000467646612737x + 0.070041843478879$	0.996
4" Wall-Mounted Average	$Y = -0.000000039273836x^3 + 0.000022008015535x^2 - 0.000482495662086x + 0.025186613063975$	0.999

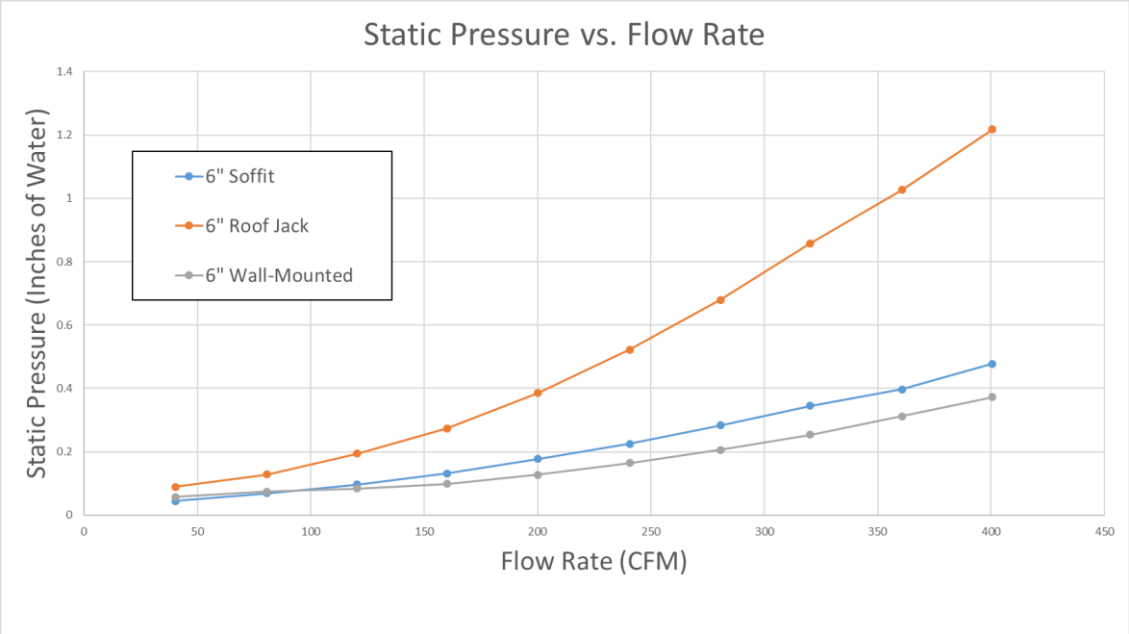

Figure 54: 6" Vent Cap Performance Average

Table 44: 6" Average Vent Cap Performance Trend Line Data

	Trend Line	R^2 Value
6” Soffit Average	$Y = -0.000000001000825x^3 + 0.000002492640125x^2 + 0.000271808902902x + 0.030254214829606$	0.999
6” Roof Jack Average	$y = -0.000000008004988x^3 + 0.000011470275755x^2 - 0.000500280229749x + 0.094821362198793$	0.999
6” Wall-Mounted Average	$Y = 0.000000000737472x^3 + 0.000001728023913x^2 - 0.000019961177385x + 0.058323935446546$	0.999

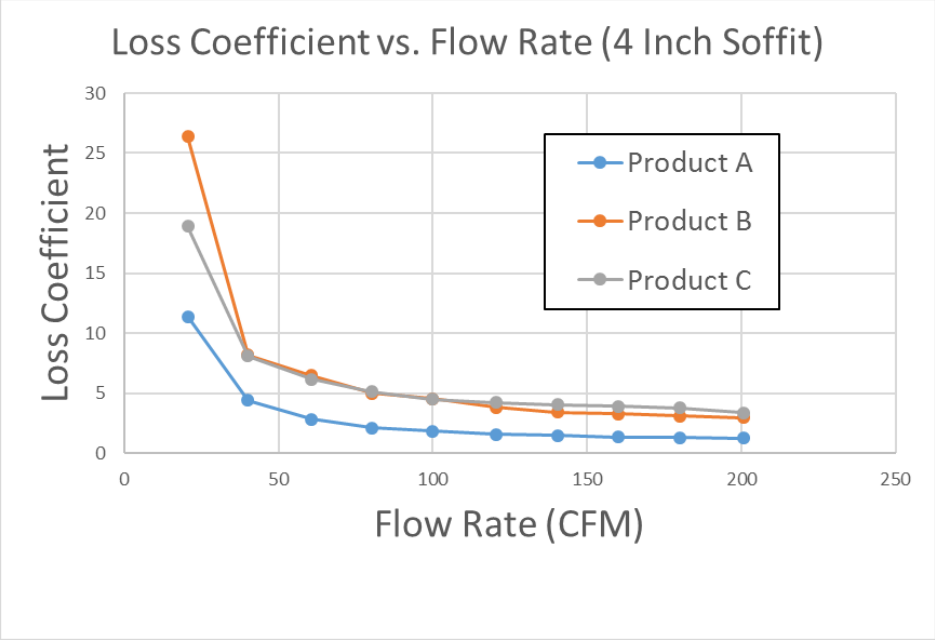

Figure 55: 4” Soffit Loss Coefficient Performance

Table 45: 4" Soffit Loss Coefficient Performance Trend Lines

	Trend Line	R^2 Value
Product A	$Y = -0.000007502983989x^3 + 0.003043595200705x^2 - 0.390909710502144x + 17.265465626530200$	0.940
Product B	$Y = -0.000017861034786x^3 + 0.007148088704415x^2 - 0.901641791473548x + 39.101558711493400$	0.900
Product C	$Y = -0.000011428674650x^3 + 0.004585102698202x^2 - 0.583329914190493x + 27.441531504464400$	0.942

Table 46: 4" Soffit Data and Trend Line Comparison

Product A			
CFM	**K(Exp)**	**K(Eqn)**	**%Diff**
200.6	1.23	0.758635	38.32234
180.1	1.31	1.754339	33.91901
160.1	1.36	1.904402	40.02958
140.4	1.47	1.612415	9.688089
120.5	1.57	1.226712	21.86549
100	1.82	1.107463	39.15041
80.4	2.11	1.611172	23.64114
60.7	2.81	3.073311	9.370493
40.1	4.4	6.000316	36.37083
20.7	11.38	10.41124	8.512872

Product B			
CFM	**K(Exp)**	**K(Eqn)**	**%Diff**
200.6	2.96	1.695743	42.71137
180.5	3.09	4.205718	36.10737
160.6	3.26	4.679039	43.5288
140.9	3.43	4.007902	16.84847
120.1	3.82	2.97739	22.05784
100.6	4.52	2.553159	43.51418
80.1	5	3.563074	28.73852
60.8	6.49	6.691279	3.101369
40.3	8.18	13.20551	61.43661
20.4	26.36	23.53118	10.73148

Product C			
CFM	**K(Exp)**	**K(Eqn)**	**%Diff**
200.4	3.36	2.701603	19.59514
180.3	3.77	4.334233	14.96638
160.4	3.89	4.67785	20.25322
140.9	4.03	4.308534	6.911519
120	4.2	3.718671	11.46022
100.6	4.49	3.525805	21.47429
80	5.12	4.268314	16.63449
60.3	6.17	6.432776	4.258925
40.7	8.09	10.52467	30.0948
20	18.89	17.51754	7.265511

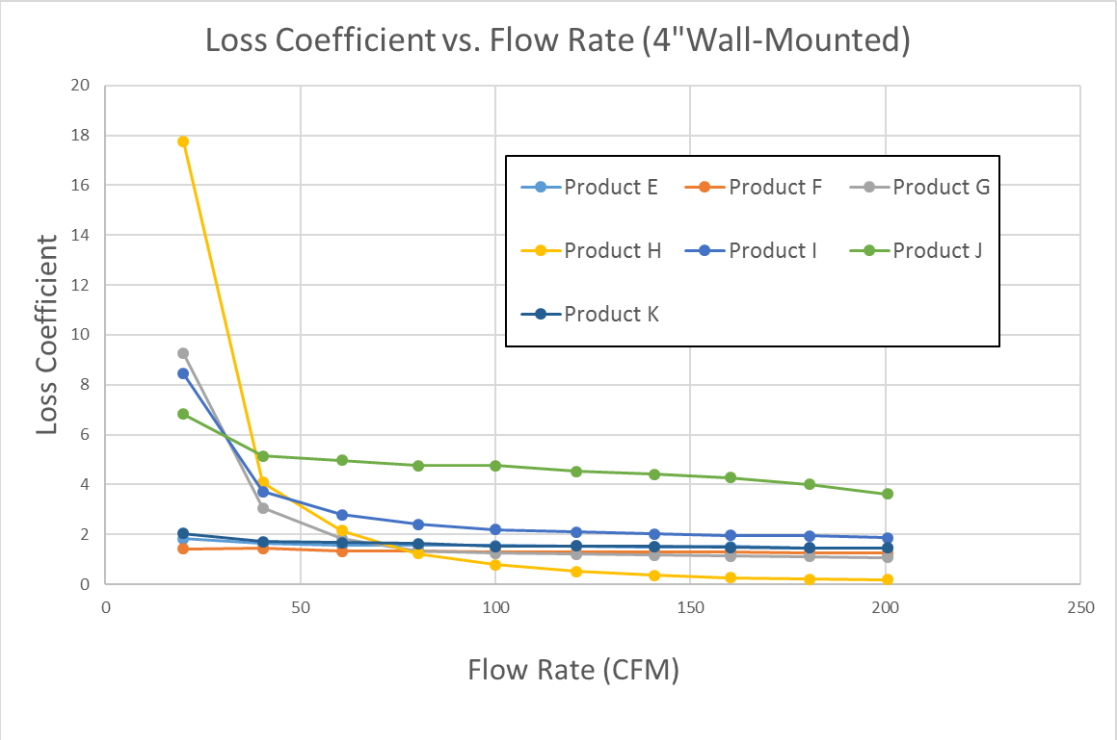

Figure 56: 4" Wall-Mounted Loss Coefficient Performance

Table 47: 4" Wall-Mounted Loss Coefficient Performance Trend Lines

	Trend Line	R^2 Value
Product E	$Y = -0.000000242755804x^3 + 0.000091086092031x^2 - 0.011421576281925x + 1.999938158115090$	0.951
Product F	$Y = -0.000000000000804x^6 + 0.000000000557444x^5 - 0.000000152204894x^4 + 0.000020593634177x^3 - 0.001413495016317x^2 + 0.043334893560863x + 0.963719027015243$	0.944
Product G	$Y = 0.000000085339505x^4 - 0.000044570394215x^3 + 0.008290814802670x^2 - 0.647489694978875x + 19.069552871851600$	0.983
Product H	$Y = 0.000000192188800x^4 - 0.000099066694448x^3 + 0.018162525928795x^2 - 1.399218761790700x + 38.858310358369500$	0.976
Product I	$Y = 0.000000063857723x^4 - 0.000033167310191x^3 + 0.006147853312269x^2 - 0.482469973950667x + 15.732301080637300$	0.983
Product J	$Y = 0.000000022521801x^4 - 0.000011953606368x^3 + 0.002197266967744x^2 - 0.170196060522990x + 9.420641704275400$	0.978
Product K	$Y = 0.000000003913492x^4 - 0.000001988991867x^3 + 0.000364523121574x^2 - 0.029748155172206x + 2.484648031241150$	0.965

Table 48: 4" Wall-Mounted Data and Trend Line Comparison

Product E			
CFM	**K(Exp)**	**K(Eqn)**	**%Diff**
200.5	1.43	1.414948	1.052618
180.7	1.46	1.477914	1.22697
160.3	1.51	1.509685	0.020892
140.7	1.49	1.519943	2.00963
120.8	1.54	1.521471	1.20321
100	1.56	1.525886	2.186818
80.1	1.56	1.544722	0.979389
60.6	1.56	1.588267	1.812017
40.4	1.64	1.671166	1.900391
20	1.83	1.805999	1.311529

Product F			
CFM	**K(Exp)**	**K(Eqn)**	**%Diff**
200.2	1.24	1.237106	0.233367
180.6	1.27	1.277177	0.565103
160.4	1.29	1.27759	0.961977
140.3	1.29	1.290677	0.052489
120.1	1.29	1.304393	1.115698
100.1	1.31	1.305854	0.316509
80.8	1.33	1.30904	1.575974
60.1	1.32	1.346537	2.010379
40.3	1.43	1.416687	0.930945
20.8	1.41	1.412487	0.176348

Product G			
CFM	**K(Exp)**	**K(Eqn)**	**%Diff**
200.8	1.08	1.226574	13.57168
180.2	1.11	0.794452	28.42775
160.1	1.12	1.081901	3.401723
140	1.17	1.403828	19.98532
120.4	1.2	1.439513	19.95938
100.3	1.24	1.196767	3.486544
80.3	1.34	1.006554	24.88406
60.5	1.83	1.516315	17.14127
40.5	3.05	3.714011	21.77087
20.2	9.26	9.020086	2.590859

Product H			
CFM	**K(Exp)**	**K(Eqn)**	**%Diff**
200.5	0.18	0.549253	205.1407
180.5	0.21	-0.54287	358.5086
160.5	0.26	0.096324	62.95239
140.9	0.35	0.918322	162.3778
120.6	0.51	1.162239	127.89
100.3	0.79	0.722888	8.495151
80.6	1.22	0.310493	74.54972
60.2	2.15	1.358101	36.83252
40.9	4.08	5.772581	41.48482
20.3	17.74	17.14267	3.367155

Product I			
CFM	**K(Exp)**	**K(Eqn)**	**%Diff**
200.2	1.87	1.994385	6.651625
180.8	1.93	1.679361	12.98648
160.3	1.96	1.9138	2.357149
140.5	2.01	2.199642	9.434937
120.1	2.1	2.293572	9.217702
100.2	2.2	2.183802	0.736251
80.2	2.41	2.11397	12.28339
60.7	2.78	2.547155	8.375702
40.5	3.72	4.244779	14.10696
20.1	8.45	8.259533	2.254042

Product J			
CFM	**K(Exp)**	**K(Eqn)**	**%Diff**
200.1	3.62	3.677641	1.592288
180.6	4.01	3.896489	2.830693
160.1	4.27	4.23561	0.805378
140.3	4.41	4.507699	2.215398
120.2	4.53	4.651326	2.678274
100	4.75	4.672279	1.63623
80.7	4.75	4.668392	1.718053
59.9	4.96	4.830564	2.609587
40.4	5.15	5.402797	4.908679
20.7	6.83	6.7372	1.358714

Table 48 Continued

Product K			
CFM	**K(Exp)**	**K(Eqn)**	**%Diff**
200	1.46	1.465594	0.383159
180.3	1.46	1.448794	0.767541
159.9	1.47	1.474744	0.322743
140.6	1.52	1.509161	0.713081
120.3	1.53	1.538184	0.534889
100	1.51	1.557421	3.140468
80.7	1.63	1.578576	3.154865
60.6	1.66	1.630708	1.76458
40.6	1.7	1.755261	3.250673
20.5	2.03	2.011557	0.9085

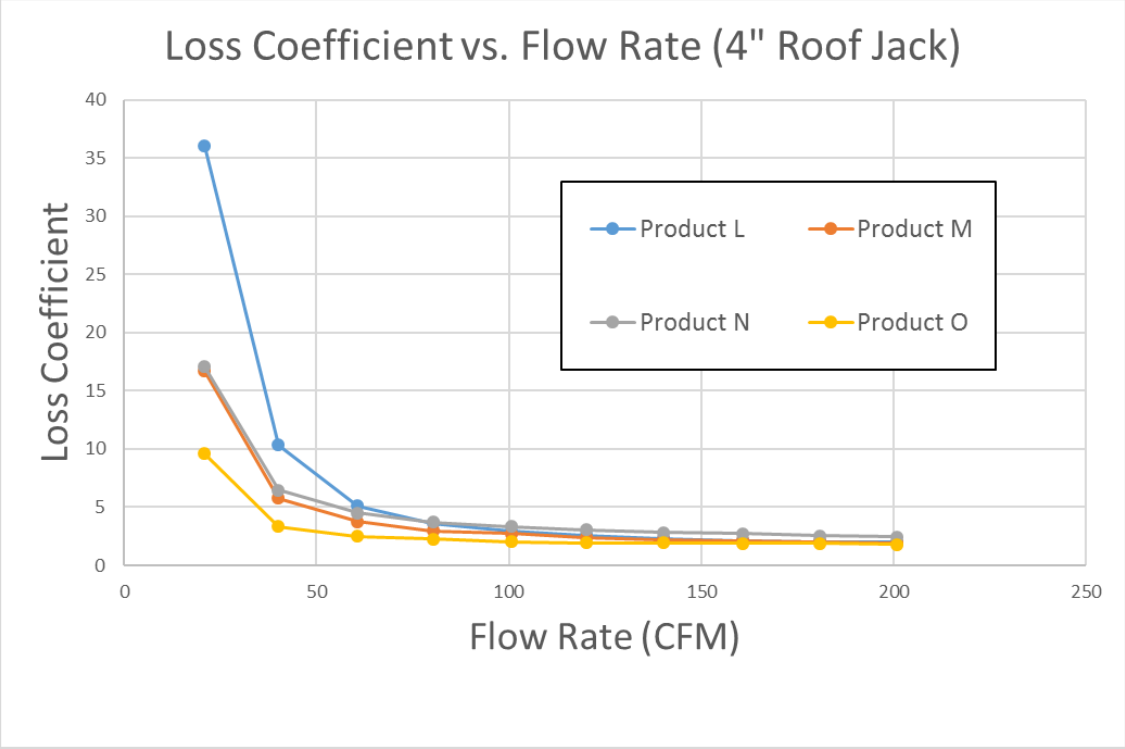

Figure 57: 4" Roof Jack Loss Coefficient Performance

Table 49: 4" Roof Jack Loss Coefficient Performance Trend Lines

	Trend Line	R^2 Value
Product L	$Y = 0.000000378531422x^4 - 0.000196296019439x^3 + 0.036202901648828x^2 - 2.800795268744190x + 79.205321168137800$	0.978
Product M	$Y = 0.000000153162889x^4 - 0.000079435249402x^3 + 0.014661941540244x^2 - 1.139842011849310x + 34.051458891107800$	0.982
Product N	$Y = 0.000000154239172x^4 - 0.000079672397595x^3 + 0.014633390957259x^2 - 1.132476369826380x + 34.431398611421700$	0.979
Product O	$Y = 0.000000089540091x^4 - 0.000046265815523x^3 + 0.008475706313371x^2 - 0.648074865927437x + 19.367626425909100$	0.970

Table 50: 4" Roof Jack Data and Trend Line Comparison

Product L			
CFM	**K(Exp)**	**K(Eqn)**	**%Diff**
200.9	1.96	2.666106	36.0258
180.9	2.04	0.592463	70.95768
160.7	2.13	1.855614	12.88196
140.1	2.3	3.44605	49.82824
120.1	2.57	3.726841	45.01328
100.7	2.91	2.757452	5.242196
80.3	3.63	1.841085	49.2814
60.6	5.11	3.847476	24.70693
40	10.36	13.50425	30.34989
20.9	35.99	34.76266	3.410215

Product M			
CFM	**K(Exp)**	**K(Eqn)**	**%Diff**
200.7	1.93	2.206944	14.34945
180.5	2.01	1.440259	28.34532
160.6	2.14	2.008979	6.122487
140.6	2.23	2.701611	21.14847
120.3	2.41	2.899883	20.32709
100.9	2.71	2.587643	4.515021
80.5	2.97	2.300889	22.529
60.4	3.74	3.229099	13.66046
40.8	5.78	6.982149	20.79842
20.4	16.69	16.25254	2.621072

Product N			
CFM	**K(Exp)**	**K(Eqn)**	**%Diff**
200.4	2.43	2.714214	11.69605
180.4	2.54	1.968258	22.50952
160.4	2.73	2.577415	5.589204
140.3	2.84	3.322489	16.98903
120.1	3.07	3.564568	16.10969
100	3.35	3.269191	2.412215
80.5	3.71	3.010234	18.86162
60.4	4.48	3.911835	12.68225
40.3	6.45	7.750752	20.1667
20.7	17.07	16.58104	2.864413

Product O			
CFM	**K(Exp)**	**K(Eqn)**	**%Diff**
200.7	1.78	1.958532	10.02987
180.3	1.87	1.498966	19.84137
160.3	1.89	1.823334	3.527312
140.1	1.94	2.204057	13.61117
120.6	1.95	2.272145	16.52023
100	2.01	2.005397	0.229028
80.1	2.24	1.745941	22.05618
60.5	2.5	2.136569	14.53724
40.6	3.33	4.173824	25.34007
20.5	9.57	9.261235	3.226383

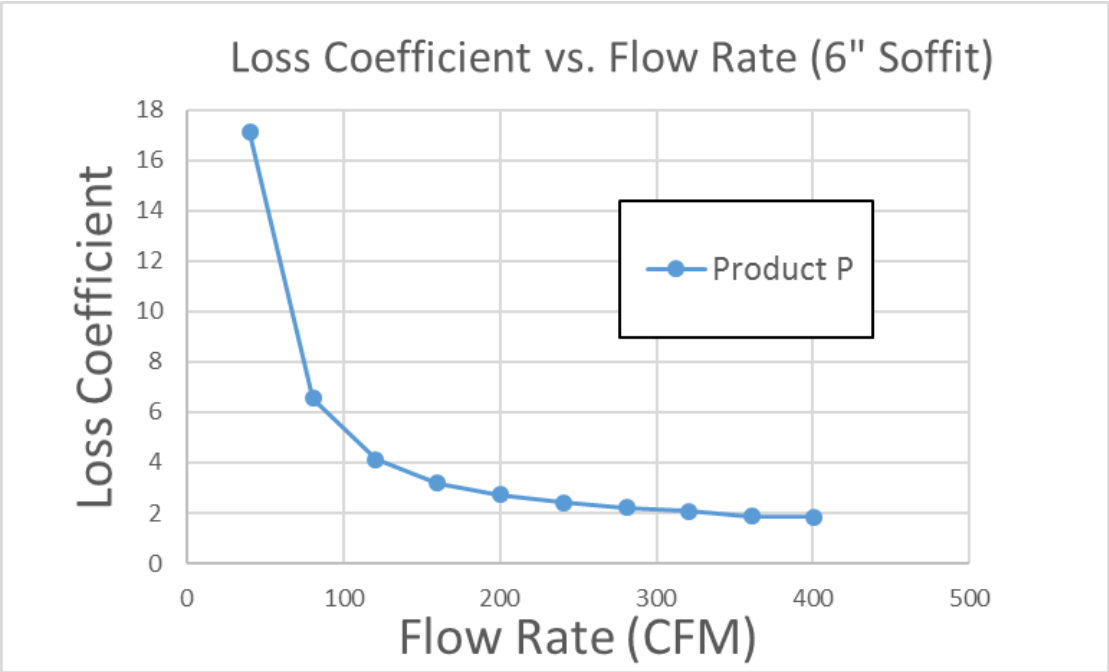

Figure 58: 6" Soffit Loss Coefficient Performance

Table 51: 6" Soffit Loss Coefficient Performance Trend Line

	Trend Line	R^2 Value
Product P	$Y = 0.000000008952307x^4 - 0.000009316184529x^3 + 0.003464137537811x^2 - 0.547161797968593x + 33.718453426644900$	0.987

Table 52: 6" Soffit Data and Trend Line Comparison

Product P			
CFM	**K(Exp)**	**K(Eqn)**	**%Diff**
400.5	1.84	2.081295	13.11387
360.7	1.88	1.398006	25.63798
320.3	2.08	1.947777	6.356864
280.7	2.22	2.60984	17.56035
240.7	2.4	2.849112	18.71299
200.1	2.73	2.646513	3.058131
160.2	3.17	2.560904	19.21438
120.5	4.12	3.672647	10.85808
80.7	6.54	7.606153	16.30203
40.3	17.1	16.70777	2.29377

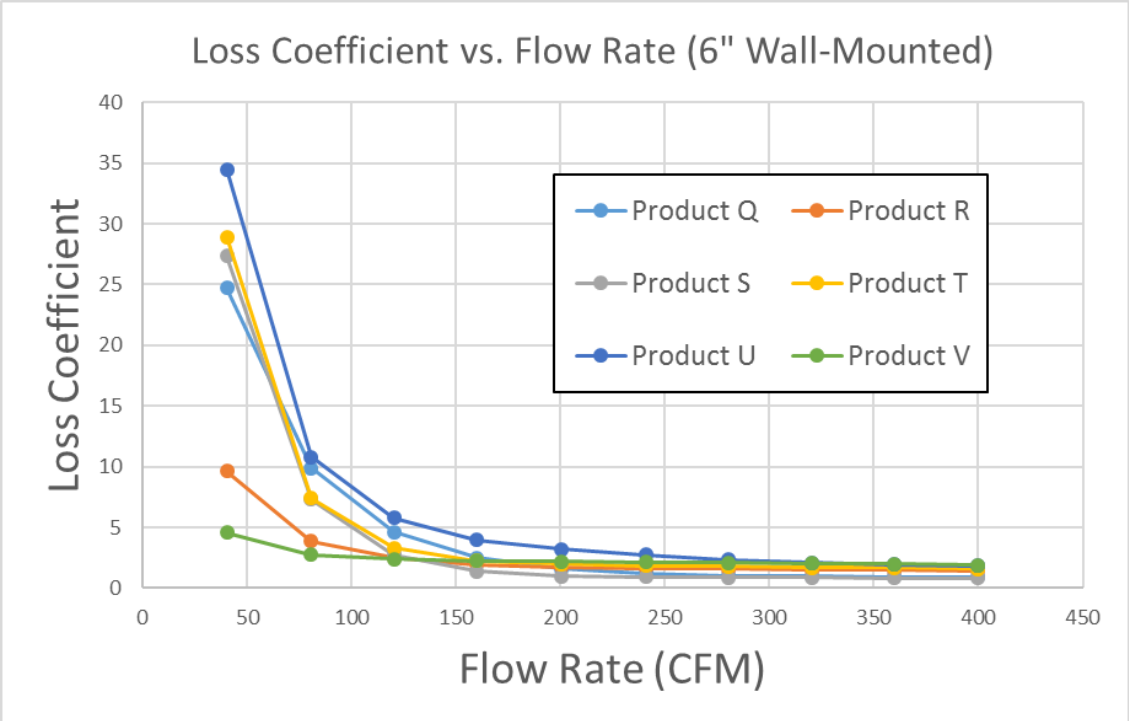

Figure 59: 6" Wall-Mounted Loss Coefficient Performance

Table 53: 6" Wall-Mounted Loss Coefficient Performance Trend Line

	Trend Line	R^2 Value
Product Q	$Y = -0.000002112080405x^3 + 0.001746545130630x^2 - 0.457973640129686x + 38.929646832895700$	0.971
Product R	$Y = 0.000000005081348x^4 - 0.000005285032753x^3 + 0.001963597332251x^2 - 0.308762727116739x + 19.088508378370500$	0.986
Product S	$Y = 0.000000017497547x^4 - 0.000018274469839x^3 + 0.006804166644077x^2 - 1.063299226831710x + 59.544766086712000$	0.984
Product T	$Y = 0.000000019458676x^4 - 0.000020139252034x^3 + 0.007403612048989x^2 - 1.136511627431660x + 62.938337917714400$	0.981
Product U	$Y = 0.000000020981251x^4 - 0.000021739972901x^3 + 0.008033425376963x^2 - 1.253420517517990x + 72.723240377885000$	0.984
Product V	$Y = 0.000000001546267x^4 - 0.000001608561834x^3 + 0.000594389038045x^2 - 0.092844299130024x + 7.361322661647100$	0.982

Table 54: 6" Wall-Mounted Data and Trend Line Comparison

Product Q			
CFM	**K(Exp)**	**K(Eqn)**	**%Diff**
400	0.95	0.014266	98.49834
360	0.95	1.870162	96.85915
320.5	0.98	2.021074	106.2321
280.5	1.05	1.273435	21.2795
240.8	1.22	0.432037	64.58712
200.7	1.59	0.291351	81.67602
160	2.51	1.714338	31.69966
120.3	4.65	5.43446	16.87011
80.6	9.88	12.25726	24.06132
40.3	24.7	23.17162	6.187781

Product R			
CFM	**K(Exp)**	**K(Eqn)**	**%Diff**
400.1	1.46	1.602021	9.727449
360.6	1.48	1.183967	20.00226
320.7	1.49	1.451931	2.554959
280.8	1.58	1.791889	13.41067
240.4	1.66	1.887642	13.71339
200.1	1.77	1.730259	2.245272
160.6	1.96	1.635426	16.55988
120	2.49	2.233914	10.28456
80.1	3.85	4.448152	15.53641
40.8	9.64	9.414807	2.336026

Product S			
CFM	**K(Exp)**	**K(Eqn)**	**%Diff**
400.7	0.84	1.325057	57.7449
360.9	0.85	-0.14803	117.4152
320.3	0.87	0.684196	21.35674
280.3	0.87	1.651771	89.8587
240.7	0.92	1.707882	85.63934
200.2	0.99	0.856975	13.43687
160.5	1.39	0.217316	84.36574
120.7	2.75	1.910545	30.52565
80.2	7.29	9.329855	27.98156
40.3	27.36	26.59446	2.798027

Product T			
CFM	**K(Exp)**	**K(Eqn)**	**%Diff**
400.1	1.6	2.151705	34.48157
360	1.67	0.516366	69.07987
320.1	1.68	1.497038	10.8906
280	1.79	2.665326	48.90088
240.1	1.86	2.779109	49.41446
200	1.98	1.80036	9.072741
160.4	2.23	0.893027	59.95393
120.2	3.33	2.384321	28.39878
80.6	7.41	9.708193	31.01475
40	28.93	28.08455	2.922384

Table 54 Continued

Product U			
CFM	**K(Exp)**	**K(Eqn)**	**%Diff**
400	1.86	2.464854	32.51901
360.7	1.96	0.724109	63.05564
320.4	2.09	1.864175	10.805
280.1	2.34	3.310112	41.45779
240	2.74	3.704988	35.21853
200.5	3.22	3.037652	5.662968
160.2	3.97	2.533304	36.18881
120.3	5.8	4.742421	18.23411
80.8	10.78	13.32035	23.56539
40.8	34.48	33.53806	2.731834

Product V			
CFM	**K(Exp)**	**K(Eqn)**	**%Diff**
400.6	1.92	1.966222	2.407372
360.1	1.99	1.89231	4.909062
320.8	2.03	2.017885	0.596814
280.7	2.09	2.156297	3.172092
240.6	2.13	2.208876	3.703102
200.6	2.18	2.174376	0.258
160.2	2.26	2.14712	4.994683
120.8	2.41	2.313148	4.018737
80.7	2.75	2.959929	7.633783
40.3	4.56	4.483836	1.670273

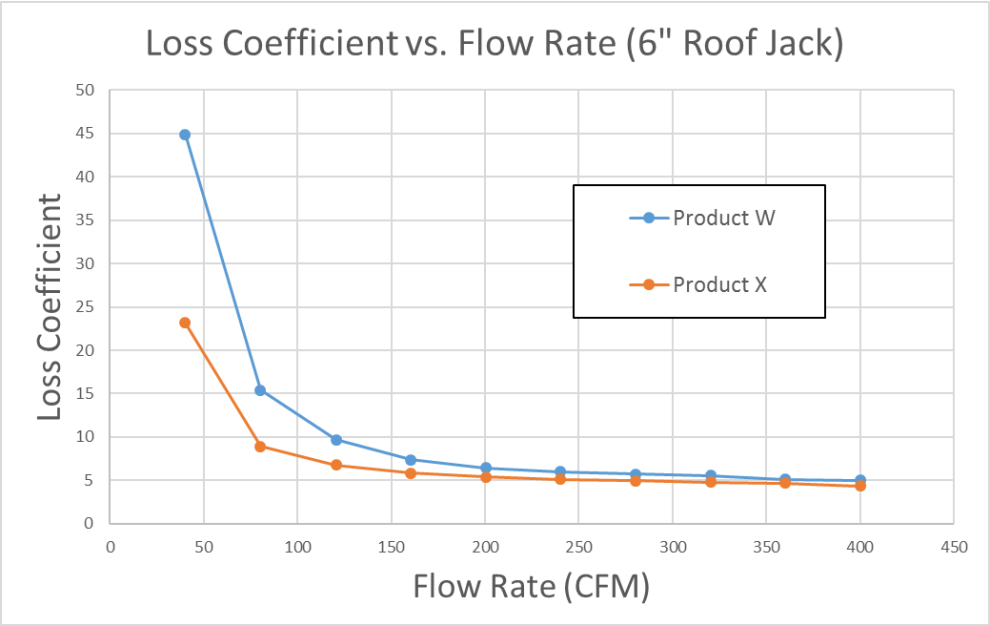

Figure 60: 6" Roof Jack Loss Coefficient Performance

Table 55: 6" Roof Jack Loss Coefficient Performance Trend Lines

	Loss Coefficient	R^2 Value
Product W	$Y = 0.000000025580723x^4 - 0.000026546648339x^3 + 0.009813534335733x^2 - 1.527959326453810x + 90.835656321675500$	0.982
Product X	$Y = 0.000000012564783x^4 - 0.000012992932634x^3 + 0.004768516337487x^2 - 0.733818940802917x + 45.173710135760400$	0.976

Table 56: 6" Roof Jack Data and Trend Line Comparison

Product W			
CFM	**K(Exp)**	**K(Eqn)**	**%Diff**
400.2	5.02	5.724364	14.03115
360.1	5.11	3.700893	27.57548
320.2	5.53	5.137437	7.098794
280.3	5.71	6.860533	20.14943
240.2	6.02	7.276768	20.87654
200.3	6.46	6.350269	1.698629
160.5	7.36	5.614755	23.71257
120.7	9.7	8.128547	16.20054
80.3	15.41	18.7373	21.59182
40.1	44.91	43.69913	2.696208

Product X			
CFM	**K(Exp)**	**K(Eqn)**	**%Diff**
400.6	4.36	4.756534	9.094822
360.7	4.65	3.835625	17.51344
320	4.8	4.646604	3.19574
280.7	4.94	5.554039	12.42994
240.4	5.14	5.798169	12.80484
200.3	5.38	5.315719	1.19482
160	5.81	4.852102	16.48706
120.1	6.76	5.929348	12.28775
80.7	8.91	10.7138	20.24469
40.3	23.18	22.52805	2.812554

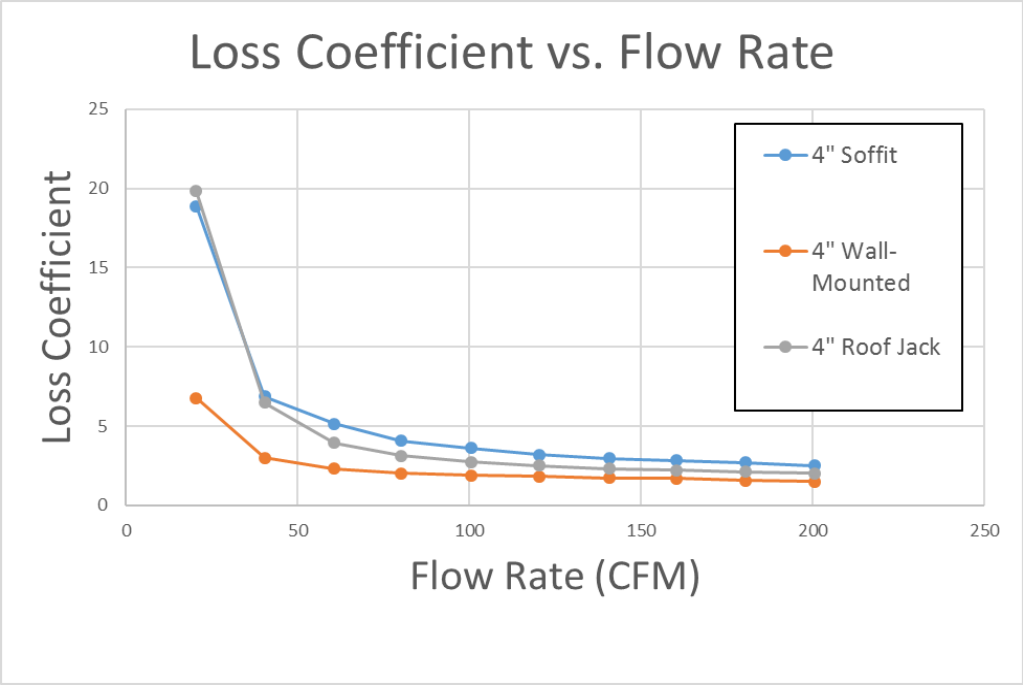

Figure 61: 4" Loss Coefficient Average

Table 57: 4" Average Loss Coefficient Trend Lines

	Trend line	R^2 Value
4" Soffit	$Y = 0.000000164586257x^4 - 0.000085023593626x^3 + 0.015635361757982x^2 - 1.215146538346710x + 37.257739975101200$	0.975
4" Wall-Mounted	$Y = 0.000000052999510x^4 - 0.000027495478246x^3 + 0.005066382287185x^2 - 0.393163572498291x + 12.733647660206400$	0.981
4" Roof Jack	$Y = 0.000000192292517x^4 - 0.000099613509935x^3 + 0.018351720167471x^2 - 1.420388594366280x + 41.545973874910200$	0.979

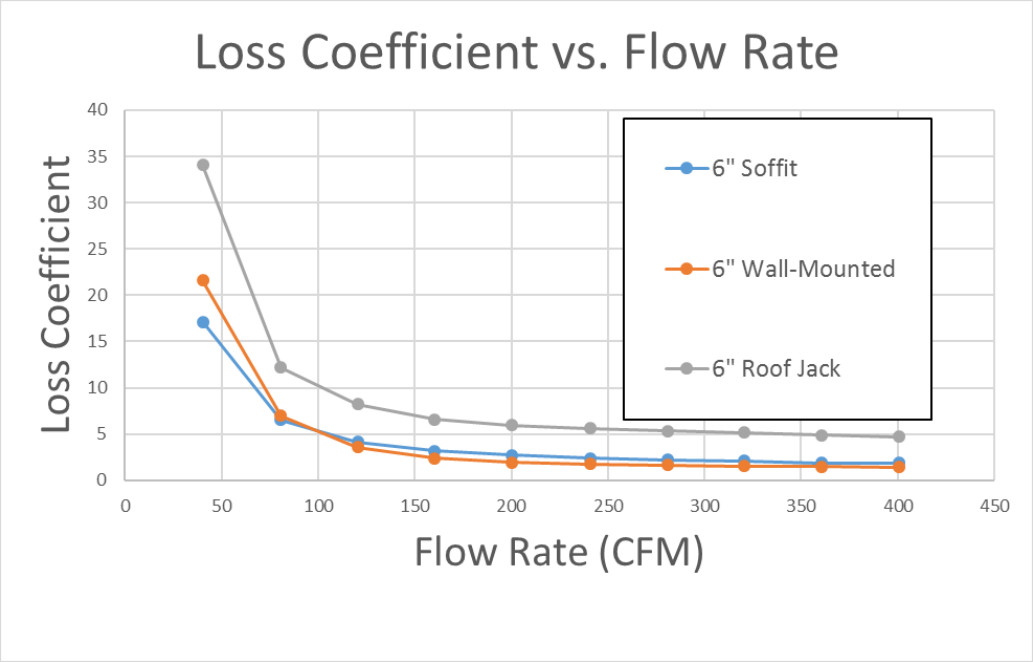

Figure 62: 6" Loss Coefficient Average

Table 58: 6" Average Loss Coefficient Trend Lines

	Trend Line	R^2 Value
6" Soffit	$Y = 0.000000008952307x^4 - 0.000009316184529x^3 + 0.003464137537811x^2 - 0.547161797968593x + 33.718453426644900$	0.987
6" Wall-Mounted	$Y = 0.000000012549039x^4 - 0.000013101856965x^3 + 0.004885928893674x^2 - 0.769321178584029x + 45.009112209659600$	0.986
6" Roof Jack	$Y = 0.000000019069397x^4 - 0.000019773155680x^3 + 0.007294798552891x^2 - 1.131824910128220x + 68.068679762996400$	0.980

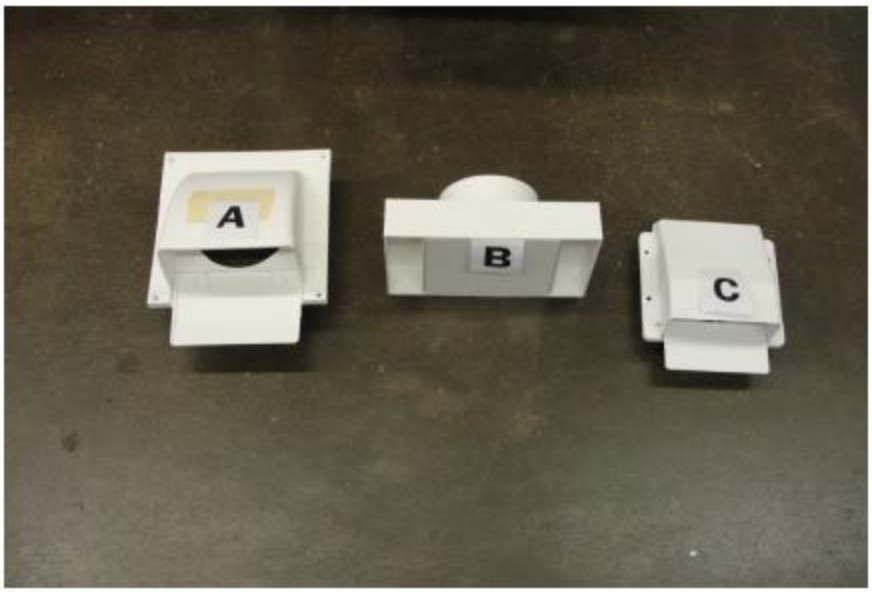

Figure 63: 4" Soffit Vent Caps

Figure 64: 4" Wall-Mounted Vent Caps

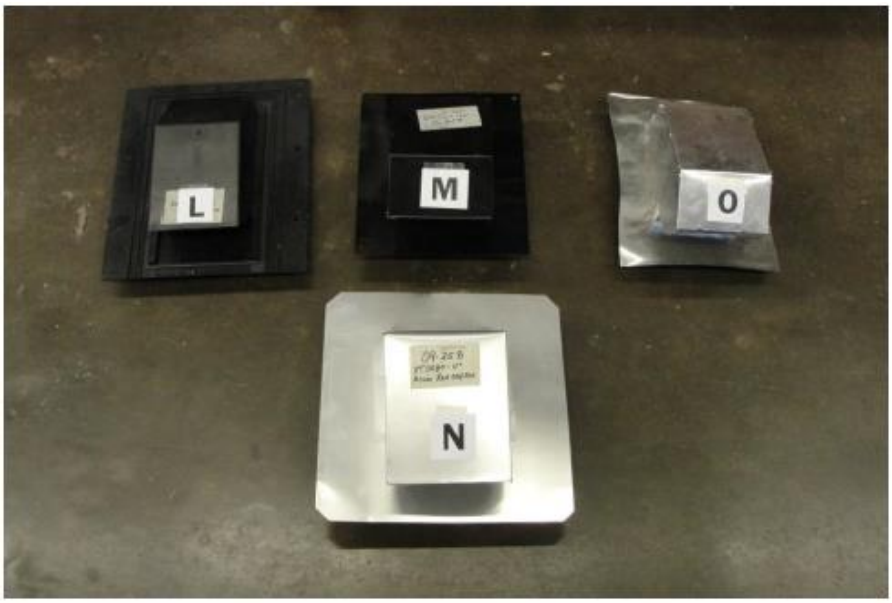

Figure 65: 4" Roof Jack Vent Caps

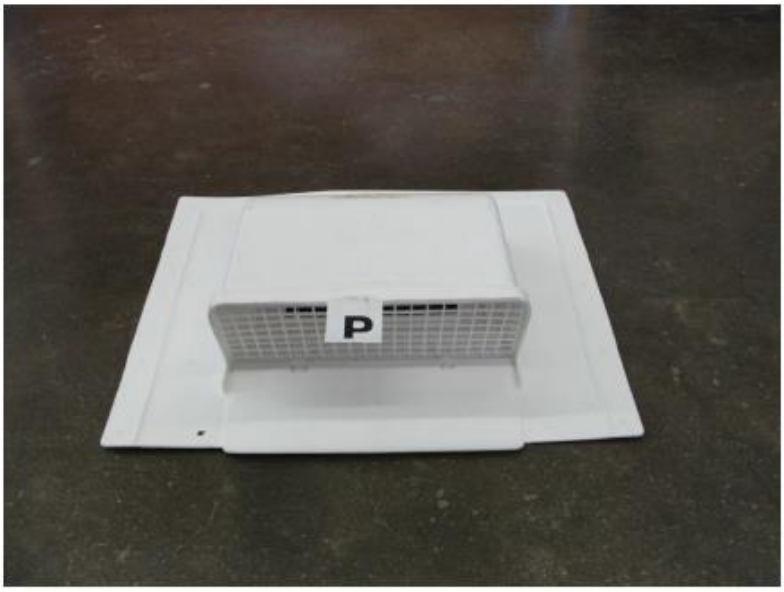

Figure 66: 6" Soffit Vent Cap

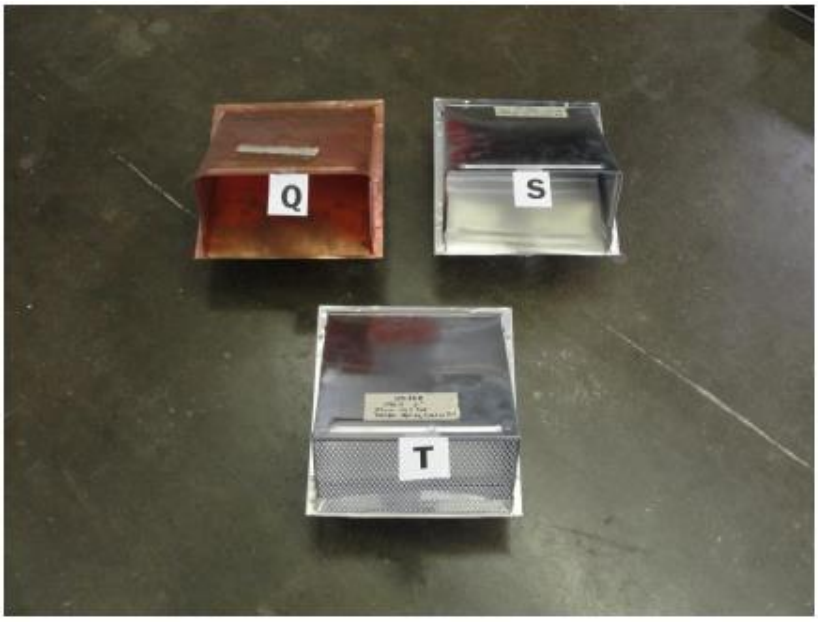

Figure 67: 6” Wall-Mounted Vent Caps

Figure 68: 6” Wall-Mounted Vent Caps

Figure 69: 6" Roof Jack Vent Caps

APPENDIX C: ELBOW DATA (ASHRAE, 2005)

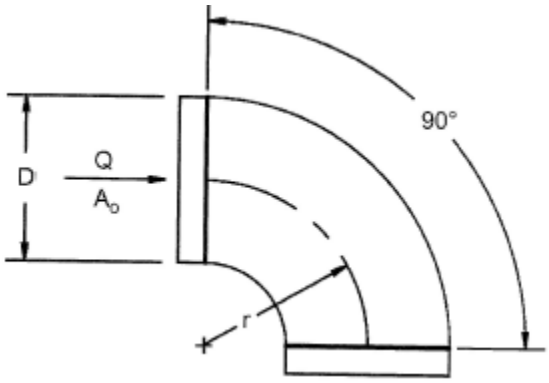

Figure 70: CD3-1 Elbow, Die Stamped, 90°, r/D=1.5

Table 59: CD3-1 Elbow, Die Stamped, 90°, r/D = 1.5

Diameter (Inches)	3	4	5	6	7	8	9	10
Loss Coefficient	0.30	0.21	0.16	0.14	0.12	0.11	0.11	0.11

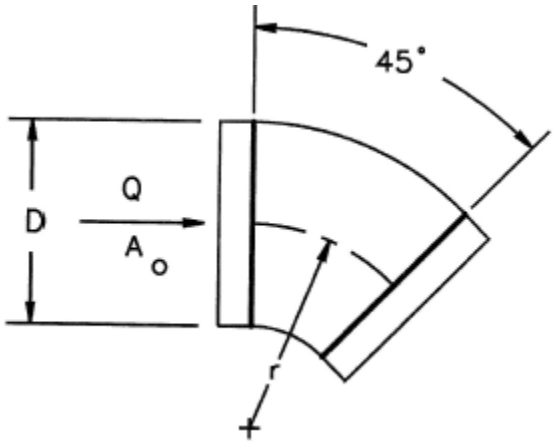

Figure 71: CD3-3 Elbow, Die Stamped, 45°, r/D = 1.5

Table 60: CD3-3 Elbow, Die Stamped, 45°, r/D = 1.5

Diameter (Inches)	3	4	5	6	7	8	9	10
Loss Coefficient	0.18	0.13	0.1	0.08	0.07	0.07	0.07	0.07

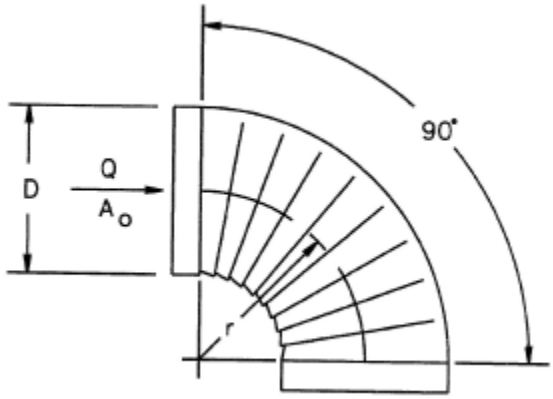

Figure 72: CD3-5 Elbow, Pleated, 90°, r/D = 1.5

Table 61: CD3-5 Elbow, Pleated, 90°, r/D = 1.5

Diameter (Inches)	4	6	8	10	12	14	16
Loss Coefficient	0.57	0.43	0.34	0.28	0.26	0.25	0.25

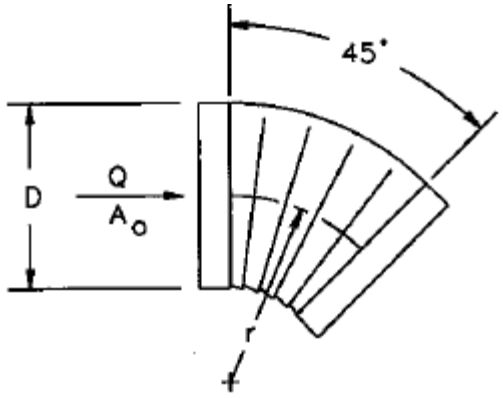

Figure 73: CD3-7 Elbow, Pleated, 45°, r/D = 1.5

Table 62: CD3-7 Elbow, Pleated, 45°, r/D = 1.5

Diameter (Inches)	4	6	8	10	12	14	16
Loss Coefficient	0.34	0.26	0.21	0.17	0.16	0.15	0.15

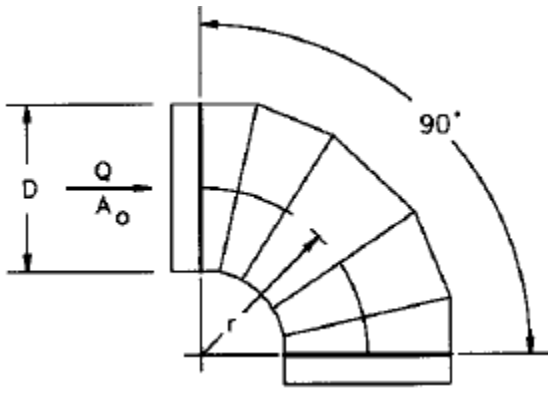

Figure 74: CD3-9 Elbow, 5 Gore, 90°, r/D = 1.5

Table 63: CD3-9 Elbow, 5 Gore, 90°, r/D = 1.5

Diameter (Inches)	3	6	9	12	15	18	21	24	27	30	60
Loss Coefficient	0.51	0.28	0.21	0.18	0.16	0.15	0.14	0.13	0.12	0.12	0.12

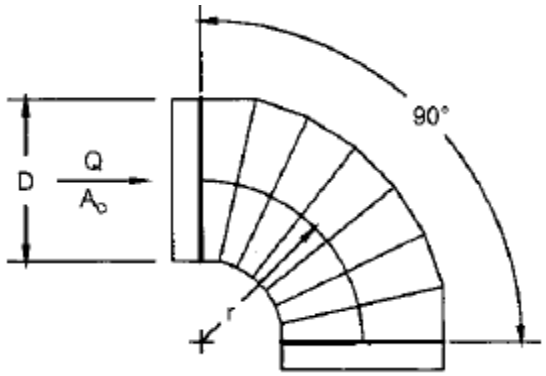

Figure 75: CD3-10 Elbow, 7 Gore, 90°, r/D = 2.5

Table 64: CD3-10 Elbow, 7 Gore, 90°, r/D = 2.5

Diameter (Inches)	3	6	9	12	15	18	27	60
Loss Coefficient	0.16	0.12	0.10	0.08	0.07	0.06	0.05	0.03

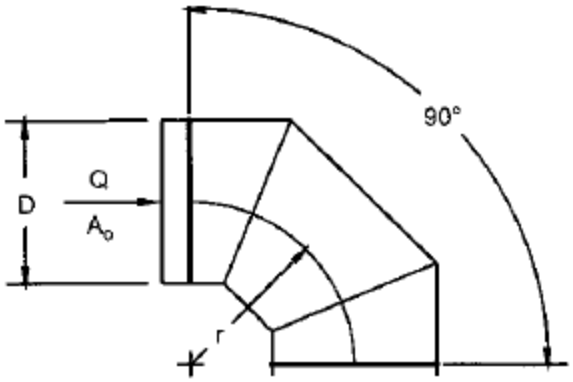

Figure 76: CD3-12 Elbow, 3 Gore, 90°, r/D = 0.75 – 2.0

Table 65: CD3-12 Elbow, 3 Gore, 90°, r/D = 0.75 – 2.0

r/D	0.75	1.00	1.50	2.00
Loss Coefficient	0.54	0.42	0.34	0.33

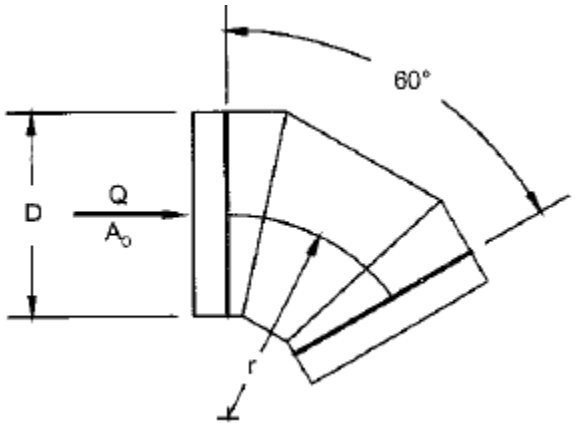

Figure 77: CD3-13 Elbow, 3 Gore, 60°, r/D = 1.5

Table 66: CD3-13 Elbow, 3 Gore, 60°, r/D = 1.5

Diameter (Inches)	3	6	9	12	15	18	21	24	27	30	60
Loss Coefficient	0.40	0.21	0.16	0.14	0.12	0.12	0.11	0.10	0.09	0.09	0.09

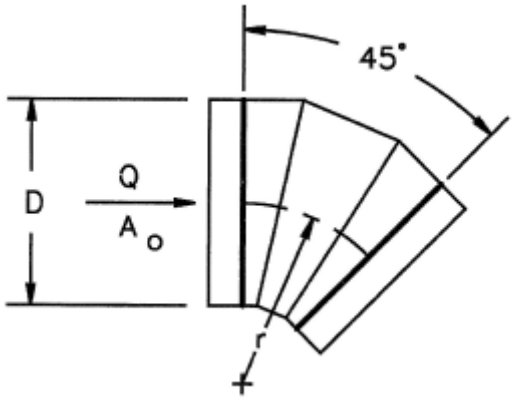

Figure 78: CD3-14 Elbow, 3 Gore, 45°, r/D = 1.5

Table 67: CD3-14 Elbow, 3 Gore, 45°, r/D = 1.5

Diameter (Inches)	3	6	9	12	15	18	21	24	27	30	60
Loss Coefficient	0.31	0.17	0.13	0.11	0.11	0.09	0.08	0.08	0.07	0.07	0.07

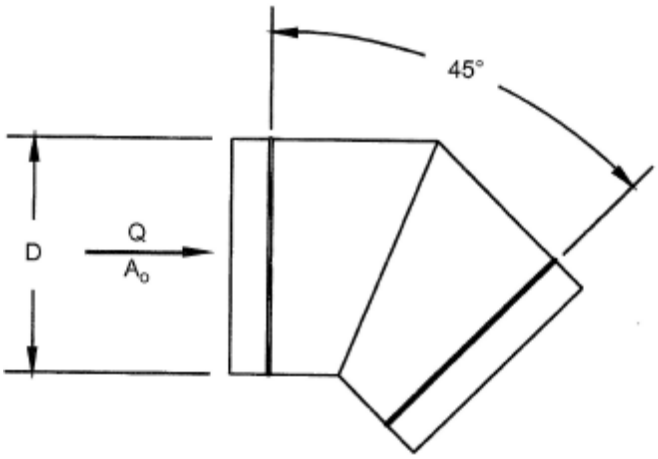

Figure 79: CD3-17 Elbow, Mitered, 45°

Table 68: CD3-17 Elbow, Mitered, 45°

Diameter (Inches)	3	6	9	12	15	18	21	24	27	60
Loss Coefficient	0.34	0.34	0.34	0.34	0.34	0.34	0.34	0.34	0.34	0.34

APPENDIX D: PERSONAL AND PHONE INTERVIEWS

The following are notes taken during phone interviews:

Johnson Supply Bryan, TX

- Some installers use B vent or flue pipe (double wall)

Erik Bergstrom, Head Engineer for kitchenfoundry.weebly.com

- Does not recommend B vent (double wall)
- Should use rigid adjustable elbows
- Round duct is easiest to install and also provides the best performance
- Square duct may be necessary if range hood is in between floors and you must go through a wall
- Recommend 5 feet of straight pipe between 90° to reduce turbulence. Turbulence will greatly reduce range hood effectiveness

Bob Seloff, Head Engineer for Vent-A-Hood

- Range hoods run air 5-6 times faster than AC handlers
    - AC handlers are approximately 300-500 ft/min
    - Range hoods are up to 1800 ft/min
- His designs make sure to never reduce cross sectional area
- Don't use vent caps that make large turns.
- No screens or exposed screws to restrict flow.
    - He mentioned using clear duct to show the position of a ping pong ball when unit was turned on. He then placed chicken wire in the duct and retested to show drastic reduction in performance.

    - 0.25” of water head loss should be a maximum
- 8” to 6” loses 43% of area and reduces velocity of fluid
- Mechanical filter on 1200cfm captures about 70% of grease. Filter is an obstacle course, air is more nimble and grease less nimble. Higher speed makes filter effective, and on average ASHRAE says 28% at 300cfm.
- Vent-A-Hood uses a squirrel cage as a centrifuge to catch grease, no mechanical filters.
- Laminar flow above 30ft/s becomes turbulent. Resistance goes up squared for doubling velocity.
- Effects of duct diameter:
    - 600cfm through 6” duct gives 3100 ft/min and requires 3” of water to push air 100 ft of duct.
    - 600cfm through 8” duct gives 1800 ft/min and requires 0.65” of water to push air 100 ft of duct.
    - 600cfm through 10” duct gives 1100 ft/min and requires 0.2” of water to push air 100 ft of duct.
- Exhaust gas process
    - Collect gases: Use the canopy to collect the inverted cone of gases
    - Blower: Use the blower to create a pressure gradient
    - Ductwork: Use the ductwork to move the gases out of the house
- Large canopy increases the capture efficiency of the range hood
- Types of range hoods

    - Ducted hoods
    - Ductless hoods
    - Air Recovery Hood
- Recommends single wall ducting to keep cross sectional area up and flow rate down (Less turbulent).
- Recommends rigid segmented elbows sold at Lowe's and Home Depot.
- Best capture efficiency ever constructed: 48%

The following are notes taken during a personal interview

Roquey Schofield, Construction Specialist at Integrity Comfort Solutions – Conroe, TX

- Typically, 100CFM (High setting) minimum range hood installation
- 95% of the time it is 6" ductwork
- Star cap is most common vent cap (Chinaman's cap)
- Stainless steel hoods are somewhere around 1200CFM and may need makeup air.
    - He built 1500 homes a year, about 20 houses (1.3%) required makeup air.
- Formicary corrosion is a problem for evaporator coils in AC units. Range hoods help reduce this problem.
- In AC units, builders have experimented with aluminum evaporator coils instead of copper because it corrodes less, has better heat transfer, but is harder to weld.
- For exhaust ventilation ductwork through the slab, you can use schedule 40 PVC, otherwise single wall galvanized steel.
- On average, there is about three feet from the stovetop to the range hood.

- Most common type of elbow is the adjustable 4 segmented elbow.
- For AC units, there should be about 400 ft^3/min per ton of air conditioning.
- Windows are 50% of heat gain in a conventional house.
- Typically, insulation: R-13 in the walls, and R-38 in the ceilings.